Design of Magnetorheological Gear Profile Finishing Tool and Experimental Investigations for Enhancing Gear Transmission Performance

A Thesis Submitted in Fulfillment of the Requirement for the Award of the Degree of

MASTER OF ENGINEERING

in

Production Engineering

Submitted by

RAVI DATT YADAV

Roll No. 801685015

Under Supervision of

Dr. Anant Kumar Singh
Associate Professor

THAPAR INSTITUTE
OF ENGINEERING & TECHNOLOGY
(Deemed to be University)

MECHANICAL ENGINEERING DEPARTMENT

THAPAR INSTITUTE OF ENGINEERING & TECHNOLOGY
(A DEEMED TO BE UNIVERSITY), PATIALA, PUNJAB – 147004, INDIA

JULY, 2018

DECLARATION

I, **Ravi Datt Yadav** hereby declare that the work presented in this thesis entitled "**Design of Magnetorheological Gear Profile Finishing Tool and Experimental Investigations for Enhancing Gear Transmission Performance**" in fulfilment of the requirement for the award of degree of **Master of Engineering (Production Engineering)** submitted at Mechanical Engineering Department, Thapar Institute of Engineering & Technology (Deemed to be University), Patiala is an authentic record of work carried out under supervision of **Dr. Anant Kumar Singh** (Associate Professor, Mechanical Engineering Department, Thapar Institute of Engineering & Technology) from August, 2017 to July, 2018. The matter presented in this has not been submitted either in part or full to any other university or institute for the award of any other degree.

Ravi Datt Yadav
(801685015)

Date: 09-08-2018

Dr. Anant Kumar Singh
(Associate Professor)
Mechanical Engineering Department,
Thapar Institute of Engineering & Technology
(A Deemed to be University), Patiala, Punjab.

Date: 09/08/2018

Dedicated

to

my family

for their endless love, support and encouragement

ACKNOWLEDGEMENT

I would first like to thank my thesis advisor **Dr. Anant Kumar Singh**, Associate Professor, Mechanical Engineering Department, Thapar Institute of Engineering & Technology. The door to his office was always open whenever I ran into a trouble spot or had a question about my research or writing. He steered me in the right direction whenever he thought I needed it. His guidance helped me in all the time of research and writing of this thesis.

I am also thankful to **Mr. Jhujar Singh** (General Manager), **Mr. Sandeep** (Manager, Quality Department) and their colleagues for helping me in understanding the process and discussing the problems faced during Gears operation and performance at GNA Gears Ltd., Hoshiarpur (Punjab).

I would also like to thank **Mr. Aditya Nath** (Deputy Manager) for help in measurement of gear tooth profile at Super Hobs and Broaches Pvt Ltd., Patiala (Punjab).

I would like thank to **Mr. Gurukaran Singh** (C.E.O) for helping me to fabricating the gear tooth profile and gear grinding operation at Kay-Kay gears (Brand of Kay-Kay Agro Industries), Patiala (Punjab).

Lastly, I would like to thank the Almighty and my family for their unbiased love, endless support and blessings.

ABSTRACT

The heavy loaded vehicles and high-speed running vehicles are usually produced more noise as well as vibration while reaching at high speed. The noise and vibration in gear box are developed during the meshing of gears teeth. Basic cause of these problem are gears surface asperities, dimensional accuracy, transmission error and their shape accuracy. All these problems are related to the gear cutting operations and the gear teeth profile surface finishing. The challenge related to the gear teeth finish can be overcome by the super finishing of the gear teeth profile precisely and with their more shape accuracy. A new magnetorheological fluid-based finishing process is developed for finishing gear teeth profile. In this process, to finish the gear teeth in nanometer range, a magnetorheological gear profile finishing (MRGPF) tool is designed and fabricated. The MRGPF tool is made likely similar to the gear grinding profile wheel tool. The present finishing work performed after the grinding of gear profile and compared the results obtained with the present MRGPF process. The magnetostatic finite element analysis (FEA) of the present developed MRGPF tool was done in Maxwell Ansoft V13. On the basis of FEA for magnetic flux density distribution on its finishing surface, the MRGPF tool has been designed. The present work is concerned with the influence of reduction in surface roughness on the gear performance (made with the material of EN24 having 62 HRC) after its profile finishing with present designed tool. The detailed design of experiments has been carried out using the response surface methodology. The spur gear is used in the present work with 3 module gear teeth profile and 12 numbers of teeth. The variable parameters taken are feed of tool, rotation of tool, and variable of working gaps between the tool surface and workpiece surface to optimize the process performance. The average surface roughness is reduced from 160nm to the 20nm after the present MRGPF process with a single tooth in 20 minutes. Also, the DIN standard is reduced from DIN 6 to the DIN 4. Thus, the present developed MRGPF tool is found capable to reduce the surface roughness and improve the surface characteristics after the gear grinding process. The benefits of the super-finished gear profile surface can be estimated in terms of improvement in scuffing performance, reduction of noise in gear box, reduce the wear rate on gear teeth profile surface while meshing and also give lower friction and bulk temperatures during operation.

Keywords: DIN standard, magnetorheological fluid, gear tooth profile, gear face, gear flank, gear profile/lead, EN24 steel.

TABLE OF CONTENTS

LIST OF TABLES

LIST OF FIGURES

ABBREVIATIONS

AGMA	American Gear Manufacturing Association
AFF	Abrasive Flow Finishing
ANOVA	Analysis of Variance
BEMRF	Ball End Magnetorheological Finishing
BHN	Brinell Hardness Number
CAD	Computer Aided Design
CAVSF	Chemically Accelerated Vibratory Surface Finishing
CBN	Cubic Boron Nitride
CIP	Carbonyl Iron Particle
CCC	Circumscribed Central Composite Design
CCF	Central Composite Face-centred
CCI	Inscribe Central Composite Design
CV	Coefficient of Variation
DIN	German Standard for Gears
ECF	Electrochemical Finishing
ECH	Electrochemical Honing
EDM	Electric Discharge Machining
FEA	Finite element analysis
HMI	Human Machine Interface
IEG	Inter Electrode Gap
MR	Magnetorheological
MRGPF	Magnetorheological Gear Profile Finishing
MRPF	Magnetorheological Polishing Fluid
NASA	National Aeronautics and Space Administration
PECH	Pulse-assisted Electrochemical Honing
PLC	Programmable Logic Controller

RSM	Response Surface Methodology
SEMUEF	Simulations Electromagnetic and Ultrasonic Finishing
SEM	Scan Electron Microscopy
SiC	Silicon Carbide
ULG	Ultrasonic-assisted Lapping of Gears

NOMENCLATURE

K_p	Coefficient of pinion
T_f	Operating Temperature (℃)
R20	Resistance of the coil winding at 20℃
Rf	Resistance at operating temperature
F_n	Indentation force (N)
F_t	Tangential force (N)
F_s	Shear force (N)
N_p	Number of particle
V_f	Percentage of volume fraction of particles
V_{one}	One-millimetre cubic cell
R_s	Resisting shear force (N)
V	Volume of MR polishing fluid (mm^3)
N_{cp}	Number of iron particles in a chain
B	magnetic flux density (T)
μ_o	Magnetic permeability of free space (m kg s^{-2} A^{-2})
H	Magnetic strength at a point (A/m)
M	Magnetization of a particle (A m^2/kg)
H_{xij}	Magnetic strength along x-axis (A/m)
H_{yij}	Magnetic strength along y-axis (A/m)
H_{zij}	Magnetic strength along z-axis (A/m)
I	Current through electromagnetic coil (A)
a_j	Radius of coil varying in y direction (mm)
z_i	Varying distance from measuring point along z-axis (mm)
R	Resultant of magnetic field
B_{zl}	Magnetic flux density in working gap at left-side tooth (T)
B_{zr}	Magnetic flux density in working gap at right-side tooth (T)
F_m	Normal magnetic force (N)
m_{ip}	Mass of iron particle (kg)

χ_m	Mass of magnetic susceptibility (m^3/kg)
F_n	Indenting force on abrasive particles (N)
H_{BHN}	Brinell hardness number (kgf/mm^2)
D_a	Diameter of abrasive particle (μm)
D_i	Indenting diameter (m)
d_i	Depth of indentation (m)
A_1	Area of groove generated by abrasive (m^2)
V_a	Volume removed by abrasive particle (m^3)
L_a	Actual contact length of abrasive (m)
Ra^i	Surface roughness in ith stroke (nm)
Ra^{i-1}	Surface roughness in (i-1)th stroke (nm)
L_w	Length of workpiece (mm)
h	Total height of material removed (μm)
N_{ab}	Number of active abrasives
A_{cf}	Area of cube face (mm^2)
V	Material removal in ith stroke (mm^3)
f	Tool reciprocation feed (mm/min)
r	Tool rotation (rpm)
g	Working gap (mm)
V_r	Resultant velocity (mm/min)
V_{ro}	Rotational speed of tool (rpm)
V_a	Axial feed of tool (mm/min)
Ds	Distance travelled by one active abrasive (mm)
D_{ac}	Distance at gear profile (mm)
F	Function of response
E_{Ra}	Experimental surface roughness
T_{Ra}	Theoretically surface roughness
Ra	Arithmetic average of the absolute value of profile heights
Rq	Root mean square average of the profile heights
Rz	Average maximum height of the profile

fHa	Profile angle deviation for gear profile (μm)
Fa	Total profile deviation for gear profile (μm)
ffa	Profile form deviation for gear profile (μm)
fHB	Profile angle deviation for gear lead (μm)
FB	Total profile deviation for gear lead (μm)
ffB	Profile form deviation for gear lead (μm)
fr	Pitch line runout (μm)
fp	Single pitch deviation (μm)
Fp	Total cumulative pitch deviation (μm)

CHAPTER 1

INTRODUCTION

The principal objective of the present work is to improve the performance of the gear teeth profile. The super finished gear teeth profile reduces the noise in gear box, wear rate of teeth, friction, bulk temperatures during operation and improves the scuffing performance. For example, different kind of super finish gear arrangement use in gear box of racing car and the main gear box of the helicopter for the smooth transmission. Gear fabricated in many ways such as forging, hobbing, shaping and wire EDM. Finishing is the last procedure for most of the manufacturing technology. Finishing process technology for greatly increasing the surface quality of a machined objects. It maintains stable precision and improve the machining precision grade. Super finish gear teeth profile reduces transmission error at high load condition of gear box in different situation. Finishing of gear teeth with high precision is transformed in many ways; such as traditional and non-traditional method. During transmission of gears, gear teeth face, flank and line of gear teeth profile much more effect on another meshing gear. At the high-speed transmission, the gear face is predominated the life of gears. The microscopic effect of the gear meshing classified of friction noise in two categories according to the load [1]. In low load condition, noise is generated by surface roughness and this type of noise is called roughness noise. In high load condition, the load is generated by mechanical instabilities such as stick-slip and sprag-slip. The meshing of gear is the process like rubbing of two stone each other, wear rate start producing roughness noise after some time. Cause of the problem, small asperities in between the two surfaces and roughness peaks start tearing off [2]. The nature of material removal based on shear forces. Superfinishing material remove surface asperities, wear of material, frictional losses and noise problem. Advanced manufacturing processes are suitable to remove these problems, the cost of manufacturing is less as compare to the traditional processes. In traditional finishing process, more heat is generated while finishing of workpiece. Thermal damage for vasco X2M gear steel of helicopter based on specific grinding energy determined from grinding force measurements [3]. The national aeronautics and space administration (NASA) test spiral bevel gears in OH-58D helicopter. Purpose of this test is to modify the gear teeth geometry to reduce transmission error and noise. Noise, vibration, and tooth strain tests are performed. Significant gear stress and noise reductions are achieved [4]. The advanced manufacturing process is best option to remove these problems. The use of magnetorheological (MR) polishing fluids for finishing is one of the most promising

smart processes [5]. For the fabrication of ultra-fine surfaces, particularly three-dimensional millimeter or micrometer structures. In this process heating of workpiece is less as compare to traditional processes. Merits and demerits of traditional and non-traditional finishing process for gear teeth profile are discussed below.

1.1 TRADITIONAL FINISHING PROCESSES

Traditional finishing process are contact type of material removal from the surface of the workpiece. For producing gear teeth with these processes are grouped into three main classes. The first group classified with forming process; such as stamping and fine blanking of gear, extrusion and cold drawing, gear rolling and gear forging. The second group classified with material removal process; gear milling, broaching, gear cutting on a shaper, hobbing, shaping and gear planning. The third group classified with additive process; gear casting, powder metallurgy and injection molding of plastic gear. All these processes are used for fabrication of gears. Accordingly, finishing process of conventional method are discussed below.

1.1.1 Gear Shaving

Gear shaving is a finishing process that applied after the processes of cutting or forming of the gear teeth. The shaving cutter process working on gear teeth surfaces, material removal of hair like chips. Slow speed of cutting tool prefer to avoid thermal loading on the cutting edges. The cutter provided with special type of serrations. It works as cutting edges at the flank area of the gear cutting teeth. The performance of this process depends on the material of shaving cutter, gear workpiece material, gear geometry, shaving allowance, and fundamental process parameter associated with the shaving. This process normally used for finishing of gear in automobile industry. This process can be classified on basis their geometry as shown in Figure 1.1 [6].

1.1.2 Gear Grinding

Gear grinding process is frequently uses for high strength and hardened materials whose Rockwell hardens on C scale approximately 45 to 62 HRC. The material removal process on the teeth face and flank surface in the form of chips by the action of abrasives. The grinding wheel most commonly used of abrasive grains are silicon carbide (SiC), alumina oxide (Al_2O_3), and cubic boron nitride (CBN). Gear grinding working principle similar to gear hobbing cutter. In this process grinder abrasives size influencing the surface roughness of teeth. For good geometrical and for high production, this process capable is best to achieve the DIN 6 standard with high qualified operator [6].

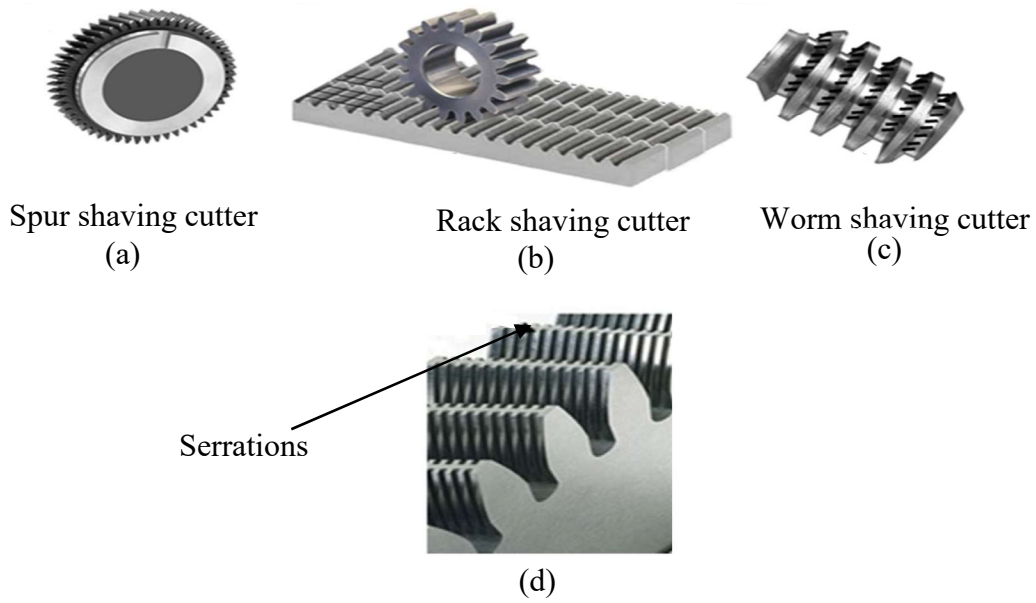

Figure 1.1 Shaving cutter based on geometry (a) spur shaving cutter, (b) Rack shaving cutter, (c) worm shaving cutter and (d) Serration at the face of gear teeth [6]

The material removal rate classified in three ways such as rubbing, ploughing and cutting. The workpiece gear and gear grinder wheel rotate about their axis. The indexing mechanism is the biggest factor affecting gear surface roughness and profile quality. It can be used for spur and helical gears. Rotate gear grinding wheel about its axis is to finishes those flank surfaces, for two adjacent teeth, which its outer edges are in contact. Gear finish requires all teeth with equal material removal rate. For, that indexing of teeth with gear grinding must. Gear grinding process is shown in Figure 1.2 [6].

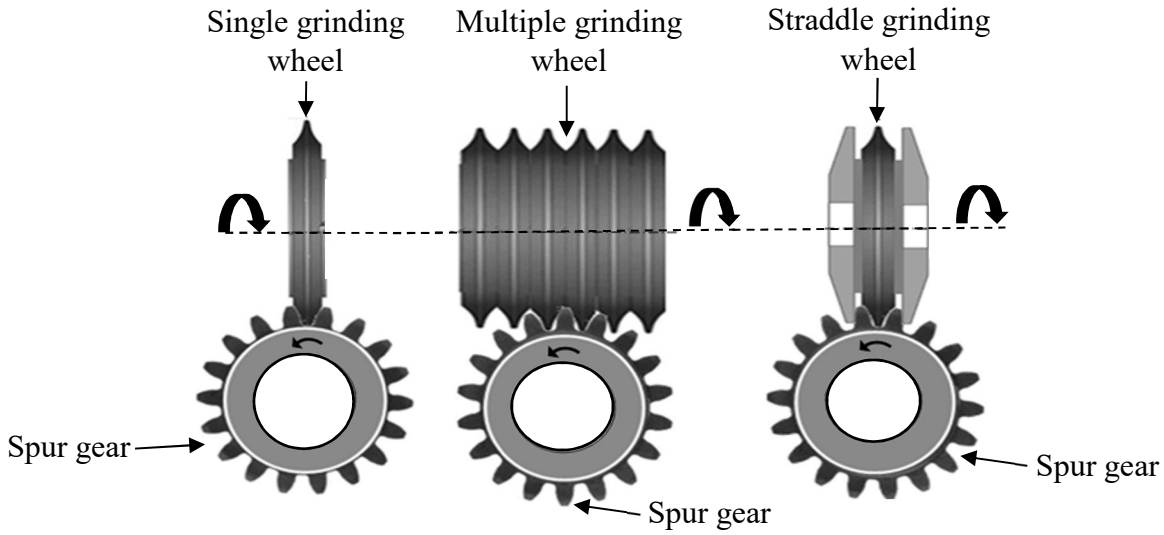

Figure 1.2 Different type finishing of a gear by gear grinding process [6]

1.1.3 Honing

Gear honing process is used to fine finish the gear either externally or internally depending on the arrangement of the workpiece gear and honing gear tool. This process is used to finish the hard material of workpiece. The honing gear drives the workpiece gear at high speed also gear reciprocated along its axis there by finish the entire face and flank width finish [7]. Gear honing removes the minor irregularities, nicks and burns from the active profile of the workpiece gear teeth. The honed workpiece surface depends upon the rotation speed, applied honing pressure, and size of the abrasive. Excessively strong bonding of abrasive may affect the finish of workpiece. The abrasive is most commonly used for cutting are Alumina, SiC, CBN and diamond. The bonded between the matrix and abrasive grain must be strong while finishing. Gear honing process shown in Figure 1.3 [7].

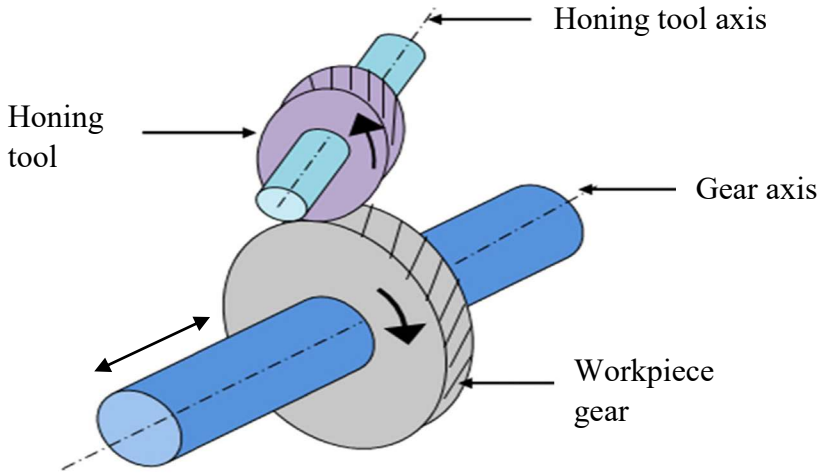

Figure 1.3 External gear honing of a single helical gear [7]

1.1.4 Gear Burnishing

Gear burnishing is a process that modifies the gear surface and geometry by cold forming instead of material removal. Low strength and/or unhardened gears are meshed accurately under pressure with ground, polished, and hardened master gears (ideal gear). This causes smearing of the minute irregularities on flank surfaces of the workpiece gear teeth by cold work. It improves surface finish and beneficial to other surface integrity descriptors. Typically, a single burnishing gear is mounted on a heavy-duty gearhead and meshed with the workpiece gear, shown in Figure 1.4 [6,8]. Two idle gears are used to provide support. The workpiece gear is mounted such that it is free to rotate. The burnishing gear is driven and drives the whole assembly by appropriately close meshing with the workpiece gear. The direction of rotation of the burnishing gear is alternated to facilitate

burnishing of both the leading and trailing side of the workpiece gear teeth. A lubricant can be used to reduce abrasive wear of the workpiece gear and to improve the surface quality.

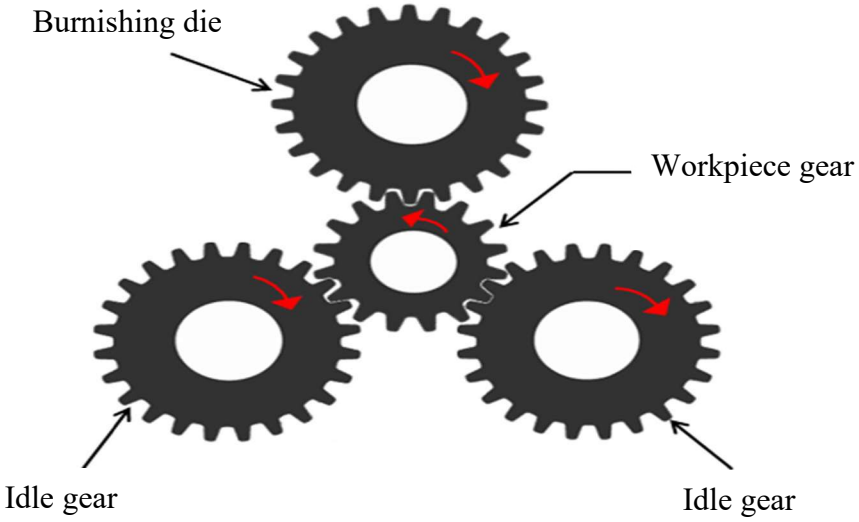

Figure 1.4 Schematics diagram of gear burnishing [6,8]

1.2 NON-TRADITIONAL FINISHING PROCESSES

There are various limitations and non-overlapping nature of the conventional finishing processes have been observed. Conventional process implemented more than one finishing station required in industries. Tool and workpiece are incorporated with a suitable heat treatment, to achieve the desired gear quality and characteristics. In non-traditional the process manufacturing productivity may be limited. But they capable to produce gear with vibration-free, low noise transmission, and extended service life (especially at higher transmission speeds). In this context, advanced finishing processes such as electrochemical honing (ECH), abrasive flow finishing (AFF), water jet deburring (WJD), etc. are emerged as processes. These processes are capable to produce high yield precision and quality finishing of gears by virtue of certain unique capabilities. These advanced processes may offer certain unique advantages. While at the same time have the potential to address some of the most significant limitations associated with conventional finishing processes.

1.2.1 Gear Finish with Electrochemical Honing (ECH)

Electrochemical honing (ECH) process is a hybridization of electrochemical finishing (ECF) and electrochemical honing as shown in Figure 1.5. These two processes work together to overcome the individual limitation while deed their advantages [9]. During hybridization process ECF

process removes the majorities of the roughness peaks area. Result of non-uniform material removal by the ECF process is selectively removing roughness peaks by honing process. The honing process is barred to removal of the forbid oxide passivating layer [10]. This process has potential to improve the quality of the gear and surface characteristics. The ECH is a good alternative to make an economical and sustainable gears.

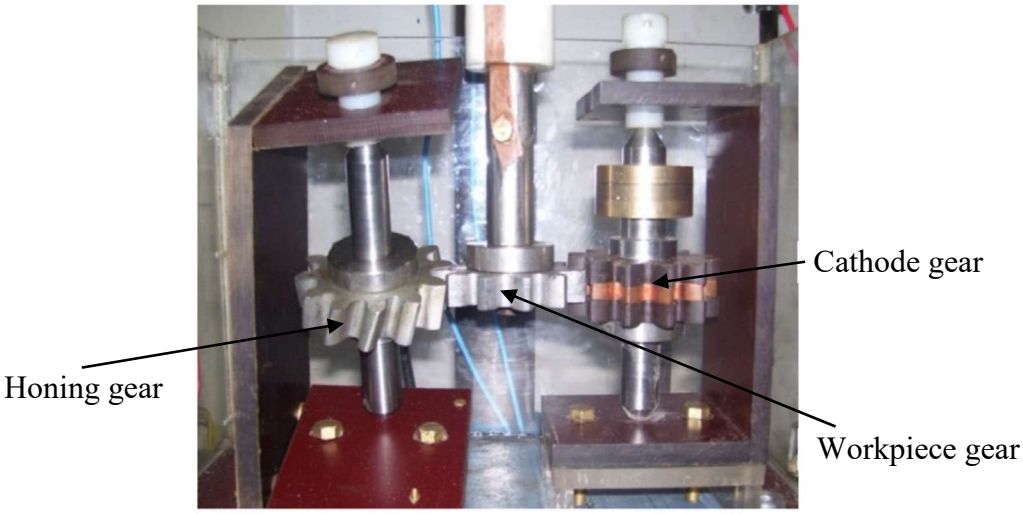

Figure 1.5 Finishing of cylindrical gears by ECH [11]

1.2.2 Gear Finish with Abrasive Flow Finishing

Abrasive Flow Finishing (AFF) process is produced a mirror-like image gear surface at minimum cost. The abrasive medium flow on gear surface profile with high extrusion pressure and high flow rate. High pressurized fluid abrasives shear off surface roughness peaks, removal of material in nano-chips and produce mirror like finish. During finishing if shape of profile restriction to the flow of abrasives where more aggressive finishing action takes place. A typical AFF machine consists of fixture or tooling for the gear, hydraulic cylinder and AFF medium, shown in Figure 1.6 [12]. For mass production modern AFF machines are fully furnished with a CNC control system. The abrasive flow finishing medium is a mixture of viscoelastic polymer, appropriate abrasive particles and a suitable lubricating oil. The path followed by abrasives is along the tooling and workpiece surface profile. Commonly used abrasives are silicon carbide (SiC), cubic boron nitride (CBN) and aluminum oxide powder (Al_2O_3). Change the ratio of polymer and lubricating oil can be controlled the viscosity of abrasive flow medium [12]. The flow rate of medium depends

upon the hydraulic pressure and size of passage. High flow rate and low viscosities are used for deburring and radiusing sharp corner, whereas slow steady rates and low viscosity are used for gear profile polishing and other finishing applications.

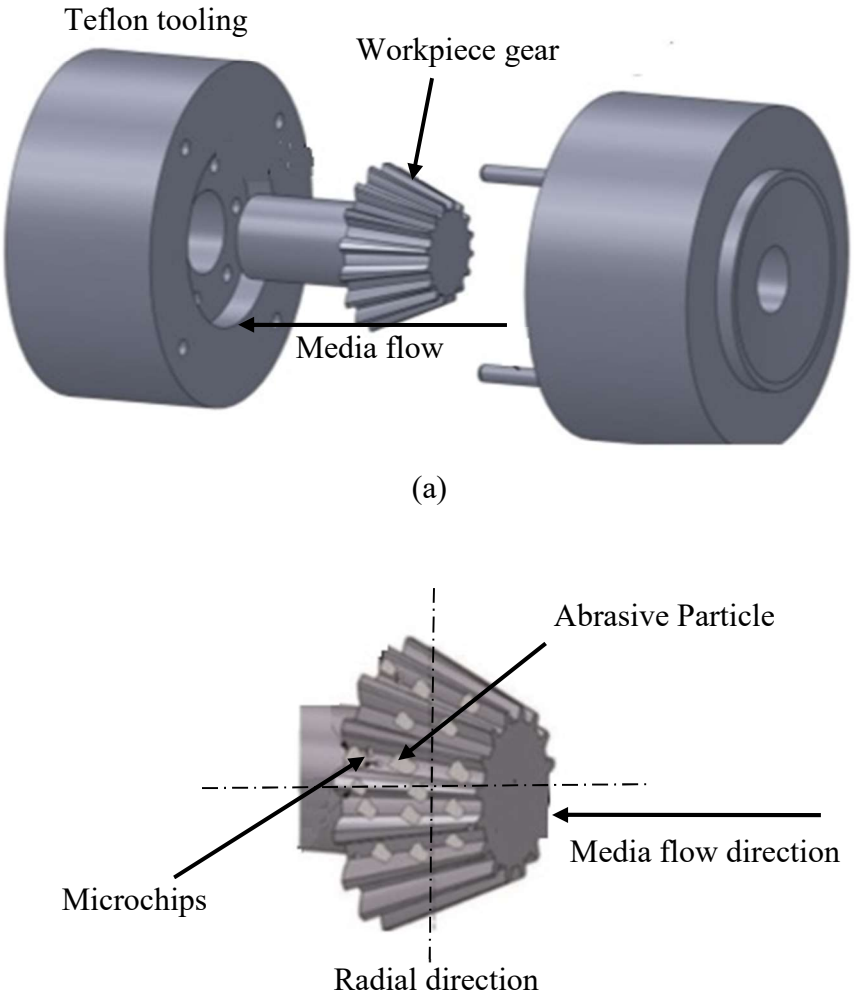

Figure 1.6 (a) Abrasive flow finishing for bevel gear and (b) schematic of a bevel gear during machining through AFM process [12]

1.2.3 Gear Lapping

Gear lapping for cylindrical gears (i.e., spur, single helical, double helical and herringbone gears) involves meshing with a gear-shaped lapping tool. Working space between lapping tool and gears is filled with pressurized abrasive grains. During finishing gear and lapping tool rotate about their axis. Lapping gear driven the workpiece gear free to rotate about its axis, shown in Figure 1.7 [13]. Due to abrasive flow velocity in working gap at gear teeth, decrease from root of a teeth to zero at

pitch line. After pitch line maximize again at the tip of teeth. Mating conical gear, no need to provide finishing allowance, both gear finish simultaneously. The most commonly abrasives used are diamond powder, aluminum oxide, silicon carbide and boron carbide. Spiral bevel gear and hypoid gear are mostly lapped with abrasive grain size 280 and 400 mesh respectively [13]. Finer abrasive or high mesh-size grain are used for highly precision gears. Large size or less mesh-size are used for coarse pitch gears.

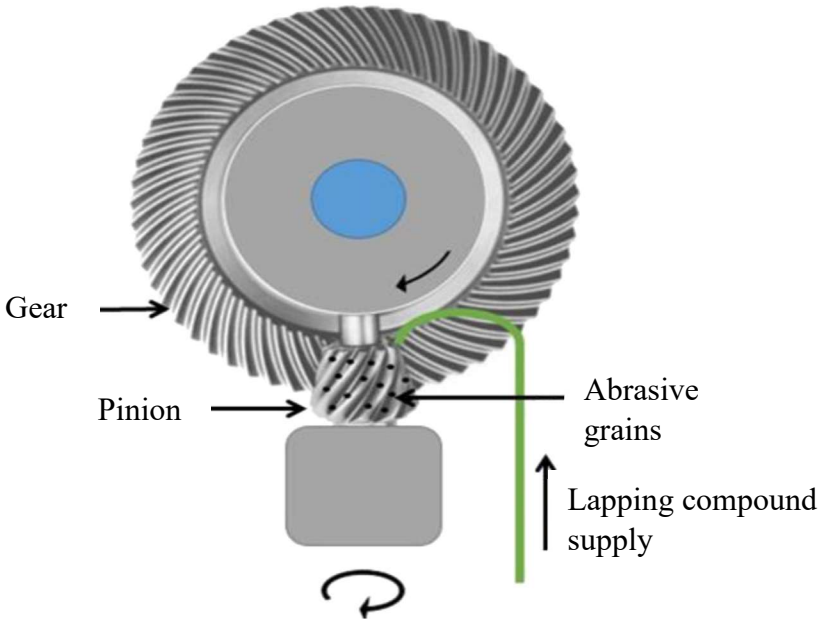

Figure 1.7 Spiral bevel gear finish by lapping process [13]

1.2.4 Water Jet Deburring

In water jet machining, highly pressurized water flow with high fluid velocity and significant kinetic energy exiting through a nozzle. This highly pressurized water jet directly strikes the workpiece surface which removes the selective materials [14]. The material removal in form of chips, burrs and debris from the gear face and flank surface without affecting the basis geometry. This process is mostly used for external spur gear, shown in Figure 1.8. Sometimes burrs and debris cannot have removed by water jet machining. If gear surface has some high material strength debris, for that water jet deburring process is used and also for the requirements of highly finished surface. In water jet deburring machine combined with mechanical deburring using a filament brush and rotary brush [14]. Frequently, spur gear faces are first mechanically deburred and then cleaned for water jet deburring for uses in precision area of gear assemblies. This process

effectively performs with material like alloy steel, cast iron, high strength steel, polymers, brass, aluminum, and composites. Soft material used low pressurized water and hard material required high pressurized water [15]. Industrial range of application water jet deburring are automotive, aerospace, fluid power, food processing, chemicals, home appliance and biomedical.

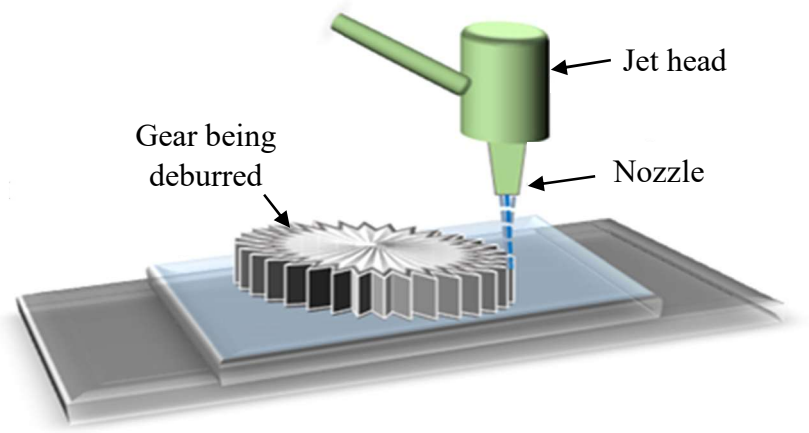

Figure 1.8 Water jet lubricant for spur gear manufacturing [15]

1.2.5 Chemical Accelerated Vibratory Surface Finish

Chemically accelerated vibratory surface finishing (CAVSF), used for isotropic superfinishing of surfaces. This process is environmentally friendly and inexpensive and capable to reduce roughness peaks from the face and flank of gear teeth. The CAVSF process possibility to reduces the average surface roughness of a hardened gear from 0.3 to 0.05µm [16]. This process has a possibility to remove approximately 5µm material from the surface and thereby producing minimum change of gear geometry. The CAVSF for gear finish occurs in a vibratory tank, using a nonabrasive ceramic media with high density and a flow of chemical acid, shown in Figure 1.9 [17]. The chemical acidic solution forms a soft coating on the gear teeth face and flank. Due to vibration rubbing motion of ceramic media with gears surfaces, that can effectively remove the roughness peaks on the gear surface. The surface valley is mostly unaffected because ceramic media not mechanically influencing the same manner as for surface peaks [16]. The ceramic media formed continuously and clean surface with force to conveyance the smooth surface mechanisms. This process continuously till the required surface finish is not achieved. The gear teeth surface finished are initially clean up in tap water followed by demineralized water to rinsed the chemical

solution. The CAVSF process yields a surface texture for conduction of lubrication. It is capable to remove peak asperities, material damaged and stress raisers. Finish gear by the process are exhibit lower operating temperature, lower friction, better surface resistance, high contact fatigue resistance and less wear.

Figure 1.9 Chemical accelerated vibratory gear finish machine [17]

1.3 ADVANTAGES OF NON-TRADITIONAL PROCESSES FOR FINISHING GEAR TEETH PROFILES

- Finished gear tooth profile in nano-metric range.
- Improve the gear tooth shape accuracy and DIN standard compare with traditional finishing processes.
- Reduction of gear noise and transmission error during gear mashing.
- Removes the surface asperities.
- Reduces the gear tooth surface wear and frictional losses.
- Reduces the thermal stress on gear tooth profile.

1.4 LIMITATION OF NON-TRADITIONAL PROCESSES FOR FINISHING OF GEAR TEETH PROFILE

- Non-traditional processes are take more time to finish the gear tooth profile.

- These processes improve the DIN standard but not capable improving the DIN such as higher value. Example an electrochemical honing process improve the DIN standard from DIN 7 to DIN 6 [11].
- Gear tooth geometry are complex in shape so non-traditional process are not give the uniform surface finish as such extent.
- Non-traditional finish processes are reducing the thermal stresses when compare with the traditional process, but not improving the thermal stress as higher rate.
- These processes are removing the surface asperities at some extent as well as gear tooth surface roughness reduce up to 0.050μm but reduces more than that [11].

1.5 NEED OF MR-FLUID BASED PROCESS FOR FINISHING OF GEAR TEETH PROFILE

- Magnetorheological (MR) fluid-based process are capable to finish the workpiece up to nano-level.
- MR fluid finish the complex shape and 3-D structure with uniformly surface finish.
- Forces acting during finishing can be controlled by controlling the magnetic field.
- A very less heated surface after finish with MR fluid base process and there is no effect of thermal stresses on finished surface.
- Reduces the sub-surface defects (scratch, micro cracks)
- A MR fluid base process can finish ferrous and non-ferrous material.

CHAPTER 2

LITERATURE REVIEW

Literature review gives an idea about the past research experience in the finishing of gear teeth. This chapter shows that, what work had already done and what is the future scope. This chapter is related to literature review of gear teeth profile finish with the traditional and non-traditional method. The research performed by the various researcher regarding the gear teeth finish discussed below.

2.1 LITERATURE REVIEW

Pa [18] developed simultaneous electromagnetic and ultrasonic electro finishing (SEMUEF) method for super finishing of acid citrate dextrose 37 material surface. This process was applying electromagnetic force and ultrasonic energy simultaneously into the electrolyte. Possibility of high material removal with the super finish workpiece surface after (SEMUEF) is 0.15μm. The high electromagnetic strength (electromagnetic field intensity) result better surface finish. It is due to that the electrolyte, via electromagnetic force, can more rapidly discharge dregs from the tight machining gap. The effects of streamline on the electrochemical reaction and improve the finish quality.

Wei *et al.* [19] firstly proposed ultrasonic-assisted lapping of gears (ULG) and compared with conventional lapping in material removal process and mechanism. The material removal mechanisms of the ultrasonic lapping include hammering, impacting and acoustic cavitation. They used taguchi method find the optimum condition for a high removal rate in the ultrasonic lapping experiments of spiral-bevel gears. The optimum conditions were found as brake torque, 0.12 Nm; pinion rotational speed, 600 rpm; and slurry concentration with 20%.

Yang *et al.* [20] introduced the ultrasonic grinder (ULG) system design methodology for the middle module hypoid gear set. This paper has also introduced contact pattern test, tooth flank error measurement and vibration experiments of gear to verify the effectiveness of the proposed ULG. The experimental results show that the ease-off topographies were compared before and after ULG and the contact area is enlarged after ULG. So, the gear set will be less noisy due to its wider contact area. In the vibration experiments, the acceleration amplitude of gear mess frequency and its harmonics have been reduced after adopting ULG. The surface quality has been improved

after ultrasonic lapping. Its gear transmission quality would be relatively better than those using the traditional lapping method.

Shaikh and Jain [21] studied the effects of electrolyte composition and finishing time on geometric accuracy and surface finish, of straight bevel gears by electrochemical honing (ECH) process. The main objective was to improve their service life and operating performance. Geometry accuracy in terms of errors in pitch and runout, while surface finish was evaluated by average and maximum surface roughness values. An electrolyte composition having 75% $NaNO_3$ and 25% NaCl and finishing time of 2 min were found as the optimum combination.

Singh and Jain [22] found experimental that the pulse assisted ECH gives marginal improvement in the surface finish. At the cost of three times higher processing time as compared with direct current ECH and higher value of inter electrode gap (IEG) up to 1 mm. It helps to give controlled anodic dissolution in ECH of spur gears. The presented work on precision finishing of spur gears by using ECH and pulse assisted ECH (PECH) processes. It indicates that pulse assistant in ECH leads a marginally higher surface quality of average percentage improvement in the roughness (PIR_a) = 7.59 and maximum percentage improvement in the roughness (PIR_t) = 0.42 than the ordinary ECH process.

Mishra *et al.* [11] studied on high precision finishing of gears by electrochemical honing (ECH) process. It is an electrochemical (EC) based hybrid machining process combining the faster material removal capability of electrochemical machining (ECM) process. Therefore, it controlled functional surface generating capability of conventional honing in a single action. However, like most of the hybrid machining processes (HMPs), ECH of gears is also in the infancy stage. Therefore, a sustained global research is required to transform it into a matured manufacturing technology. To get its successful industrial applications and commercialization. This process having some advantages, like workpiece is free of thermal stresses as very little amount heat built up although very low temperature is involved with the process. This process leaves no significant residual stresses, process improves the surface finish as well as fatigue life of gears and reduces the running noise.

Jain [23] purposed gear grinding with electrochemical process as a hybrid process to finish the hardened surface. Electrolyte is supplied through the inter electrode gap between gear workpiece and gear grinding tool. This process is similar to gear electrochemical honing. Honing gear is replacing with the grinding wheel. The finishing by ECH reduces to gear finishing. Role of the mechanical honing gear wheel is insignificant to produce high quality of gear. In the

electrochemical grinding process, the material removal is slow rate for better finishing. The material removal rate in this process can be increased in two ways. One, stick in suitable abrasives into the cathode gear, second is integrating of abrasive particles into the electrolyte. Mostly uses of abrasives are such as aluminum oxide, silicon carbide, and cubic boron nitride, depending upon the hardness of gear material.

Britton *et al*. [24] investigate the effect of surface finish comparing the frictional losses of conventionally ground teeth. This process was used for those teeth which were super-finished by vibrating tank polishing process used containing water, abrasive compound (aluminum oxide) and zinc chips. Result of superfinishing was reduced 30 percent in total frictional torque at heaviest loads 67.7 Nm and at highest speed of 5000 rpm. This reduction in friction was accompanied by a reduction in gear tooth bulk temperature amounting to approximately 10°C under the most severe conditions considered.

Klocke *et al.* [25] proposed that soft finishing of gears by hobbing, roughing process and finishing process. In roughing process, the most amount of the material needs to get machined. Left of material debris remove in finishing process is used to get a high-quality shape of the gear and to get low surface roughness. The investigation revealed that the use of a combination tool for finish hobbing reached a three times higher tool life in the finishing cut than the use of a conventional hob. The soft finishing compare to hard finishing offers several key benefits. One benefit is to realize a more economical process.

Jolivet *et al.* [26] measured the friction noise before and after meshing in dry and lubricated conditions. The effect of meshing teeth flank was studied with finished surface by power-honing, grinding and not finished. To accomplish this objective, a new non-destructive sensory measurement technique was developed to characterize the friction noise generated by teeth flank surface. Results demonstrate particularly that the finishing process of tooth surfaces has more impact on friction noise generation than the lubricant viscosity, roughness attenuation due to previous meshing.

Masseth and Kolivand [13] studied the effects of superfinishing and lapping on surface finish and transmission errors were discussed on ring gear and pinion. In lapping process, measurement results show that gear surface finish becomes worse after lapping while no consistent results for pinion surface finish were observed. Furthermore, lapping decreases the surface finish variation among gear sets and decreased the first three harmonics of transmission errors for both drive and coast sides. The result of measurements taken before and after superfinishing improves surface

finish drastically, the quality achieved by the superfinishing process considerably decreased when gear sets were rolled together. Also, do not have any considerable and consistent effect on transmission errors.

Sekar and Kumar [27] performed a detailed investigation on wear depth for standard and non-standard gears has been carried out using a mixed finite element method (FEM) and analytical approach. In the standard gear drive the equal tooth thickness at the pitch circle of the pinion and gear, the maximum fillet stresses in the pinion and gear are different. The maximum balanced fillet stress is achieved by adopting the unequal tooth thickness at the pitch circle of the pinion and gear. An increased tooth thickness coefficient for pinion (kp) 0.5 to 0.5463 was required to achieve the balanced maximum fillet stress. In the non-standard gear the change in the values of load share is found to be significant in the double pair contact regions. The load carrying capacities of the pinion too thin bending and contact increases due to the reduced load at the region.

Karpuschewski *et al*. [28] said in their studied that all abrasive finishing processes are nowadays under critical review due to the increased specific power demand related to the small chip thicknesses. While gear finishing already plays a major role in sustainable energy generation by wind mills, the power consumption of the manufacturing processes itself have to be further optimized. The majority of gears are still used for the purpose of our individual mobility. Even with a change from gasoline and diesel-based fluids to renewable fuels there will be a need for high quality, silent and efficient gear boxes in the automotive sector and beyond.

Venkatesh *et al.* [29] studied the abrasive flow machining (AFM) is carrier a semi viscous material that holds the abrasive particles acts as a multi-point flexible tool (deforming tool) with tiny cutting edges in the abrasive flow machining. A new tooling for fixing bevel gears was designed and developed in such a way the abrasive media passage is thoroughly restricted to abrade the gear tooth surface only. The initial surface roughness of the as received bevel gears was measured 1.4 to 1.8 micrometers. Effects of few important parameters such as extrusion pressure, abrasive mesh size, processing time and media flow rate on finishing EN-8 steel bevel gears have been investigated. Taguchi orthogonal array was used to investigate the signal to noise ratio, main effect and parametric optimization. The extrusion pressure has the highest percentage contribution (73.71%) in surface finish improvement whereas 83.60 % in material removal rate. The tooth surface morphology gets improved with an increase in extrusion pressure.

Antoniadis *et al*. [30] studied and said gear skiving is nowadays an attractive alternative in gear finishing process. They investigate the possibility to simulate the rough cut of gears with various

cutting profiles. The consequent analytical determination of the finishing material removal and the final prediction of the cutting forces course. This algorithm is supported by a computer code that offers the aforementioned parameters, with the aid of a user-friendly graphical interface, built modular and object oriented.

Fuentes *et al.* [31] proposed and investigation a modified the geometry of helical gear drives finished by plunge shaving. The geometry of the shaver tooth surfaces that will shave the helical pinion and apply the proposed surface modifications has been developed. Geometric characteristics of the proposed shaver has been discussed. The necessary face width of the shaver and the conditions for avoidance of pointing and undercutting have been studied. Partial crowning of the pinion tooth surface has been proposed as the optimal design for a helical gear drive, yielding the lower contact stresses and transmission errors when errors of alignment occur.

Heinzel and Wagner [32] achieved a high surface finish with high shape accuracy an elastic bonded grinding wheels used. The gear grinding with elastic bonded grinding wheels manifest a very low risk of grinding burn as well as it is applicable on conventional gear grinding machines. Results of this process achieving good average roughness, shape accuracy and the use of fine finishing is about four times faster compared to vibratory finishing. The workpieces were pre-ground with a conventional vitrified grinding wheel. Subsequently, a finishing process with an elastic bonded grinding wheel was conducted.

Oobayashi *et al.* [33] firstly investigated the high-accuracy fine finishing of gear teeth surfaces using a water-lubricated tribo-chemical technique. A pair of shaved gears with rather low surface roughness was rotated in water lubricant for 30 min. The wear of the tooth surface proceeded layer-by-layer as a linear function of the number of mesh contacts and preferentially at the contact point or area. Operation noise from the gear pair rotation was drastically reduced to lower than about 10–15 dB compared to conventionally machined gear surfaces (30 dB in average), as a result of the wear of the tooth surface to form a best-fit profile. Comparing the gear shape accuracy by toff process with the other finishing process.

Lopatin and Plotnikova [34] developed mathematical modelling of teeth shaving and gridding at helical-bevel gears of involute-bevel gearings. Furthermore, the opportunity of doing these operations on machines for teeth processing in common bevel gears. Methods of helical-bevel gearing finishing processing, used for helical gear with change the contact angle of the processing tool. This allows to receive high precision of helical bevel gear, which is similar to bevel gearings.

Jolivet *et al.* [1] measured the topological features of teeth surfaces finished by grinding and power-honing were measured in three locations with a three-dimensional white light interferometer. The transmission system was composed of two identical loaded gears with one degree of freedom. The simulations of meshing gear changing the load on the teeth during meshing, their effect that geometry of the gear is unchanged, so the gear meshing stiffness becomes the main parameter influencing the transmission error. The numerical results show that the choice of the finishing process has an impact on the meshing stiffness and thus on the gear vibrations.

Jung *et al*. [5] used magnetorheological (MR) fluids for finishing is one of the most promising smart processes for the fabrication of ultra-fine surfaces, particularly three-dimensional millimeter or micrometer structures. In this study, mechanisms of material removal responsible decreases on high surface hardness workpiece by a wheel type MR finishing process is examined. This new process examined with theoretical and experimental studied.

Niranjan *et al*. [35] finished workpiece surface in nanometer range and obtain defect free surface using bidispersity magnetorheological polishing fluid (MRPF) by ball end magnetorheological finishing (BEMRF) tool is presented and achieved surface roughness up to the 20 nm. Vibration sample magnetometer (VSM) used for the magnetization of magnetic abrasives. Two grade of carbonyl iron particle (CIP) that is CS and HS grade. Their different composition studied in MR polishing fluid. Final conclusion of the research work is to 20 to 20 % of CIP and 15 to 20% silicon carbide (SiC) is a better composition for finishing of steel workpiece.

Degroote *et al*. [36] studied the magnetorheological polishing process is consisting of micronized magnetized carbonyl iron particle, nonmagnetic polishing abrasives and base fluid paraffin and water. Used this MR polishing fluid for finishing of glass. A mathematical model represents drag force, surface mechanical properties of glass, chemical durability of the glass, polishing abrasive size and concentration, the glass composition and MR fluid ph. Individual validate of all term and combination of all term to compared with the experimental data.

Barman *et al.* [37] studied the finite element analysis of magnetic field assisted finishing process. In this study magnetic field to the finishing zone is applied by the permanent magnet. Studied of the magnetic field distribution of the workpiece and tool surface. magnetic field move from tool to the workpiece surface observing using Ansoft Maxwell. On, the basis of this magnitude magnetic force calculated and surface roughness model was designed for the improvement in process.

Jha and Jain [38] developed magnetorheological abrasive flow finishing process was developed for the stainless-steel internal workpiece. In this study different combination of CIP and SiC particles are used to improvise the finishing quality. Magnetic force is studied at individual particle of CIP in the working gap. Studied of CIP chain structure in gap. Magnitude of fluid abrasive particles studied and calculated the effect of surface roughness.

Li *et al.* [39] surface roughness of the optical glass is obtaining 0.56nm. Magnetorheological finishing machine process is used to finish optical glass. Viscoplastic MR fluid was produced and applied at different variation of gradient magnetic field. Study of magnetic field in the working gap, variation of gap. Magnetorheological polishing fluid is better than the traditional finishing for glass finishing.

Sagbas [40] studied the response surface methodology (RSM) had been developed for the optimization study of process parameter. In this study RSM is used for the ball burnishing process of 7178 aluminum alloy. A rotatable central composite design with quadratic regression model prepares to predict surface roughness. For the validation of the report surface roughness model predict value compare with the experimental data. If the average surface roughness error is less than the predict experimental process parameter are suitable for experiment. If it is high variation than study need some new parameter which influencing the surface roughness. In the present study average error between experimental and predict value is 2.82%. That means the parameter decide for improvising surface roughness are enough.

Oktem *et al*. [41] developed better methodology to determine the optimum parameter leading to reduce the surface roughness. For the best optimization of the process response surface methodology is used to development of genetic algorithm. A forth order response surface model was developed for reduce the desired surface roughness. The genetic algorithm reduces the average surface roughness for the mold cavity process from 0.412μm to 0.375μm, almost 10% improvement. Therefore, the response surface methodology gives the optimum parameter for the material removal of surface roughness.

2.2 GAP IN LITERATURE

From the literature review, it has been found that number of problems shooting by the finished surface of gear during meshing in transmission. Reason for that the gear teeth are physical contact at high rpm and heavy loaded shaft driven. From the past work found that the number of operations is employed to reduce the surface roughness of gear teeth surface. Some of the traditional and non-

traditional method are used for finish. The traditional methods are produced temperature stress while finishing of gear teeth profile. These traditional methods are mostly for mass production industry, where less loads are applied during its operation. A highly finished gear profile with less stress required in helicopter and high-speed racing cars. Requirements these finishing levels are fulfilled by the non-traditional processes. Non-traditional method is achieved a surface roughness in nano-metric range. Most of the process are discussed above and observed during finishing there are less heat produced heat less on the gear teeth profile, that why chance of thermal stresses is negligible in the non-traditional finishing processes. A semi-finished or an unfinished gear causes a lot of problem as mentioned below.

- More gear noises
- Transmission error
- Thermal damage
- Power loss at gear teeth level
- High level of gear teeth stress
- More wear rate of teeth face
- At high load unwanted vibration
- Shape accuracy not attain
- Another surface imperfection
- DIN standard (gear standard) not maintain

Problem discussed above are encountered by the most of the non-traditional finishing process which are already developed for finishing gear teeth. But, some of the major problem like shape accuracy and thermal damage of gear teeth are stilled challenged for smooth operation of the gear teeth profile.

2.3 IMPORTANCE OF THE PROPOSED PROJECT IN THE CONTEXT OF CURRENT STATUS

From the literature review it was found that the traditional finishing processes are mostly used for finishing the gear tooth profile. Even after using these traditional finishing processes, the finished gear tooth surface gets many defects such as shape accuracy, dimensional accuracy, surface asperities and pitch circle deviation. The non-traditional finishing process are improving surface characteristics but their uses are less to finish the gear tooth profile. After finish gear tooth profile with non-traditional methods get some defects such as gear runout, gear lead and profile error and

take more time to finish the gear tooth profile. Therefore, to improve the further surface characteristics of gear tooth profile the MR polishing fluid-based finishing process is required. MR polishing fluid-based finishing processes are capable to improve surface finishing at nano-level. Therefore, the MR finishing process can be more useful to improve surface characteristics of gear tooth profile after the traditional finishing processes. In proposed research, the functional applications of gear tooth profile would be investigated before and after using the improved MR finishing process.

2.4 OBJECTIVES

- Design and development of magnetorheological fluid-based gear profile tool for finishing of gear teeth profile.
- To perform finishing of ferromagnetic gear teeth profile with the present developed process.
- Analysis of material mechanisms to understand the magnetic forces on abrasive particles and reduction of final surface roughness.
- Optimization of process parameters to obtain the minimum surface roughness
- Compare of DIN standard result as obtained by the present MR finishing process with the DIN standard result obtained by the existing processes for highly finished gear.

2.5 METHODOLOGY OF THE PRESENT RESEARCH

Embracing literature survey and followed by analysis of gaps, based on that a new process is designed known as magnetorheological fluid base finishing gear teeth profile finishing. After newly designed tool for gear teeth profile finishing, study of process parameters are performed. Analysis the behavior of the magnetorheological fluid while finishing of gear teeth and their effect on surface finish are performed. For the successful designed of a newly tool the proposed methodology is followed, shown in Figure 2.1.

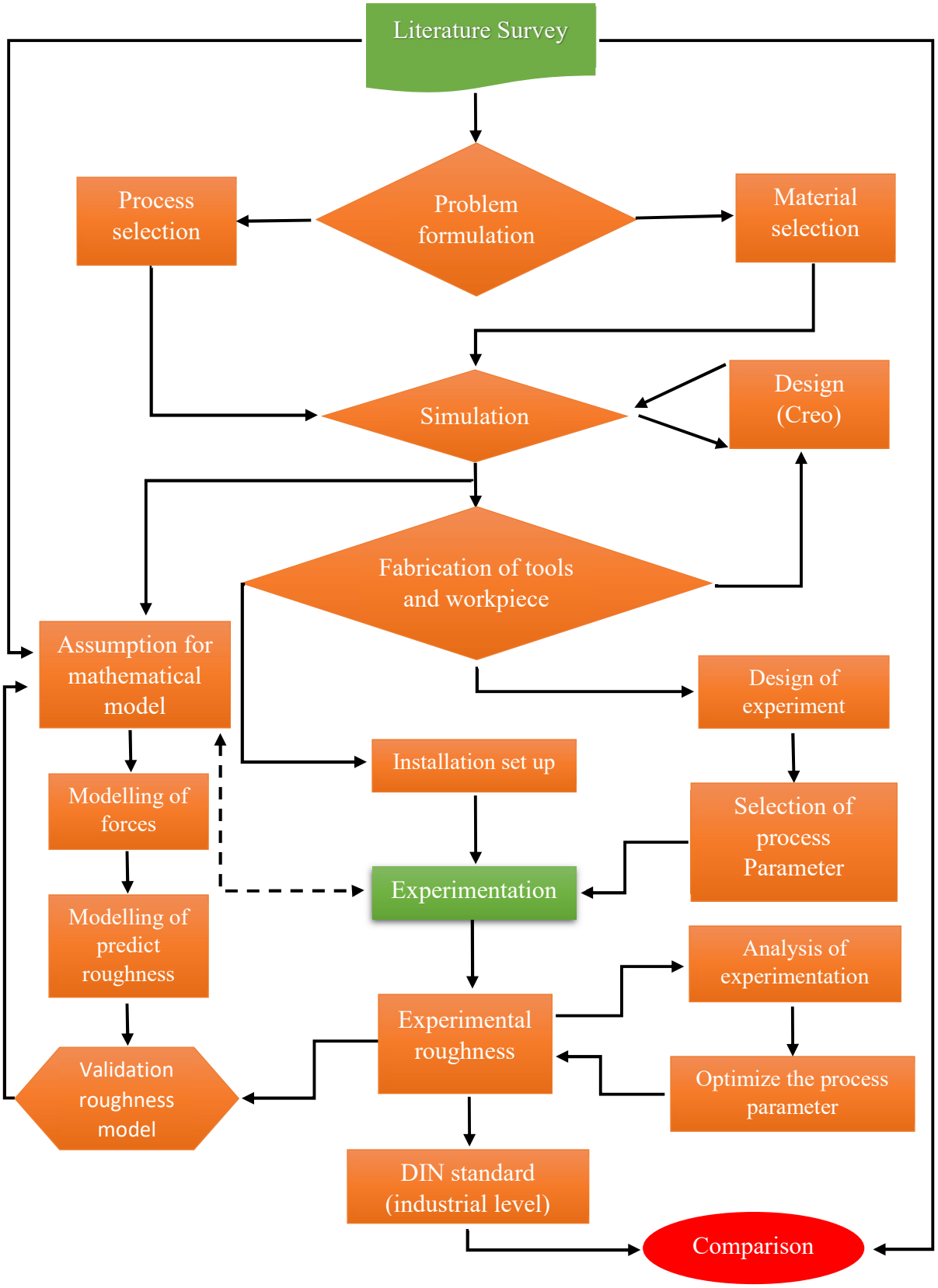

Figure 2.1 Methodology to carry out present research work

CHAPTER 3

DESIGN OF TOOL FOR FINISHING GEAR TEETH PROFILE

In automotive gear manufacturing industries, the big challenge is to satisfy the costumer in the fastest world. The manufacturing of gear box for high speed cars, bike and heavy vehicle in gear box many type of problem occurred as discussed in literature gap. With all these challenges the manufacturing industries have difficultly to produce quality of gear tooth with conventional machining. The non-conventional machine methods are suited best for producing the quality of gear teeth profiles. The literature review chapter revealed that the finishing of gear and their effect on the performance of gear box. Therefore, to meet the requirements of the precision finishing of the gear teeth profiles, a magnetorheological polishing fluid-based finishing tool is design and developed.

3.1 DESIGN OF MAGNETORHEOLOGICAL (MR) FLUID-BASED TOOL FOR GEAR TEETH FINISHING

As it has been studied in the previous chapter and found that there are number of tools design have been used for finishing of gear teeth profile. Also, a number of researches carried out based on MR fluid for superfinishing of ferrous and non-ferrous materials of different shapes. It has been proven that the finishing of ferromagnetic workpiece by MR fluid-based processes are very effective in term of nano-finishing and texture of the workpiece surface. The MR fluid-based finishing process is new concept for the finishing of gear profile effectively. The main aim of this MR fluid base process tool design is to perform more effective finishing and then compare the MR finished surface with the existing process used in industry. For the development of the tool firstly analyses the finite element analysis of tool, prepare final CAD model and fabricate the tool design. The tool is designed for the finishing of left and right sides of the gear teeth profile at a time by the stiffened MR polishing fluid. Based on the distribution of magnetostatic magnetic field, the tool has been designed. The tool is designed in such of way that the it can finish equally both sides of the gear teeth profile. The single teeth gear profile grinder is the best studied for designing and implementation of the novel magnetorheological fluid-based tool.

3.1.1 Electromagnetic Model for Finite Element Analysis

The finite element analysis (FEA) of magnetorheological polishing fluid tool for gear profile is performed in Maxwell Ansoft V13. The pre-CAD model of tool is made based on the earlier study shown in Figure 3.1. The magnetostatic FEA simulation has been performed to analysis the magnetic field with the tool tip surface along with the MR polishing fluid in the working gap and ferromagnetic gear teeth profile workpiece surface. Maxwell Ansoft V13 solve the electromagnetic field problem of a given model by assigning materials, boundaries and source conditions applying Maxwell equations over a finite region or space. To check the magnetic field for the feasibility of the tool. The Creo model was imported to the Maxwell Ansoft. The properties were assigned to each component of the model as given in Table 3.1 [42,43].

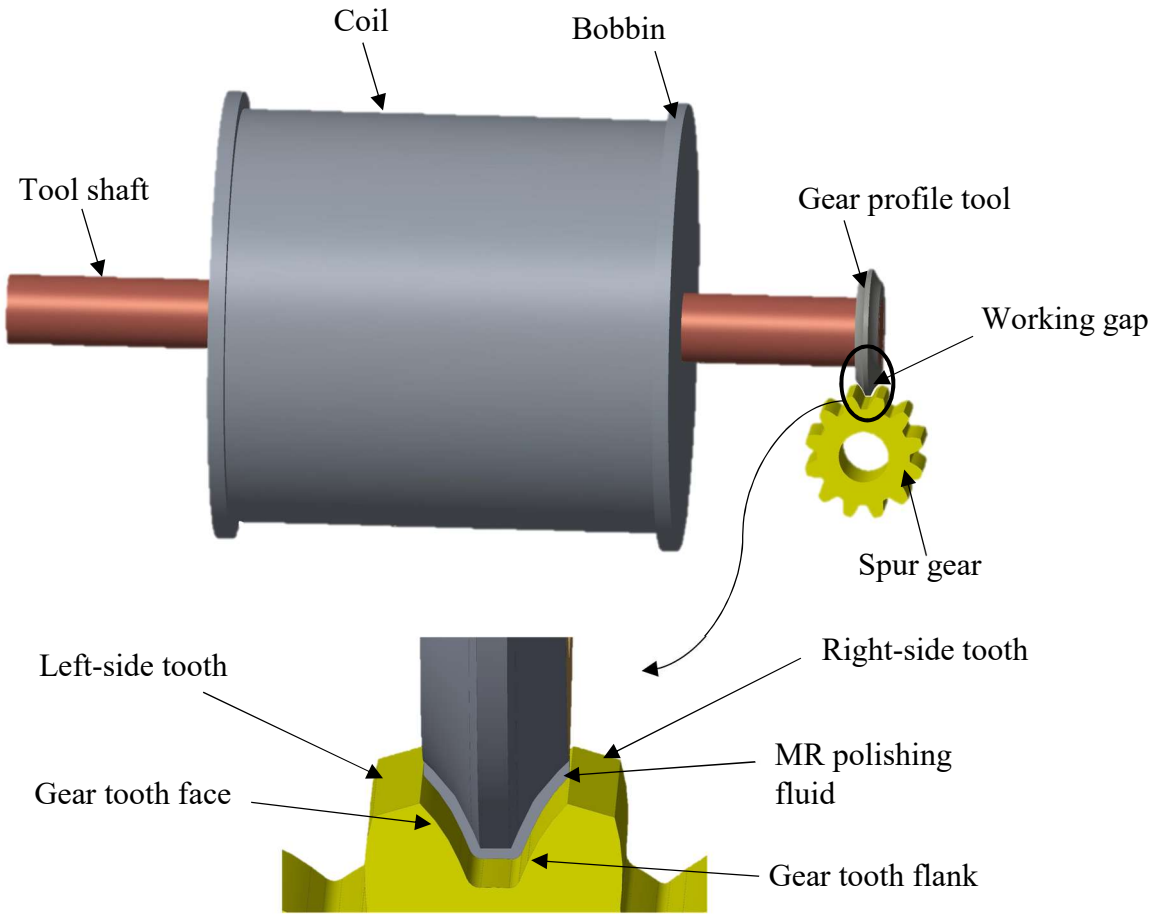

Figure 3.1 CAD model of electromagnetic tool along with MR polishing fluid and ferromagnetic spur gear workpiece prepared for magnetostatic simulation on Creo 3.0

Table 3.1 Input parameter for analyzing of magnetostatic magnetic field

Component	Material	Relative permeability
Bobbin	Aluminum	1
Coil	Copper	0.99
Rotating shaft	Mild steel	200
Finishing medium	MR polishing fluid	5
Ferromagnetic spur gear	EN24 steel	40

Environment was created around the model. Excitation assign to the current and current density in term of, number of turns per unit ampere. On, the basis of these parameters and their variable of level find the design of the electromagnet tool is performed. For FEA analysis of the ferromagnetic gear teeth surface with the gear profile tool, the permeability of the gear material is obtained. The gear material permeability plays major role as flowing of magnetic flux density from the tool surface and the workpiece surface though gap. From the literature review, industry experience and design of gear books it is found that the steel grade are mostly use for the manufacturing of gear [44, 45]. On the basis of the that assign the EN24 material with permeability 40 for the FEA of tool has been assigned. With these parameters, the effects of magnetic field in the working gap between the tool finish surface and workpiece surface has been analyzed. The tool number of turns per ampere is assigned as 5200. These 5200 turns per ampere can be expressed in many ways in term of gauge diameter of copper coil and current, basically its match the combination between the current and coil gauge diameter. When the gauge diameter increases resistance of the coil decreases, 20-gauge wire is best for producing electromagnet magnet [46]. The designing of the tool with workpiece, studied the magnetic flux density in the working gap. In workpiece gap, magnetorheological polishing fluid ribbon is putting of a 0.6mm thickness to check the flow of field distribution.

3.1.2 Magnetostatic Finite Element Analysis (FEA)

For distribution of magnetitic flux density at the gear teeth profile in working gap is shown in Figure 3.2. From this distribution of magnetic flux density, clearly visible that the highest value of magnetic flux density at the tool surface. Gear teeth workpiece has two profiles one over left-hand side is called left-side teeth profile and right-hand profile called right-side teeth profile.

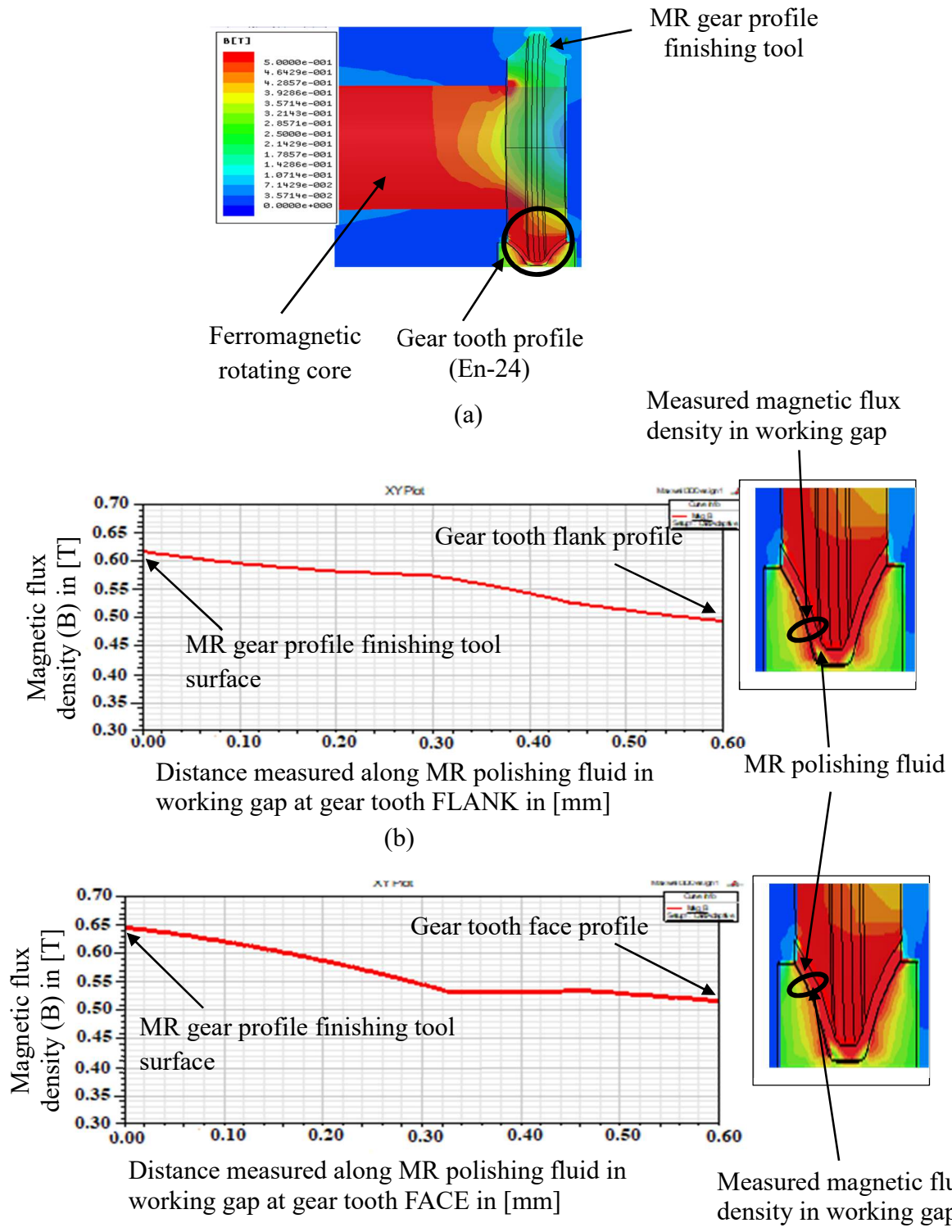

Figure 3.2 Magnetic flux density distribution in FEA (a) in working gap between the tool surface to gear tooth profile (side view), (b) 2D plot of magnetic flux density in working gap near flank of gear tooth profile and (c) 2D plot of magnetic flux density in working gap near face of the gear tooth profile

Figure 3.2(a) shows the distribution of magnetic flux density. It shows that the magnetic flux density is equally distributed on both teeth profiles. The involute gear teeth profile has two faces, one is gear teeth face and another is gear teeth flank. The shape of the gear face is curved shape and gear flank have a slight straight vertical shape. Figure 3.2(b) magnetic flux density at tool surface is 0.63T to the workpiece gear tooth flank surface is 0.53T. The magnetic flux density continuous decrease from tool surface to the gear tooth flank surface. This slope indicates that the magnetize iron particle in MR polishing fluid stuck at tool surface and they apply force to abrasive particle in MR polishing fluid to indent in the gear tooth surface. Figure 3.2(c), magnetic flux density at tool surface is 0.64T to the workpiece gear tooth face surface is 0.54T. This magnetic flux density slope again indicates the same thing which shows by the gear tooth flank. The FEA study at gear tooth face and flank conclude that the magnetic flux density at the tool surface and gear tooth surface is almost same and their magnetic flux density slope are almost same. It means that the uniformity of magnetic flux density at the gear tooth profile. The uniform magnetic flux density indicate that the material removal is same during MR fluid-based finishing.

The parallel flow of magnetic flux lines from the electromagnet passes through the solid core to gear profile tool than medium of magnetorheological polishing fluid to the gear tooth profile workpiece. This indicate that the magnetic flux is accumulated and high in the placing of direction towards the ferromagnetic workpiece. It is better for the strength of the iron particles chains in MR fluid. The distribution of the parallel magnetic flux line shown in Figure 3.3.

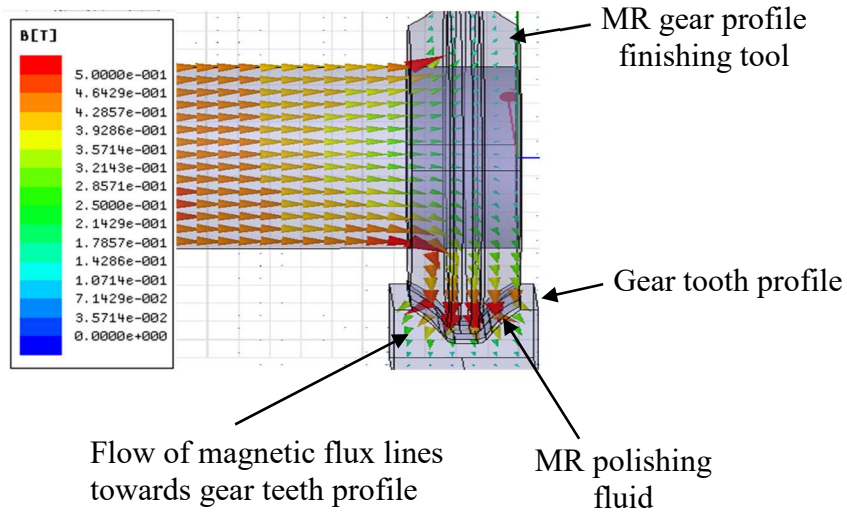

Figure 3.3 Parallel flow of magnetic flux lines towards gear teeth profile

The magnetic flux lines are stronger when ferromagnetic workpiece come in their contact due to that workpiece get magnetize. All the magnetic lines flow between the tool surface to the workpiece surface gap when MR polishing fluid comes in contact of magnetic lines in gap it gets magnetize. When higher the magnetization of MR fluid means iron particle in MR fluid are magnetize and the align iron particles are stuck to the tool surface. In the working gap higher, the magnetization means that higher the depth of indentation of abrasive particles in workpiece surface.

3.1.3 FEA of Right-Side Gear Teeth Profile

For the FEA of the right-side gear teeth profile, an inclined plane at the right-side profile shown in Figure 3.4(a). When the gear profile tool at the center of the gear teeth face width, at that point the distribution of the magnetic flux density on the right-side gear tooth profile shown in Figure 3.4(b). Magnetic flux lines from the center of the gear profile tool, distribution of magnetic flux on the gear teeth right-side profile as shown in Figure 3.4(c). The distribution of the magnetic flux from the center Y-axis of the tool, represent that the left side and right side from Y-axis equally magnetic flux distribute at 1mm on gear tooth surface. At the center of Y-axis gear profile tool, the magnetic flux density is 0.54T and distribution of magnetic flux density from the center Y-axis at 1mm distance is 0.47T. From this plotting of magnetic flux density shows that the field at the center is maximum. Moving from the right and left side at 1mm of distance is small decay. The distribution of magnetic flux density at right-side gear tooth profile signifies that the strong magnetic field in 2mm region. This strong magnetic field region shows that the almost equal amount of material removal in this area. This strong magnetic field improves the indentation of abrasive particle in MR polishing fluid to the workpiece surface. This strong magnetic field region helps to design of the outer diameter of the gear profile tool for the finishing of the gear profile teeth. For the finishing of the gear teeth with strong field distribution is give strength to the iron particle chain in magnetorheological fluid contact with gear teeth profile.

3.1.4 FEA of Left-Side Gear Teeth Profile

Gear teeth left-side profile FEA analysis is similar to the right-side teeth profile. Analysis an inclined plane at the gear teeth left-side shown in Figure 3.5(a). Similar to the right-side analysis, distribution of the field from the central Y-axis of the gear profile tool shown in Figure 3.5(b). Magnetic flux lines from the center of the gear profile tool, distribution of magnetic flux on the gear teeth right-side profile as shown in Figure 3.5(c).

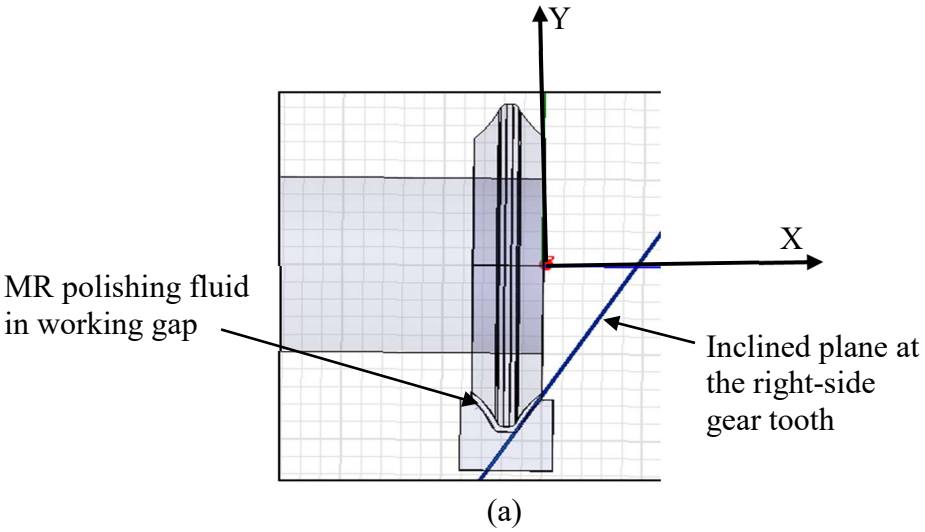

(a)

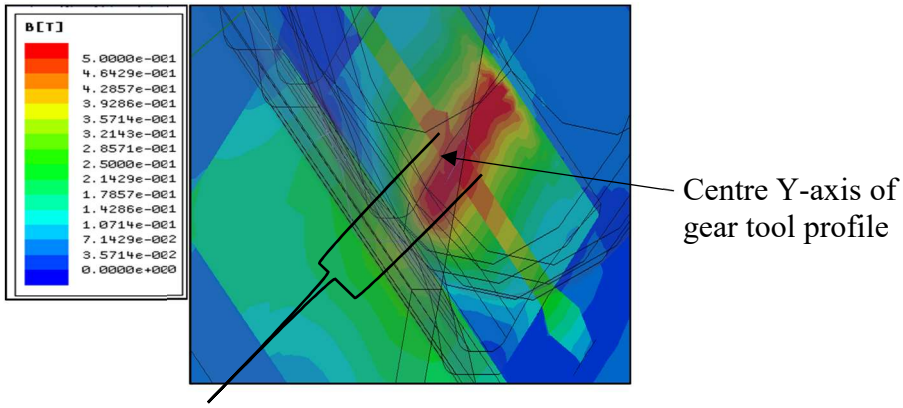

Distribution of magnetic flux density on the right-side of gear tooth profile surface

(b)

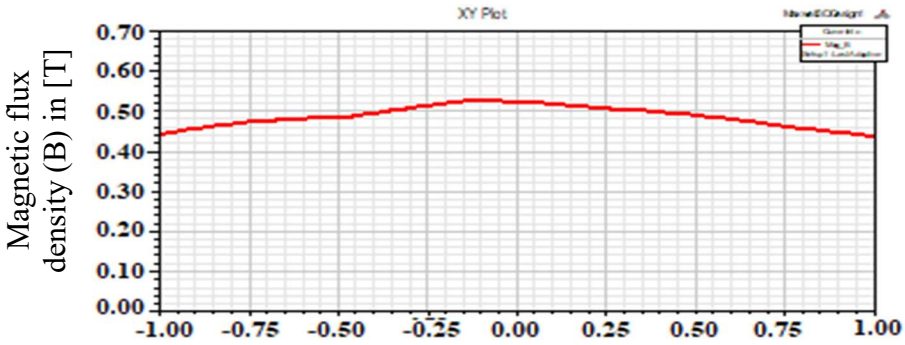

Distance measured at the center of gear profile MR finishing wheel tool

(c)

Figure 3.4 Magnetic flux density distribution at the right- side of gear teeth profile from the tool central Y-axis (a) inclined plane on right-side teeth, (b) distribution of magnetic flux density and (c) 2D plot of magnetic flux from center axis of tool

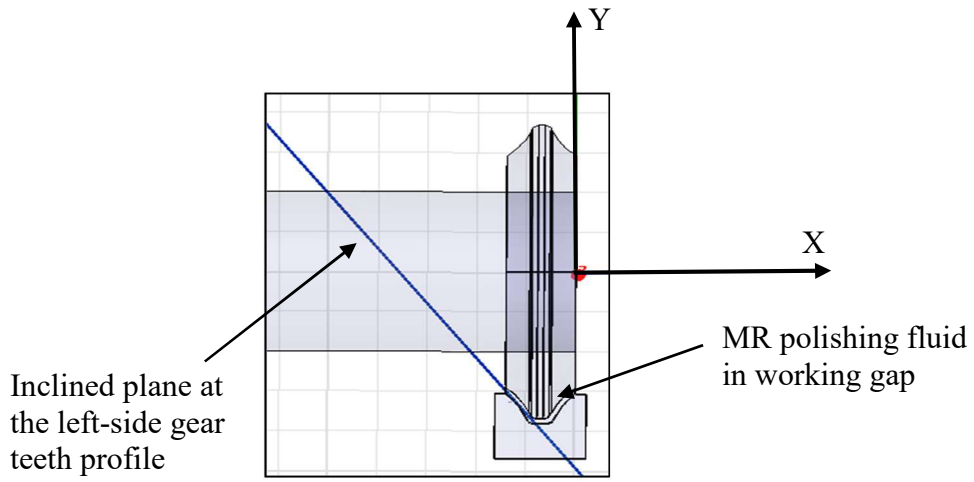

(a)

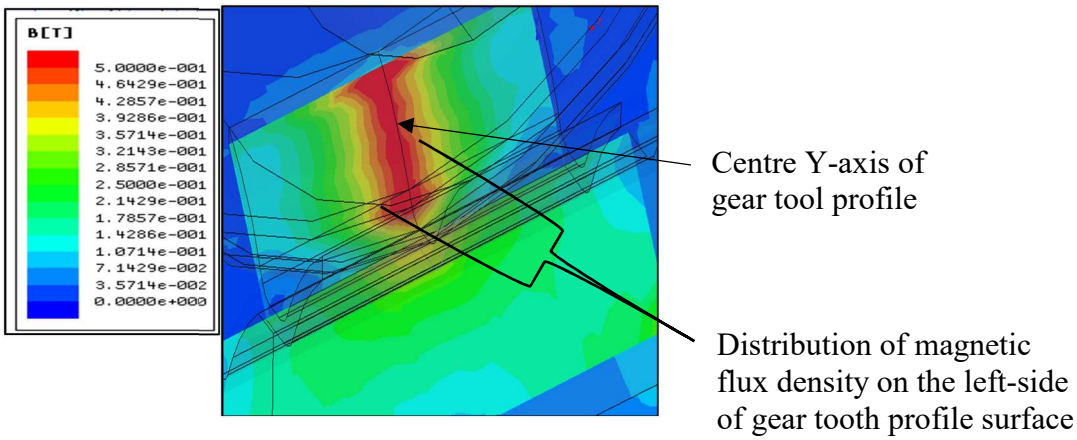

(b)

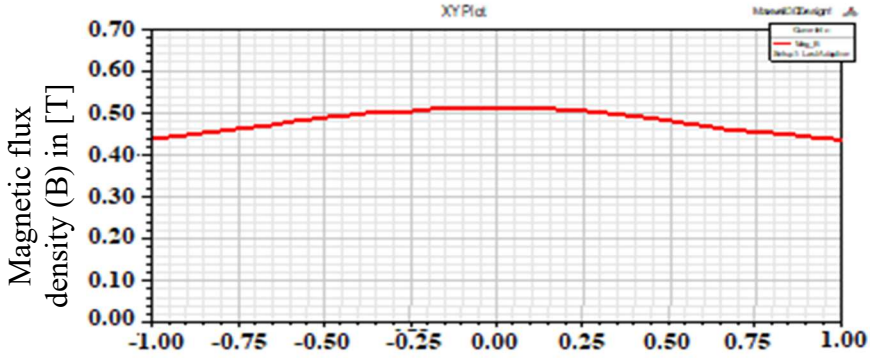

(c)

Figure 3.5 Magnetic flux density distribution at the left- side of gear teeth profile from the tool central Y-axis (a) inclined plane on left-side teeth, (b) distribution of magnetic flux density and (c) 2D plot of magnetic flux from center axis of tool

Magnetic flux density at the center y-axis is 0.53T and at 1mm distance from the center Y-axis is 0.46T graph shown in Figure 3.5(c). From this plotting of magnetic flux density shows that the field at the center is maximum. Moving from the right and left side at 1mm of distance is small decay. The distribution of magnetic flux density at left-side gear tooth profile signifies that the strong magnetic field in 2mm region. This strong magnetic field region shows that the almost equal amount of material removal in this area. This strong magnetic field improves the indentation of abrasive particle in MR polishing fluid to the workpiece surface.

Analysis of the magnetic flux density distribution on the right-side and left-side gear tooth profile shows that the higher magnetic flux region both sides is almost same at 2mm from the central Y-axis. It signifies that the during MR fluid-based finishing the material removal on both-sides is same. The distribution of magnetic flux density at gear tooth profile helps to find the outer diameter of the gear profile tool, working gap and shape of the gear tool profile

3.2 CAD MODELS OF FINAL MAGNETORHEOLOGICAL GEAR PROFILE FINISHING TOOL

On the basis of the FEA analysis of the gear profile tool and workpiece, its final design created in the PTC Creo 3.0 design software. In the designing of new set up for gear finishing, design the gear profile tool, indexing fixture, bobbin, cooling jacket and design of MR gear profile finishing tool. The design of programmable logic controller (PLC) and Human Machine Interface (HMI) is taken from the earlier designed ball end tool [46].

3.2.1 Design of Gear Profile Tool

Designing of gear profile tool has been performed on the basis of result obtained from the magnetostatic FEA. The curvature of the gear tool is similar to the gear teeth profile. So that the distribution of the magnetic flux density at the gear profile is uniform. The design of the gear profile is shown in Figure 3.6. For the finishing of the gear teeth profile, the tool profile is taken a 3-module spur gear. This gear tool profile used for finishing of the three-module gear teeth profile, with the stiffened magnetorheological polishing over its end profile surface.

3.2.2 Design for Holding Spur Gear Indexing Fixture

For the finishing of single gear tooth profile at a time, it is required to hold it tightly. To maintain the uniform working gap between gear profile tool to gear tooth profile an indexing of gear teeth has been done with provide uniform gap without any error.

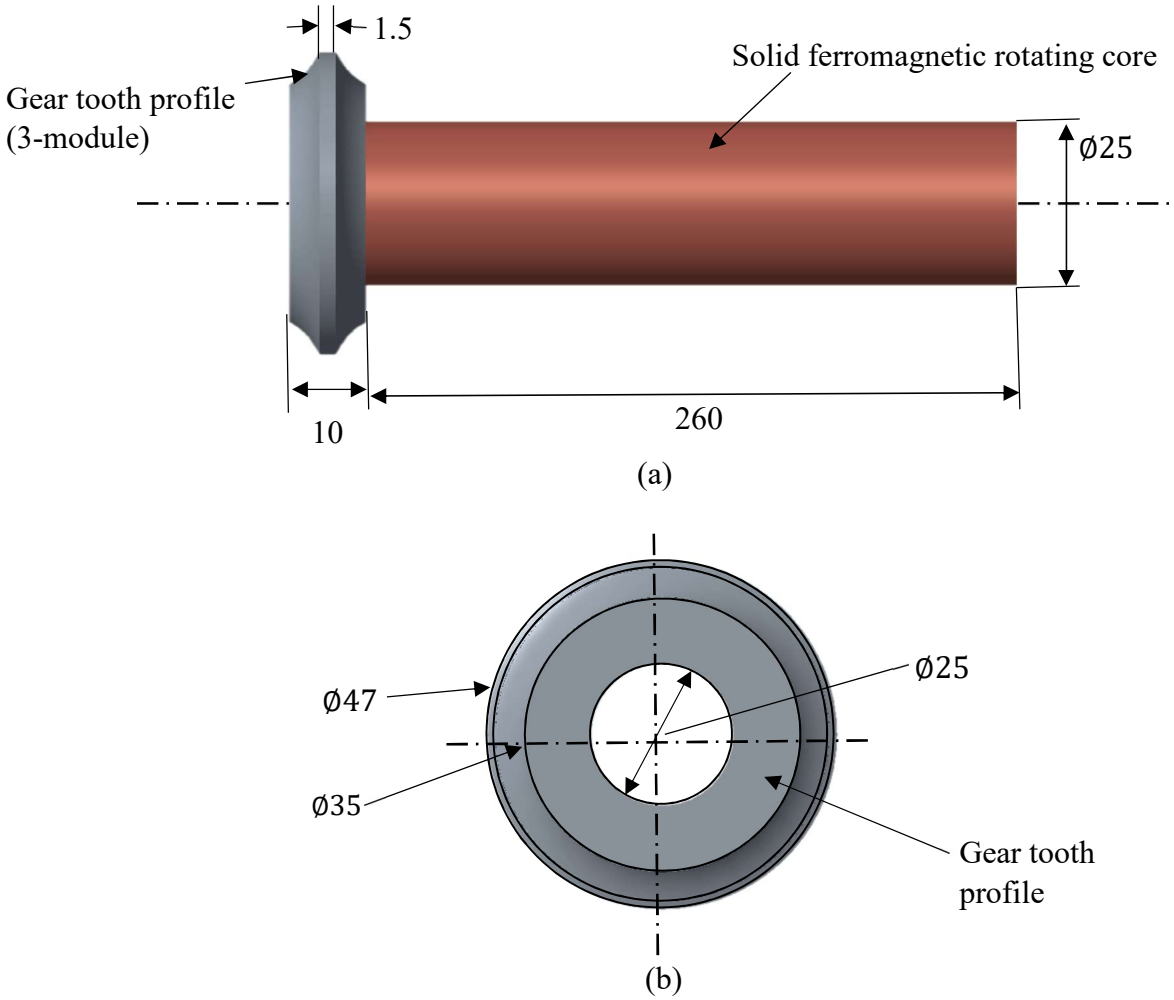

Figure 3.6 CAD model of the rotating core with gear wheel tool profile (a) from top view and (b) side view, all dimensions in (mm)

The manually indexing fixture design help in achieving final dimension accuracy. It is a replica of one big gear that is called indexing gear to the finishing of spur gear. The gear is having three module and involute profile. The indexing gear is employed on rotating shaft and indexing gear teeth profile tightly hold by the profile nob. The main function of the indexing gear teeth is to maintain the highly accurate shape of the spur gear teeth profile. For the indexing of the gear teeth, the indexing gear teeth is to be multiplication of natural number of finishing gear teeth. The important factor for the finishing is to be the setting of indexing with proper gap. The indexing fixture is shown in Figure 3.7, the indexing gear is manually operated. For the precision in finishing, need of skill operator. Otherwise, the precision hydraulic operated fixture is required which is costly.

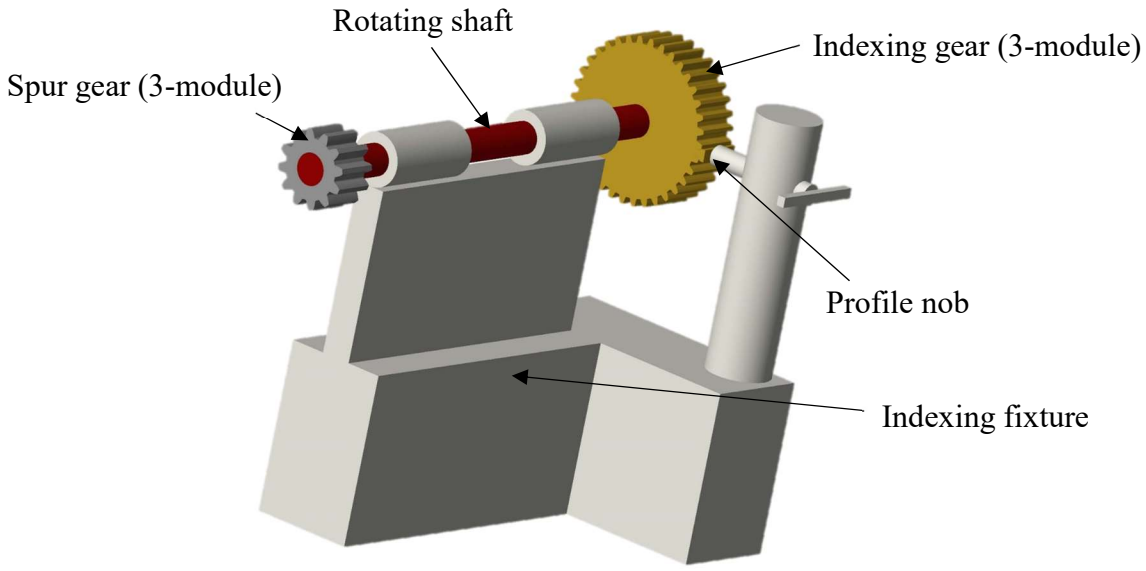

Figure 3.7 CAD model of indexing fixture for holding spur gear profile teeth during its teeth profile finishing

3.2.3 Design of Bobbin

Design of bobbin getting the idea from the analysis of the FEA analysis. Its decided that the number of turns copper coil is 2600, for that using 20-gauge wire. On the basis that design and dimension of bobbin shown in Figure 3.8. Aluminum material use for the bobbin is lighter in weight, easy to machine and that could restrict the magnetic field it has non-ferrous material. The thickness of bobbin sheet is not to take thin or not too thick, because that can work as a heat transfer while heating of coils.

3.2.4 Design of Cooling Jacket

Form the FEA analysis, design of cooling jacket depends upon heating of coils. Coil heating are mainly due to number of turns per ampere. When the coil gets start heating, it increases the temperature of atmosphere. So, the oil is circulating around the coil also start heating. To maintain the required atmosphere temperature, the coil should absorb the heat. On the basis of resistance operating temperature, the cooling jacket is designed, using the Equation 3.1 [47].

$$Rf = R20\,[1 + 0.00393(Tf - 20)] \tag{3.1}$$

Where

R20 = the resistance of the coil winding at 20℃

0.00393 = a physical constant of copper representing the change in resistance due to change in temperature

Tf = the operating temperature

Rf = the resistance at the operating temperature

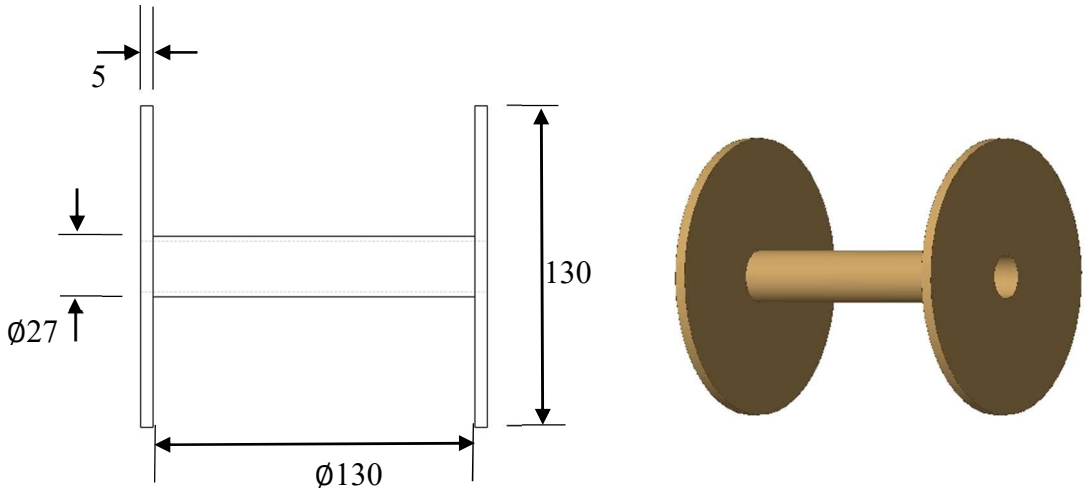

Figure 3.8 Bobbin (a) drawing and (b) CAD model, all dimension in (mm)

For design of cooling jacket, firstly find that the how much change of temperature when working with any period of cycle. For the cooling of electromagnet, different substances use like transformer oil, air cooling and fins cooling system. For the gear profile MR finishing tool, cooling of electromagnet transformer oil is used, it is good heat absorbent. On the basis of the resistance change at operating temperature, the suitable cooling jacket is designed. In cooling jacket inlet, valve for supply the chilled transformer oil and outlet of the jacket is returned in chilling plant. The design of the cooling jacket is shown in Figure 3.9. The cooling jacket is pressure fitted with bobbin.

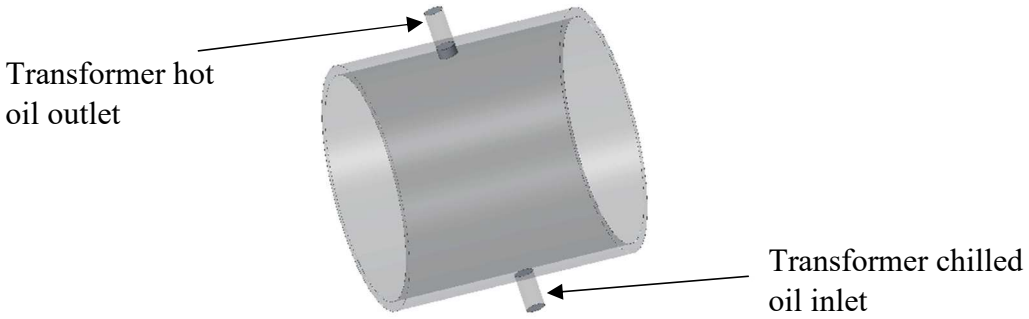

Figure 3.9 CAD model of cooling jacket over electromagnet

3.2.5 Design of MR Gear Profile Finishing Tool Setup

Design of overall assembly of electromagnet MR polishing fluid tool is shown in Figure 3.10. This tool set up is finishing of spur gear teeth profile using the MR polishing fluid. This set up is working with 3-axis PLC controlled system. Tool is mounted with the horizontal Z-axis and provide the tool reciprocation and tool rotation for the finishing of the single gear teeth profile. The spur gear workpiece is tightened with indexing fixture.

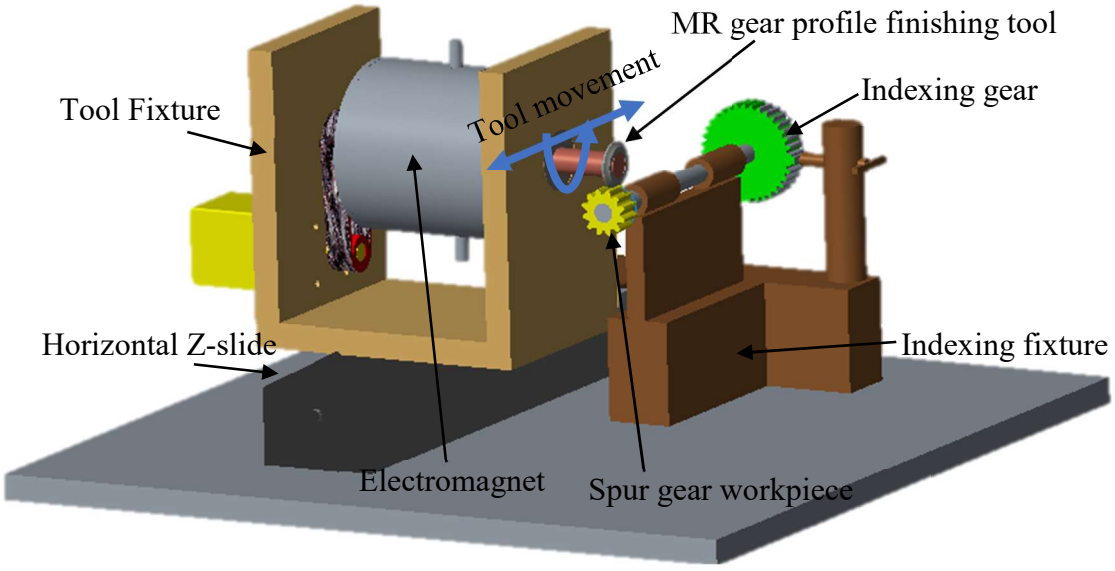

Figure 3.10 CAD model of MR gear profile finishing tool set up

After completing the design portion fabricating the all individual parts with precision. The fabrication assembly of gear profile MR polishing wheel tool is completed and is ready to use with practical application.

3.3 CONCLUSIONS

On the basis of result obtained from FEA as uniform magnitude of magnetic flux density, the magnetorheological gear profile finishing (MRGPF) tool is designed for finishing of ferromagnetic gear tooth profile. The following specific results are drawn.

- Magnetic flux density of gear profile tool surface was found as 0.63T and decrease towards the gear tooth profile face linearly to value of 0.54T.
- Magnetic flux density of gear profile tool surface was found as 0.64T and decrease towards the gear tooth profile flank linearly to value of 0.54T.
- The magnetic flux density uniform throughout the gear tooth profile surface, conclude that the magnetic flux density starts with tool surface at 0.63T average and decrease towards the gear tooth profile 0.54T average.
- Distribution of magnetic flux density on right-side gear tooth profile was found as 0.54T at the central Y-axis and decreasing with minor linear slope the magnetic flux density was 0.47T at 1mm distance on gear tooth profile from the central Y-axis.
- Distribution of magnetic flux density on left-side gear tooth profile was found as 0.53T at the central Y-axis and decreasing with minor linear slope the magnetic flux density was 0.46T at 1mm distance on gear tooth profile from the central Y-axis.
- The distribution of magnetic flux density on both sides of gear tooth profile shows that the higher magnetic flux density region on gear tooth profile both side is same.
- Decision of MR gear profile finishing tool outer diameter on the basis of the distribution of magnetic flux density on gear tooth profile and their magnetic flux density strength.
- Effective design of the cooling jacket to avoid the magnetic flux property change during working, found the better design of electromagnet using Equation 3.1 as per atmospheric condition.
- The designed indexing fixture ensure the high accuracy in working gap while finishing the gear tooth profile.

CHAPTER 4

THEORETICAL ANALYSIS OF SURFACE FINISHING OF GEAR TEETH PROFILE WITH THE NEWLY DESIGNED MAGNETORHEOLOGICAL GEAR PROFILE FINISHING (MRGPF) TOOL

Magnetorheological (MR) fluid-based finishing processes demand is increasing due to its ability in improvement on surface characteristics as compared to traditional finishing processes. Magnetic fluid-based finishing processes are precision finishing processes. In this chapter, the mechanism of material removal is analyzed in term of surface roughness model. This includes study the various parameters such as magnetic flux density, magnetic force, indentation force and then surface roughness model are affecting the performance of the process. Variation on the performance of the process is discussed for different machining parameters. The efficiency of the process in term of surface roughness reduction and time can be improved by studying the effect of various parameters. The unit cell structure is derived for the composition of MR polishing fluid used. The unit cell structure was used to calculate the active abrasive particles and the magnetic iron particles in the working gap. For validation of the theoretical calculation surface roughness values, the experiments were performed. Percentage error was calculated for the surface roughness results obtained in theoretical and experimental analysis.

4.1 COMPOSITION OF MAGNETORHEOLOGICAL (MR) POLISHING FLUID

For the finishing of workpiece material, rheological properties of the MR polishing fluid determine the finishing capability of the process [38]. The rheological behavior of the MR polishing fluid depends on the MR polishing fluid composition. The MR polishing fluid consists of iron particles, silicon carbide (SiC) abrasives and base fluid. The MR polishing fluid composition was selected on the basis of literature review for finishing of ferromagnetic workpiece and these are reported in Table 4.1 [48–52].

Table 4.1 Composition of MR polishing fluid

Components	% volume concentration
Iron particle of 500 mesh size	20
Abrasive particles of 800 mesh size	20
Carrier medium (Paraffin oil and AP3 grease)	60

The MR polishing fluid is applied on the tool surface in working gap to finish the workpiece surface. The magnetic flux density in the working gap results dipoles are formatting in iron particles. Dipoles of iron particle attract each other and form the chains structure in the region of magnetic flux density. The yield strength of the chain structure depends on the strength of magnetic field.

4.2 MAGNETIC FIELD BASE PRESENT FINISHING PROCESS

In this process, the gear tooth profile surface is finished by the use of magnetorheological gear profile finishing (MRGPF) tool. The rheological behavior of MR polishing fluid is controlled by the magnetic field. The working gap of 0.6mm is created between the tool surface and gear tooth profile surface with the help of gear indexing mechanism. The MR polishing fluid applied in the working gap and under the effect of magnetic field forms brush on the tool surface. For the finishing of gear tooth profile, the MRGPF tool is given rotation as well as reciprocation motion and gear workpiece are fixed its axis. Material is removed in the form of micro-chips due to the MR polishing fluid retained over the tool surface moves over the workpiece surface.

4.3 MECHANISM OF MATERIAL REMOVAL DURING GEAR TOOTH PROFILE FINISHING

The material is removed in the form of micro-chips by the interaction of abrasive particles and the gear tooth profile surface. To understand the mechanisms of material removal during finishing, it was necessary to study the forces acting on the abrasive particles. The mechanism of material removal is shown in Figure 4.1. Under the effect of magnetic field, the magnetic iron particles arranged themselves in the form of chains in the working gap. The iron particles move toward high magnetic field region towards tool surface whereas abrasive particles move toward region of lower magnetic field towards gear tooth profile surface. The abrasive particles which are responsible for the removal of workpiece material are known as active abrasives [38, 53]. The active abrasive particles get indented on the workpiece surface due to magnetic force applied on it, this is also known as indentation force (F_n) [54]. For the finishing of gear teeth profile with MRGPF tool is rotated and reciprocated about its axis shown in Figure 4.1(a). Tool rotation gives the tangential force (F_t) to the active abrasives while finishing of gear teeth profile. The F_t force is acting at θangle with respect to X-axis, reason for that the tool profile is curved. Tool reciprocation carry the active abrasive in the feed direction X-axis.

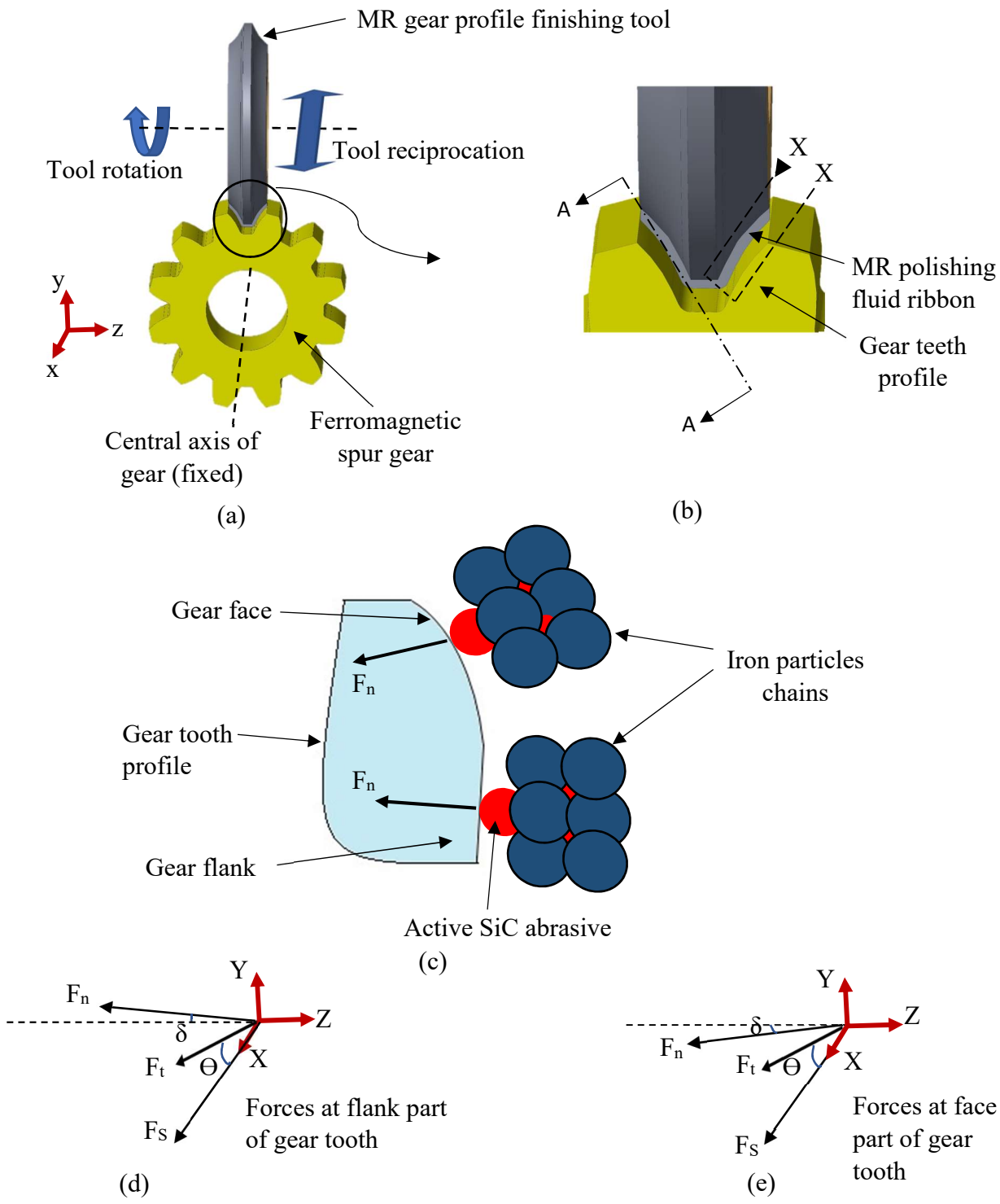

Figure 4.1 (a) Mechanisms of material removal and forces during finishing of gear teeth profile, (b) cross-sectional view (A-A) and (X-X) of intersection of MR fluid with gear teeth profile, (c) active Sic abrasive indent on gear tooth face and flank through the iron particle chains, (d) forces acting on gear tooth flank and (e) forces acting on the gear face during the finishing operation

This should be axial shear force (F_s) due to tool reciprocation motion on the workpiece roughness peaks. The active abrasive particles attain three kinds of forces during finishing viz. indentation force (F_n), shear force (Fs) and tangential force (F_t) [55].

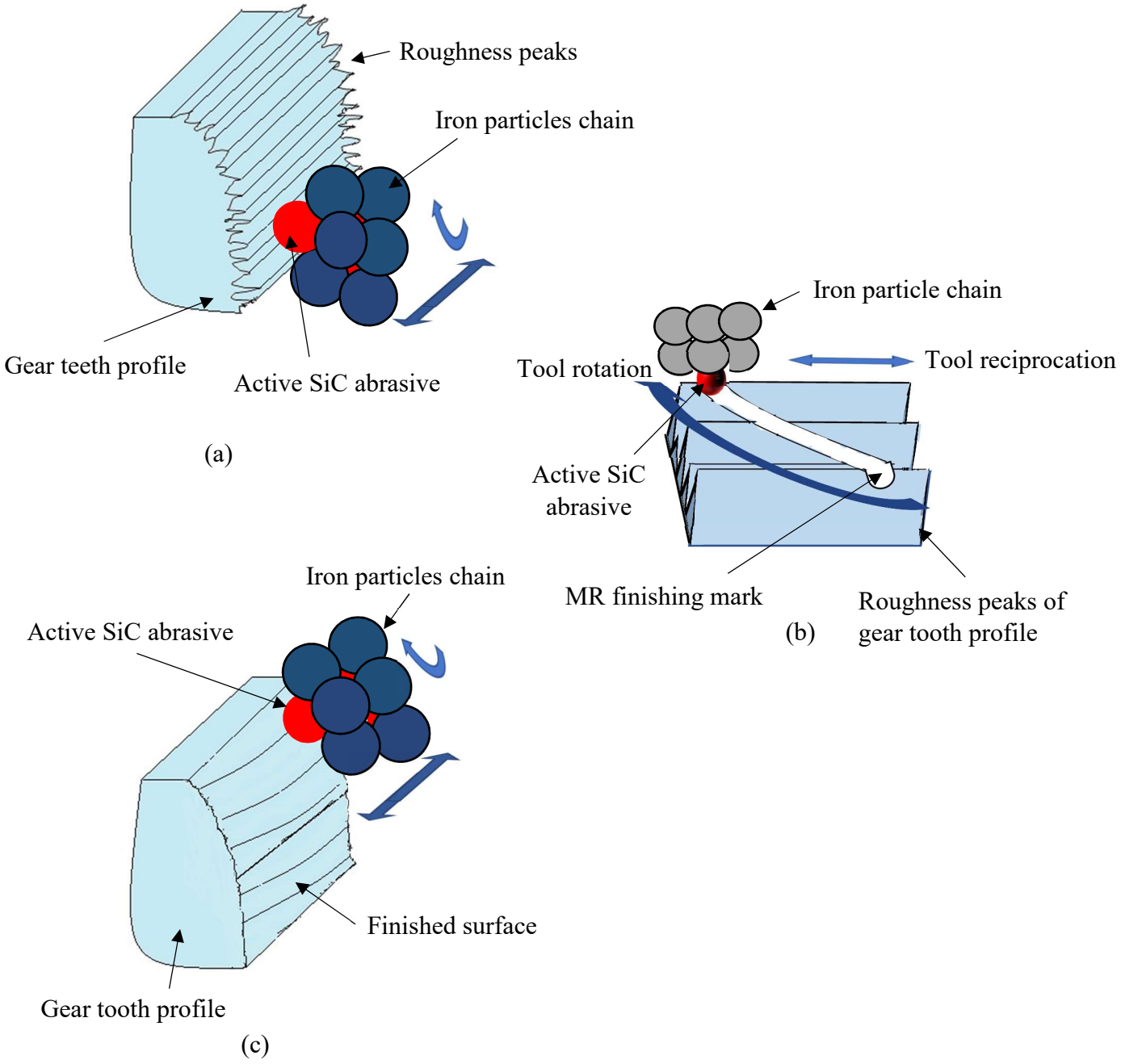

Figure 4.2 Magnified view of surface finishing gear teeth profile (a) surface peaks after gear grinding (X-X) view, (b) ploughing by single abrasive (A-A) view and (c) after MR finishing (X-X) view during MR finishing operation

Gear teeth profile is taken as involute profile, face of the gear teeth curved and flank of gear teeth is slight angle to the Y-axis. The indentation force and tangential force at an angle as per the shape of gear teeth flank, shown in Figure 4.1(d). Same as the shape of gear teeth face is shown in Figure 4.1(e).

The strength of magnetic flux density in working gap is responsible for yield strength of iron particles chains [54]. The MR polishing fluid iron particle chains yield strength provides the gripping to the active abrasives. If the chains yield strength higher than the resisting force of roughness peaks, active abrasive remove material on the workpiece surface. If it is not, then chains yielding take place and active abrasives slither over the roughness peaks [51, 56]. Figure 4.2(a) shows the finishing of gear tooth profile after gear profile grinder operation where roughness peaks and grinding lays aligned in almost horizontal straight lines. Figure 4.2 (b) shows, The active abrasive particles indent by the indentation force at some depth in workpiece surface. On the same time resultant force of (shear and tangential force) acted on the active abrasive, it starts ploughing of material on the workpiece surface. Figure 4.2(c) shows, super finished gear tooth profile after MR polishing fluid finishing take place on the gear tooth profile. For the super finished gear tooth profile was caused by the active abrasives indentation force and resultant force (shear and tangential force).

4.4 SURFACE ROUGHNESS MODEL FOR MAGNETORHEOLOGICAL FINISHING OF GEAR TEETH PROFILE

The mechanism of material removal in term of reduction in surface roughness can be analyzed by understanding various forces acting on the abrasive particle. Various forces play an important role in removal of roughness peaks. It was predicted that three forces are acting on active abrasives, though the theoretical analysis of reduction in surface roughness of the gear teeth profile. Normal force is responsible for indentation of abrasives on workpiece surface, tangential and axial shear forces are responsible for overcoming the shear strength of roughness peaks. The following assumption are considered to simplify the mathematical modelling.

- Throughout the working gap between the MRGPF tool surface with gear teeth face and flank for both the left and right side of gear teeth profile is same.
- Tangential and axial shear force are responsible for shearing of roughness peaks and magnetic normal force credit for indentation of active abrasives in workpiece.

- After grinding surface roughness was uneven but it was considered uniform surface roughness values.
- MR polishing fluid iron particle and SiC abrasive particle uniformly distributed throughout the working gap.
- Shape of SiC abrasive and iron particle are of spherical and uniform shape.
- Magnetic leakages and losses are neglected.
- MR polishing fluid not neutered by the nano-chips of workpiece, due to low material removal rate.

4.4.1 Unit Cell and Iron Particle in Chain Structure

It was assumed that the shapes of iron particles and abrasive particle are spherical in MR polishing fluid composition. After applying the magnetic field, the spherical shape iron particles are arranged in a chains form. Every chain of iron particle accumulated the spherical shape of abrasive particle. For calculating the number of iron particles in a chain, it was assumed that the unit cells are repeated in the MR polishing fluid column. So, the main focus was on to study the number of abrasives and iron particles in a unit cell.

4.4.1.1 Unit Cell

For the present study, MR polishing fluid concentration combination was taken as 20% of SiC abrasives, 20% of iron particles and 60% of base fluid (80% of heavy paraffin and 20% AP3 grease) [48-50]. The size of abrasive and iron particles can be calculated the kirk mesh Equation 4.1 [57].

$$\text{microns} = \frac{15000}{\text{mesh}} \tag{4.1}$$

It gives the approximately estimation of particle diameter in microns. The mesh number is increasing, diameter is decreasing, so kirk equation gives estimation. Using this equation find the 800-mesh size particle diameter 19μm, and 500-mesh size particle 30μm. These calculated values are used for the modelling of surface roughness.

The MR polishing fluid mixture having numbers of particles of abrasive SiC and iron particles. After calculating the diameter of the SiC and iron particle, calculate the number of particles in one-millimeter cubic volume cell is calculated using the Equation 4.2 [58].

$$N_p = \frac{V_f \times V_{one}}{V_p} \tag{4.2}$$

Where N_p is number of particles, V_f is the percentage of volume fraction of particles, V_{one} is the volume of one-millimeter cubic cell of MR polishing fluid and (V_p) volume of single particle. Using Equations 4.2, V_f of SiC particle is 0.2 mm^3 and V_{one} is 1 mm^3 and V_p is volume of one SiC particle is 3.59×10^{-6} mm^3. The number of SiC abrasive particles in 1 mm^3 is 55689. Similarly, the number of iron particles in 1mm^3 is calculated 14147.

For the study of MR fluid volume, one-millimeter of cubic cell MR polishing fluid V_{mr1}. To calculate the V_{mr1} using Equation 4.3 [58].

$$V_{mr1} = \frac{V_{one}}{N_p} \tag{4.3}$$

The volume of one-millimeter cubic cell V_{mr1} is based on the larger diameter size of the particles. The cube around an iron particle, volume accumulated in the that cell it is 7.06×10^{-5} mm^3. The edge length of the cube was found to be 41µm. The ratio of the number of iron particles to the number of SiC particles in one-millimeter cubic cell indicated number of iron and SiC particles in a cube. One of iron particle is accumulated with approximately four number of SiC particles. The placement of the abrasive particles in a cube depend on appropriate force applied by the single iron particle, it is assumed. Placement of particles in a cube any of two diagonals out of four diagonals of a cube. Adjacent cube having placement of abrasive particles in opposite diagonals. The diagonal length of the abrasive is consisting of one iron particles and two abrasive particles. One face of the cube is consisting of two abrasive particles. The indentation forced applied by single iron particles in cube on the active face of the cube abrasives. The hypothetical arrangement of the cube is shown in Figure 4.3 [38].

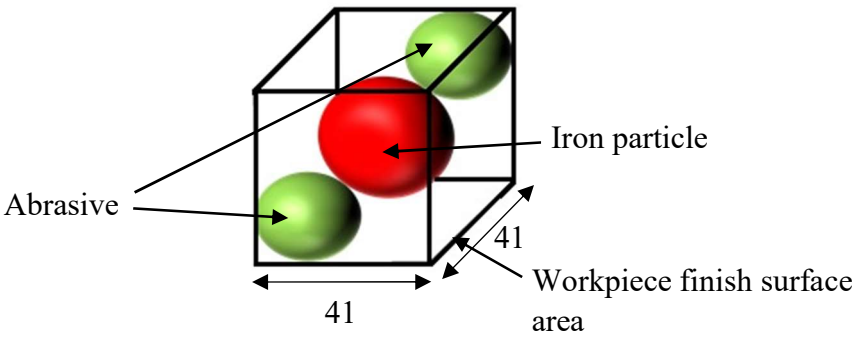

Figure 4.3 Configuration of SiC and iron particles in cube [38]

4.4.1.2 Magnetic Iron Particle in Working Gap

Working gap is fixed for finishing of gear teeth profile using MRGPF tool surface to gear tooth profile surface. The uniform working gap was taken as 0.6mm for finishing of ferromagnetic workpiece [52] shown in Figure 4.4. For the study of chain structure, edge length cube of iron particles of the consider that is having one iron particles. One of the iron particles in a cube, formation of the chain with the adjacent of the cube iron particles. Number of iron particles present in a chain calculated using Equation 4.4 [38].

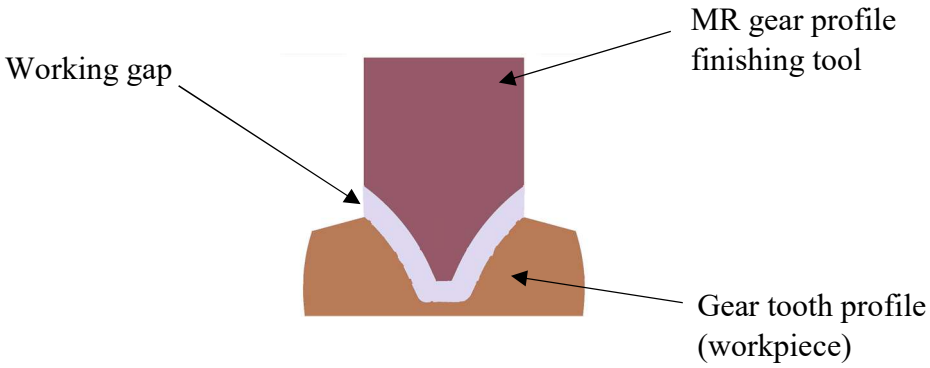

Figure 4.4 Schematic of working gap between tool surface and workpiece surface.

$$N_{cp} = \frac{\text{Working gap}}{\text{Edge length of cube}} \tag{4.4}$$

Where N_{cp} is number of iron particles formation of single chain in a working gap. Working gap was consider 0.6 mm and edge of cube length drive was 41 µm. Number of iron particles N_{cp} in a chain was found as 14.

4.4.2 Modelling of Magnetic Flux in Working Gap

To calculate the magnetic flux density in the working gap was calculated based on electromagnet design. The Bio-savart law was used to calculate the magnetic field strength. In this law, study of the one coil which is localized at the one end center of core at point 'O'. Number of turns wound in radial and longitudinal direction, to drive the filled requirement at the point P (x, y, z) as Shown in Figure 4.5 [47]. The radius of the existing coil 'a' and current 'I' flowing take a microsection of coil 'dl' to get the effect of change in magnetic flux density at point 'P'. Same as, take all three-

direction magnetic field strength shown in Equation 4.5, 4.6, 4.7 [59]. Consider same amount of current (2A) passes through the coil.

Calculated point 'P' was at the tool surface where x = 0mm and y =20.5, for right-side teeth z = 52.5mm and for left-side teeth z = 49.5mm, all these dimensions from the 'O' at the one end of center of core.

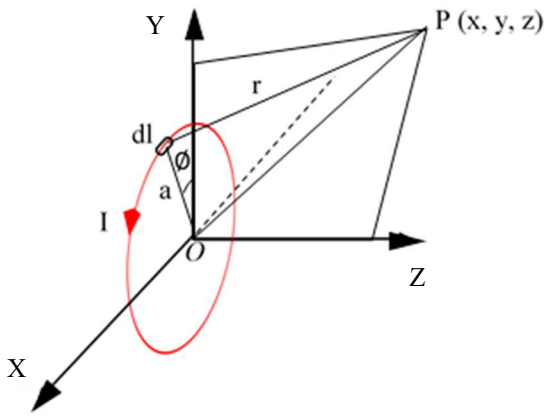

Figure 4.5 Representation co-ordinate of magnetic field strength at a point [47]

$$H_{xij} = \frac{I{a_j}^2}{4(R^2 + {a_j}^2)^{\frac{3}{2}}}\left[\frac{3xz_i}{(R^2 + a_j^2)} + \frac{105a_j^2x^3z_i}{8(R^2 + a_j^2)^3} + \frac{105a_j^2xy^2z_i}{8(R^2 + a_j^2)^3}\right] \quad (4.5)$$

$$H_{yij} = \frac{I{a_j}^2}{4(R^2 + {a_j}^2)^{\frac{3}{2}}}\left[\frac{3yz_i}{(R^2 + a_j^2)} + \frac{105a_j^2y^3z_i}{8(R^2 + a_j^2)^3} + \frac{105a_j^2yx^2z_i}{8(R^2 + a_j^2)^3}\right] \quad (4.6)$$

$$H_{zij} = \frac{I{a_j}^2}{4(R^2 + {a_j}^2)^{\frac{3}{2}}}\left[2 - \frac{3(x^2 + y^2)}{(R^2 + a_j^2)} + \frac{15a_j^2(x^2 + y^2)^2}{2(R^2 + a_j^2)^2} - \frac{105a_j^2(x^2 + y^2)^2}{8(R^2 + a_j^2)^3}\right] \quad (4.7)$$

Where H_{xij}, H_{yij}, and H_{zij} represent the component of magnetic field strength in x, y and z-axis, shown in Figure 4.5 [47]. Radius 'a_i' of the coil varying in the y direction and z_i direction.

$$R = \sqrt{x^2 + y^2 + z_i^2} \tag{4.8}$$

Where R is the resultant of the measuring magnetic field at point 'P' using Equation 4.8, in the free space at x, y and z_i from the point 'O'. Varying of the parameter 'a_i' and 'z_i' is calculated by Equations 4.9 and 4.10 [59].

$$a_j = a + jd_g\,, \quad 0 < j \leq n \tag{4.9}$$

$$z_i = z + id_g\,, \quad 0 < i \leq m \tag{4.10}$$

Where 'i' and 'j' represent number of coil turns in y and z direction 'n' is radially and 'm' is longitudinally respectively. For the present model of electromagnet 'n' vary from 0 to 37.5mm and 'm' vary from 0 to -130mm. To measure the magnetic field strength 'H' in the working gap tool surface and workpiece surface, from Equation 4.11 [60].

$$H = \sqrt{(H_{xij}^2 + H_{yij}^2 + H_{zij}^2)} \tag{4.11}$$

Where Hxij represent component of magnetic strength along x-axis, Hyij represent component of magnetic strength along y-axis, Hzij represent component of magnetic strength along z-axis as shown in Figure 4.5.

The magnetic field present in the working gap is responsible for magnetization of ferromagnetic particles. Magnetic flux density (B) at any point in a working gap calculated by using Equation 4.12 [47], [61].

$$B = \mu_0(H + M) \tag{4.12}$$

Where μ_0 is relative permeability of air in free space, H is magnetic strength at a point, M is magnetization of a particles. Magnetization of iron particle calculate from B-M curve of iron particles. In this research, the ferromagnetic materials are tool core mild steel, workpiece EN24 and MR polishing fluid having relative permeability of 200, 40 and 5 [46], [52] respectively.

Calculation of magnetic field strength and magnetic flux density at every iron particle in working gap. The left-side gear teeth profile variation of magnetic field and magnetic flux density given in Table 4.2 and right-side gear teeth profile variation at a point in Table 4.3 using Equation 4.11 and 4.12. The left-side and right-side of gear teeth profile calculated almost having same magnetic flux in the working gap both-sides.

Table 4.2 Magnetic field strength and magnetic flux density in working gap of left-side gear tooth profile

Distance from tool surface to workpiece (Working gap) in (mm).	Magnetic field strength (H) in (A/M)	Magnetic flux density (B) in (T)
0.041	1759.88	0.538
0.082	1754.62	0.537
0.123	1749.36	0.535
0.164	1744.10	0.534
0.205	1738.84	0.532
0.246	1733.58	0.530
0.287	1728.32	0.529
0.328	1723.06	0.527
0.369	1717.80	0.525
0.410	1712.54	0.524
0.451	1707.28	0.522
0.492	1702.02	0.521
0.533	1696.76	0.519
0.574	1691.50	0.517
0.615	1686.24	0.516

The magnetic flux calculated values at left-side gear tooth profile comparison with the magnetostatic FEA analysis in the working gap shown in Figure 4.6, Both the graph had almost linear curve. Theoretical analysis data is lesser than the FEA analysis, with 17% of error. In theoretical analysis centrifugal force not consider and atmospheric environment not consider. Theoretical linear equation for variation of magnetic flux density in working gap from left-side gear tooth profile is shown in Equation 4.13.

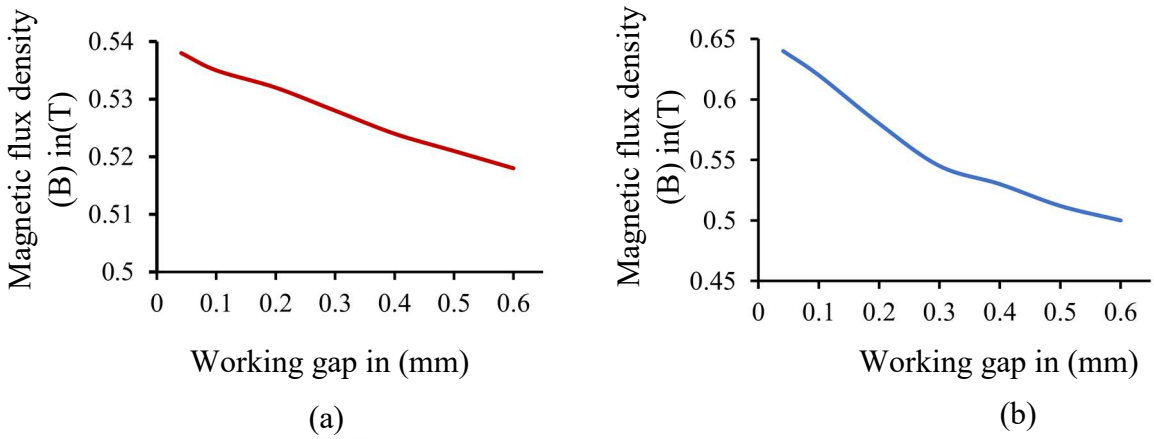

Figure 4.6 (a) Theoretically calculated variation of magnetic flux density in working gap of left-side gear tooth profile and (b) variation of magnetic flux density obtained from the finite element analysis with the MR polishing fluid and gear tooth profile workpiece

Table 4.3 Magnetic strength and magnetic flux in working gap of right-side gear teeth profile

Distance from tool surface to workpiece (Working gap) in mm.	Magnetic strength (H) in (A/M)	Magnetic flux (B) in (T)
0.041	1721.02	0.526
0.082	1714.79	0.525
0.123	1708.56	0.523
0.164	1702.33	0.521
0.205	1696.10	0.519
0.246	1689.87	0.517
0.287	1683.64	0.515
0.328	1677.41	0.513
0.369	1671.41	0.511
0.410	1664.95	0.509
0.451	1658.72	0.507
0.492	1652.49	0.505
0.533	1646.26	0.504
0.574	1640.03	0.502
0.615	1633.80	0.500

Same as the right-side of the gear teeth profile comparison of the FEA and the calculated data in Figure 4.7, and linear equation obtained is given in Equation 4.14. The graph plotted between them have an error of 16%. This error is considerable for calculating the magnetic force. The B_{zl} and B_{zr} are the values of variation in magnetic flux density in working gap from the at left-side and right-side of gear teeth profile towards the gear tooth profile surface.

$$B_{zl} = 0.540 - 0.0016z \tag{4.13}$$

$$B_{zr} = 0.528 - 0.0019z \tag{4.14}$$

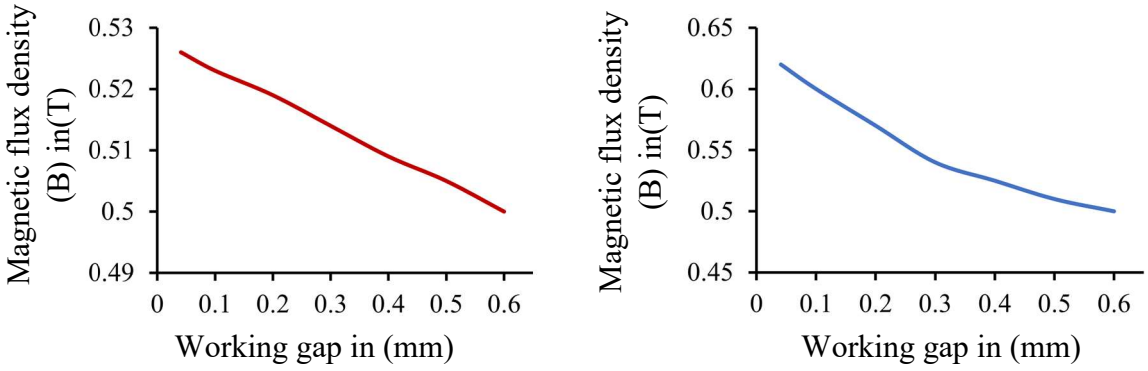

(a) (b)

Figure 4.7 (a) Theoretically calculated variation of magnetic flux density in working gap of right-side gear tooth profile and (b) variation of magnetic flux density obtained from the finite element analysis with the MR polishing fluid and gear tooth profile workpiece

4.4.3 Calculation of Magnetic Force on Iron Particle and Indenting Force on an Abrasive Particle

When the iron particles come under the effect of magnetic field exerts normal force on active abrasive particles. The indentation force of the active abrasive applied on to the workpiece surface is caused normal force applied by the iron particles. The indentation force which is responsible for finishing of the workpiece surface. The magnetic force acting on an iron particle is calculated by using Equation 4.15 [62].

$$F_n = \frac{m_{IP}\chi_m B(z)\frac{dB(z)}{dz}}{\mu_0} \tag{4.15}$$

Where F_n is the normal magnetic force exerted by the iron particles, m_{IP} is the mass of iron particles, χ_m is the mass of magnetic susceptibility, μ_0 is the magnetic permeability of free space, B(z) is variation of magnetic flux along the working gap, H is the magnetic field strength.

m_{IP} is the mass of iron particle = 2.3989×10^{-11} kg

μ_0 is the magnetic permeability of free space = $4\pi \times 10^{-7}$ (N/A^2)

Using these data calculate mass of susceptibility at every iron particle in a single chain, in the working gap. Putting the value of (B) from Figure 4.8 in the Equation 4.16 [63].

$$\chi_m = \frac{\mu_0 M}{B} \tag{4.16}$$

Where the value of (B) plotting from the linear curve left-side (Equation 4.13) and right-side (Equation 4.14) of the gear teeth profile. The magnetization of iron particle (M) is calculated from the B-M curve of CS grade iron particles, shown in Figure 4.8 [51].

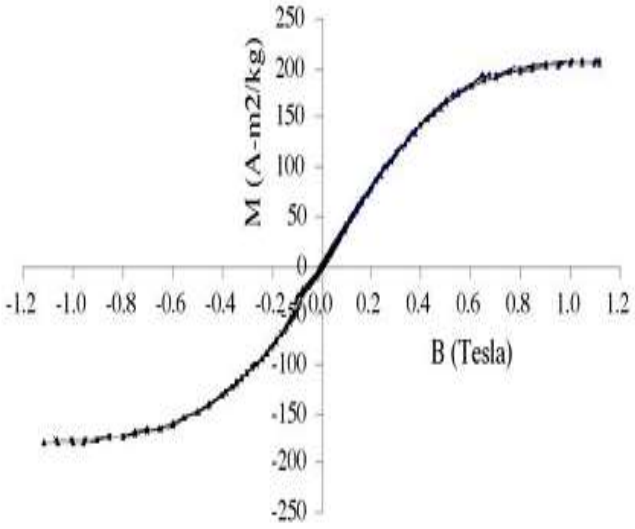

Figure 4.8 Representation of B-M curve for CS grade iron particle [51]

From all these data calculate the indentation force of active abrasive in a single chain using the Equation 4.17 [63]. These results are reported in the Table 4.4 and Table 4.5 respectively.

$$F_n = \sum_i^n \frac{m_{IP} B_i \left(\frac{dB(z)}{dz}\right)_i \chi_i}{\mu_0} \tag{4.17}$$

Where B_i is magnetic flux along every iron particle in a chain, χ_i is mass of susceptibility at individual iron particle in a chain and 'n' is the number of iron particle in a chain as value is 14.

From Table 4.4, calculate the mass of susceptibility at every individual iron particle in a iron particle chain. The indentation force exerted by the individual iron particle in the working gap of right-side gear teeth profile is reported in Table 4.4. The indentation force acting is on active abrasive particle to be sum of every individual iron particle in a chain.

On the right-side gear teeth profile indentation force was found as 8.58×10^{-11} N. Also, same as above left-side gear teeth profile indentation force at active abrasive by the single chain of the iron particles on an active abrasive particle data given in Table 4.5. The left-side gear teeth profile indentation force was found as 7.40×10^{-11} N. The indentation force difference between left and right-side is very small and take it negligible difference. Therefore, the indentation force is taken as 7.40×10^{-1} N for theoretical analysis of magnetic flux.

Table 4.4 Magnetic force acting on iron particles at working gap of right-side profile

Distance from tool surface to workpiece surface (Working gap) in mm.	Magnetic flux density (B) in (T)	Mass of magnetic susceptibility $(\chi_m) \times 10^{-4}$ (m^3/kg)	Magnetic force $F_n \times 10^{-12}$ N
0.041	0.526	3.79	-5.98
0.082	0.525	3.78	-5.95
0.123	0.523	3.76	-5.91
0.164	0.521	3.75	-5.87
0.205	0.519	3.74	-5.83
0.246	0.517	3.73	-5.80
0.287	0.515	3.71	-5.76
0.328	0.513	3.70	-5.72
0.369	0.511	3.69	-5.68
0.410	0.509	3.68	-5.64
0.451	0.507	3.66	-5.61
0.492	0.505	3.65	-5.57
0.533	0.504	3.64	-5.53
0.574	0.502	3.63	-5.49
0.615	0.500	3.62	-5.46

4.5 CALCULATION OF THEORTICAL SURFACE ROUGHNESS

4.5.1 Calculation of Material Removal by Single Active Abrasive

The indentation force (F_n) acting on an active abrasive particle was calculated in the previous section and Rs is the resisting force of workpiece material. Two indentation force was calculated, left and right-side gear teeth profile which are almost same. For further study, the left-side of the indentation force 7.40×10^{-11} N was taken. This indentation force causes of depression by active abrasive on the workpiece surface as Shown in Figure 4.9 [38]. Brinell hardness of the workpiece is matter, how much active abrasive indent. For present study hardness of the workpiece 62HRC taken, measure on Rockwell hardness tester.

Table 4.5 Magnetic force acting on iron particles at working gap of left-side profile

Distance from tool surface to workpiece (Working gap) in mm.	Magnetic flux density (B) in (T)	Mass of magnetic susceptibility $(\chi_m) \times 10^{-4}$	Magnetic force $F_n \times 10^{-12}$N
0.041	0.538	3.80	-5.15
0.082	0.537	3.79	-5.11
0.123	0.535	3.78	-5.08
0.164	0.534	3.77	-5.05
0.205	0.532	3.76	-5.02
0.246	0.530	3.75	-4.99
0.287	0.529	3.74	-4.96
0.328	0.527	3.73	-4.92
0.369	0.525	3.72	-4.89
0.410	0.524	3.71	-4.86
0.451	0.522	3.70	-4.83
0.492	0.521	3.69	-4.80
0.533	0.519	3.67	-4.76
0.574	0.517	3.66	-4.73
0.615	0.516	3.65	-4.70

Brinell model is used to calculate the indentation in the workpiece. Using Brinell hardness number calculate the indentation diameter, calculate using Equation 4.18 [63].

$$H_{BHN} = \frac{2F_n}{\pi D_a \left(D_a - \sqrt{D_a^2 - D_i^2} \right)} \tag{4.18}$$

Where F_n is the indentation force on the abrasive particles, D_a is the diameter of abrasive particles, D_i is the indentation diameter, H_{BHN} is Brinell hardness number measured in kgf/mm^2.
For $F_n = 7.40 \times 10^{-11}$N, $H_{BHN} = 658$ Kgf/mm^2 (EN24 steel), $D_a = 19$µm.
The value of D_i is calculated using Equation (4.18) as $D_i = 1.2083 \times 10^{-10}$ m.

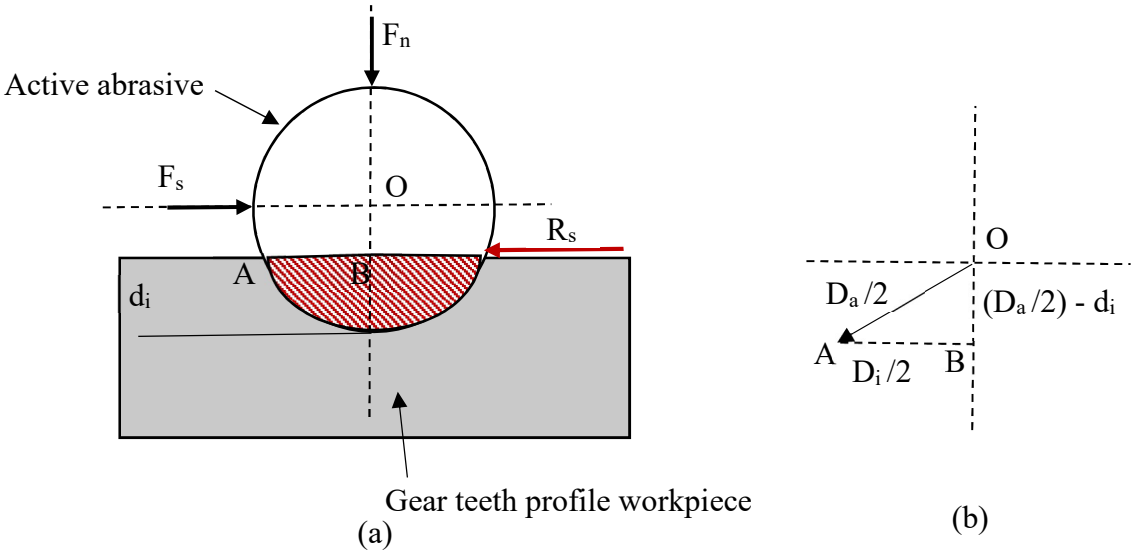

Figure 4.9 (a) Forces acting on active abrasive particle in MRGPF tool process and (b) calculation of d_i [38]

From Figure 4.9 (b) In ΔOAB, depth of indentation by active abrasive particle calculated using Equation 4.19 [38].

$$d_i = \frac{D_a}{2} - \frac{1}{2}\sqrt{D_a^2 - D_i^2} \tag{4.19}$$

For $D_a = 19$ µm, putting the calculated indentation diameter (D_i) value above, the value of depth of indentation in workpiece (d_i) is calculating using Equation 4.19 as 1.39×10^{-16} m.

From the Figure 4.8(a), the area of groove generated by abrasive particle on workpiece surface can be calculated by using Equation 4.20 [38], [63].

$$A_1 = \frac{D_a^2}{4}\sin^{-1}\frac{2\sqrt{d_i(D_a - D_i)}}{D_a} - \sqrt{d_i(D_a - D_i)}\left(\frac{D_a}{2} - d_i\right) \quad (4.20)$$

Where putting all the calculated values, diameter of abrasive (D_a) and depth of indentation (d_i), the value of area of groove A_1 is 4.88×10^{-16} m.

So, the volume removed by single active abrasive calculate by using Equation 4.21 [38].

$$V_a = A_1 \times (1 - \frac{R_a^i}{R_a^o}) \times L_w \quad (4.21)$$

Where A_1 is area of cross-section of groove, L_w is length of the workpiece, R_a^o is the initial surface roughness, R_a^i is the surface roughness in the i^{th} cycle.

4.5.2 Number of Active Abrasive

The abrasive particle which are responsible for surface finishing are known as active abrasives. The active abrasives region has been decided on the basis of the distribution magnetic flux density at the tool surface to the workpiece surface. Magnetostatic finite element analysis with workpiece was performed and their result was already discussed in 3.1.2 section. It was found that for both the left and right-side gear tooth profile having a same magnetic flux density. The details of active abrasives region are shown in Figure 4.10. The magnetic flux density was representing on the gear lead line, it was strong up to 1mm of contact that is a to D distance. In the active abrasive region magnetic flux varies from 0.52T to 0.45T. For the calculation of the active abrasive region DEFG shown in Figure 4.10, calculate using Equation 4.22.

$$\text{Active abrasive area DEFG} = [(ac \times aD) \times 2] \ \text{mm}^2 \quad (4.22)$$

To calculate the length of a to c using CMM machine and found that the 6mm. The distance of a to D was taken as 1mm. Therefore, from Equation 4.22 calculate area DGFE was 12 mm^2.

From Section 4.4.1, it was found that there are two active abrasives interacting with workpiece surface and are placed at corners of the unit cell of length 41µm.

The total number of active abrasives calculating using Equation 4.23.

$$N_{ab} = \frac{\text{Active abrasive area DEFG} \times 2}{A_{cf}} \quad (4.23)$$

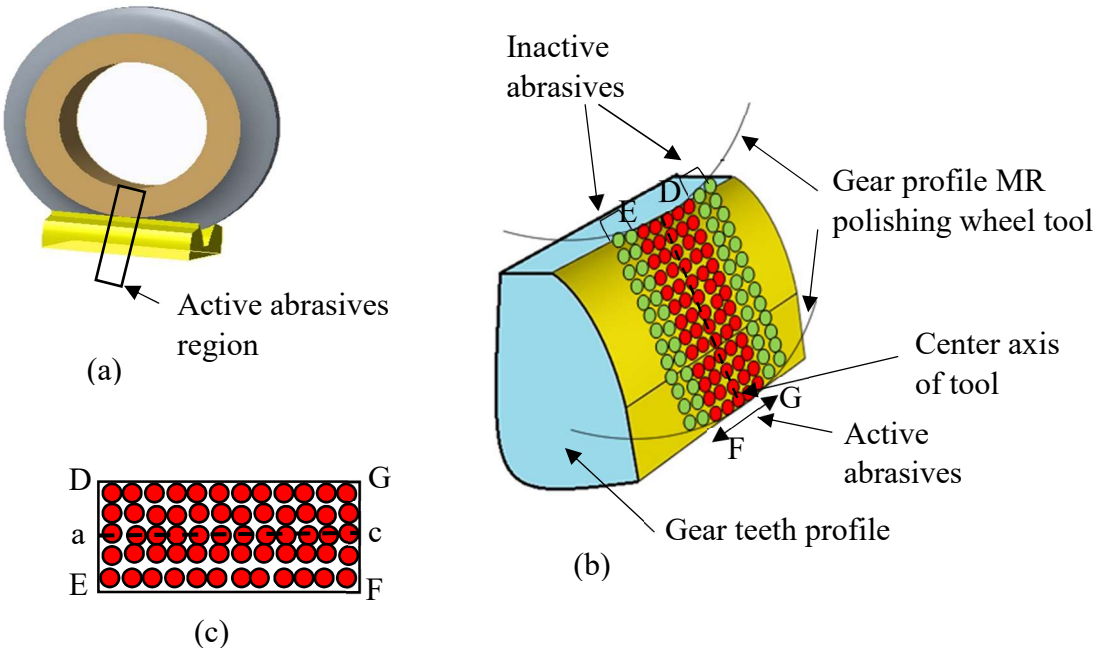

Figure 4.10 (a) Creo model section view, (b) active abrasive while finishing of gear teeth face and flank profile and (c) inclined view of active abrasive area

Where Area of cube face (A_{cf}), which is twice the edge length of the cube = 0.001681mm^2, Active abrasive area is 12mm^2. The total number of active abrasive (N_{ab}) in the active region is 14277 numbers.

4.5.3 Calculation of Change in Surface Roughness Value

Volume removed by active abrasives in ith stroke was calculated by using Equation 4.24 [38].

$$V = V_a \times N_{ab} \tag{4.24}$$

Material removed in ith stroke (V) = actual contact length × gear teeth depth (distance a to c) × total height of material removed [64]

$$V = L_a \times D_{ac} \times h \tag{4.25}$$

Substituting Equation 4.25 in to Equation 4.24, that is Equation 4.26 was obtained

$$V_a \times N_s = L_a \times D_{ac} \times h \tag{4.26}$$

Substituting the value of V_a from Equation 4.21 and $h = \frac{R_t}{R_a}(R_a^{i-1} - R_a^i)$ in Equation 4.26 [64].

$$R_a^{i-1} - R_a^i = \frac{N_{ab} \times A_1}{\frac{R_t}{R_a} \times D_{ac}} \tag{4.27}$$

Where R_a^{i-1} is the surface roughness in (i-1)th stroke, R_a^i is the surface roughness in ith stroke, N_{ab} is the number of active abrasives, D_{ac} is the projection of MRGPF tool on workpiece face it is called a to c distance discussed in Equation 4.22 and A_1 is indenting area by single abrasive, Equation 4.27 represent the material removed in single cycle.

4.5.4 Effect on Active Abrasive Area with Feed and Rotation Speed

Active abrasive area already calculated in section 4.5.2. This active abrasive area varies with the toot reciprocation feed and tool rotation shown n Figure 4.11. The active abrasive area GF and DE line varies with the rotation speed and reciprocation speed.

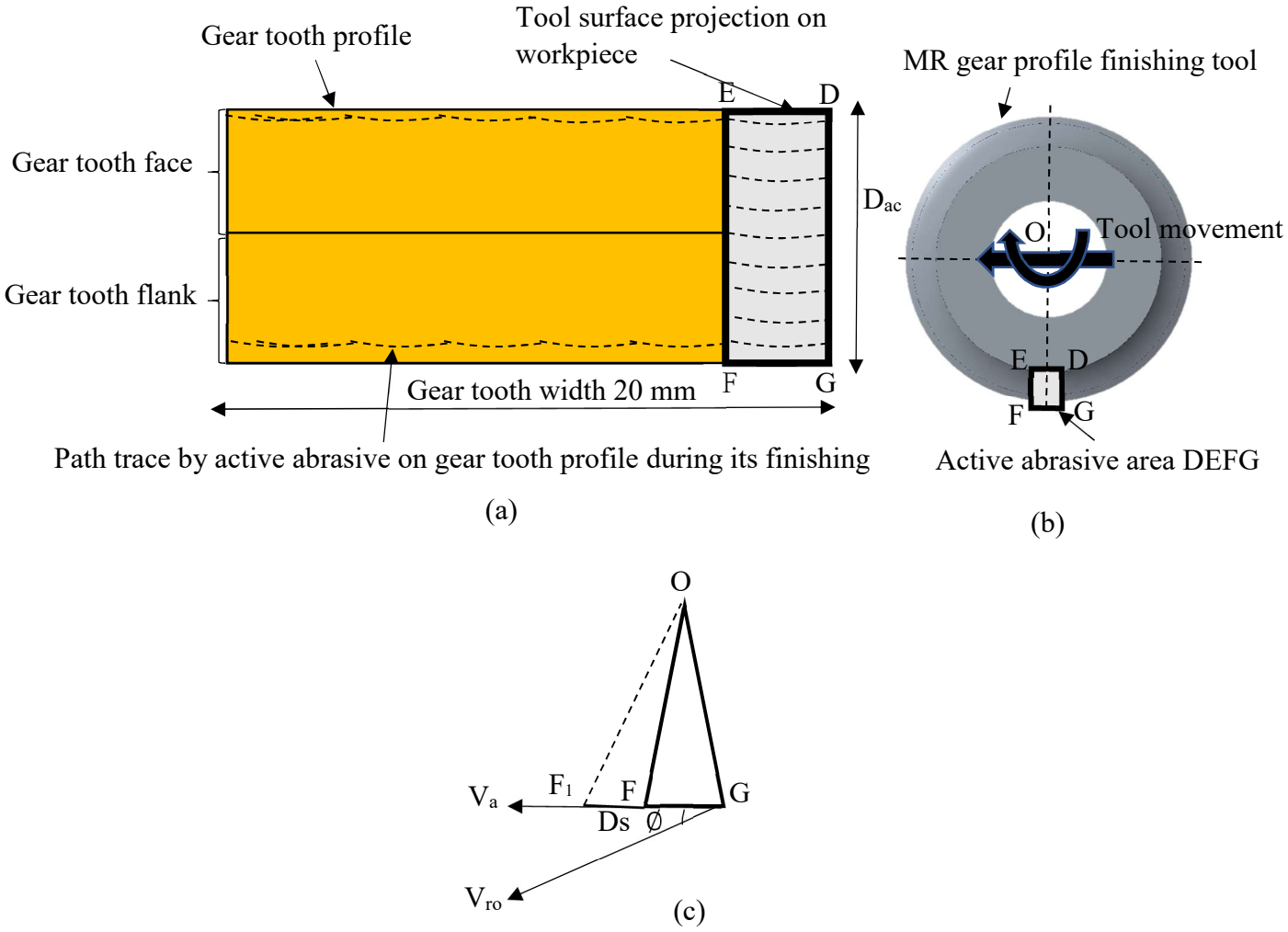

Figure 4.11 (a) Active abrasive area vary with tool reciprocation feed and rotation speed, (b) active abrasive area projected w.r.t tool and (c) schematic diagram of velocity impact in active abrasive area

For the study of active abrasive area take a line GF and study about active abrasive change their position during feed and speed of tool. From Figure 4.11(a) shows that the gear profile tooth finishing by active region of abrasive. Figure 4.11(b) shows that the active abrasive region while finishing of gear tooth profile. Resultant of feed and velocity component moving in one direction, shown in Figure 4.11 (c).

$$Vr = V_a + V_{ro}\cos\emptyset \tag{4.28}$$

Where Vr is the resultant velocity, V_a is the axial feed of tool and V_{ro} is the rotation speed of tool. Rotation speed of tool moving tangential and their component effect in axial side because the very small angle (∅) and it may be negligible. Suppose one of abrasive particle at point G in active region, calculate it's time to reach at point F, given in Equation 4.29.

$$\mathrm{T} = \frac{\mathrm{GF}}{\mathrm{V_{ro}}\cos\emptyset} \tag{4.29}$$

Due to the resultant of feed and rotation speed, distance (Ds) travelled by one active abrasive, calculated using Equation 4.30.

$$\mathrm{Ds} = \mathrm{Vr} \times \mathrm{T} \tag{4.30}$$

The length GF is having a number of active abrasive particle in GF length (G_{ab}) that is calculate by ratio of the GF length to the edge length of cube. So, at a particular line GF extend from one point to the GF_1, calculated using Equation 4.31.

$$\mathrm{GF_1} = \mathrm{Ds} \times \mathrm{G_{ab}} \tag{4.31}$$

As the active abrasive area DEFG is change to new area DE_1F_1G. So, it is change with different feed and rotation speed and the change of active abrasive area, directly affect the number of active abrasives in that reason given in Table 4.6, Calculate using Equation 4.23.

Table 4.6 Representation of active abrasive area change with feed and rotation speed

S. No	Tool feed (mm/min)	Tool rotation (rpm)	Area DE_1F_1G (mm^2)	Number of active abrasives
1	50	500	12.79	15217
2	75	300	13.98	16628
3	100	400	13.97	16621

The change of active abrasive area is for single cycle, single cycle of tool is completed when it covers the total width of the gear teeth profile in present cycle it is 20mm.

So, the Equation 4.27 rewritten as in Equation 4.32. Where $\frac{R_t}{R_a}$ is taken from grinded surface roughness graph value as 7 [38]. This change in active abrasive area to calculate the surface roughness finish of gear teeth, calculated result after 20 minutes shown and result are given in Table 4.7.

$$R_a^{i-1} - R_a^i = \frac{N_{ab} \times A_1 \times 20}{\frac{R_t}{R_a} \times D_{ac} \times GF_1} \tag{4.32}$$

Table 4.7 Change in surface roughness for single stroke

S. No	Tool feed (mm/min)	Tool rotation (rpm)	Change GF_1 (mm)	Change of surface roughness (ΔR_a) in (μm)
1	50	500	2.133	0.065
2	75	300	2.330	0.087
3	100	400	2.329	0.122

4.6 RESULTS AND DISCUSSION

The analysis of MRGPF tool was done to check its feasibility of tool to finish the EN24 spur gear tooth profile. A theoretical model was developed to calculate the magnetic flux density in working gap. Magnetic flux density varies from 0.53T to 0.51T and 0.52T to 0.50T on both left and right sides of the gear tooth profile respectively. Magnetic flux density gradient is maximum towards the tool surface and decreased towards workpiece surface. The variation in magnetic flux density gradient in working gap is almost similar to that obtained by finite element analysis. After calculating the magnetic flux density, indenting force was calculated on both left and right-side of gear tooth profiles. The indentation force at the left-side was 7.40×10^{-11} N and the right-side was 8.58×10^{-11} N. The indentation force was both of sides are almost similar for roughness model left-side indentation force was used and developed roughness model for EN24 material. The theoretical analysis has the been performed the change in surface roughness values. The

theoretical change in surface roughness has been obtained further, validated experimentally a obtained during the MR finishing of gear tooth profile.

4.6.1 Experimental Validation of Change in Surface Roughness Values

The spur gear teeth profile has been super finished by the magnetorheological gear finishing (MRGPF) tool. The finish of the gear teeth profile is validated with the theoretical analysis and compared with the experimental results data. For the experimentation, MR polishing fluid was prepared. MR polishing fluid with composition of 20% iron particles, 20% abrasive particles and 60% carrier medium (80% heavy paraffin and 20 % grease) was used. Experiment for 20 min was performed on each combination of parameters. The parameters for experiment are given in Table 4.8. The surface finish after experimentation was measured using Mitutoyo SJ-400 surf test.

Table 4.8 Parameter for experimental validation

Experiment No.	Tool Feed (mm/min)	Tool rotation (rpm)	Number of cycles
1	50	500	50
2	75	300	75
3	100	400	100

Experiments were performed to validate the theoretical roughness model given in Table 4.10. The number of cycles was calculating by using Equation 4.33 and shown in Table 4.8.

$$\text{Number of cycle} = \frac{\text{Total duration (min.)}}{\text{Cycle time}} \tag{4.33}$$

Total duration of the experiments performed was 20 minutes. The Cycle time is the ratio of tool movement and the feed of the tool. For the finish of gear tooth the tool movement was gear width that is 20mm. Result of the gear teeth profile in term of gear teeth profile finishing and error in term of percentage change of surface roughness values. The change of percentage surface roughness error ($\%\Delta R_a$ error) shown in Equation 4.34.

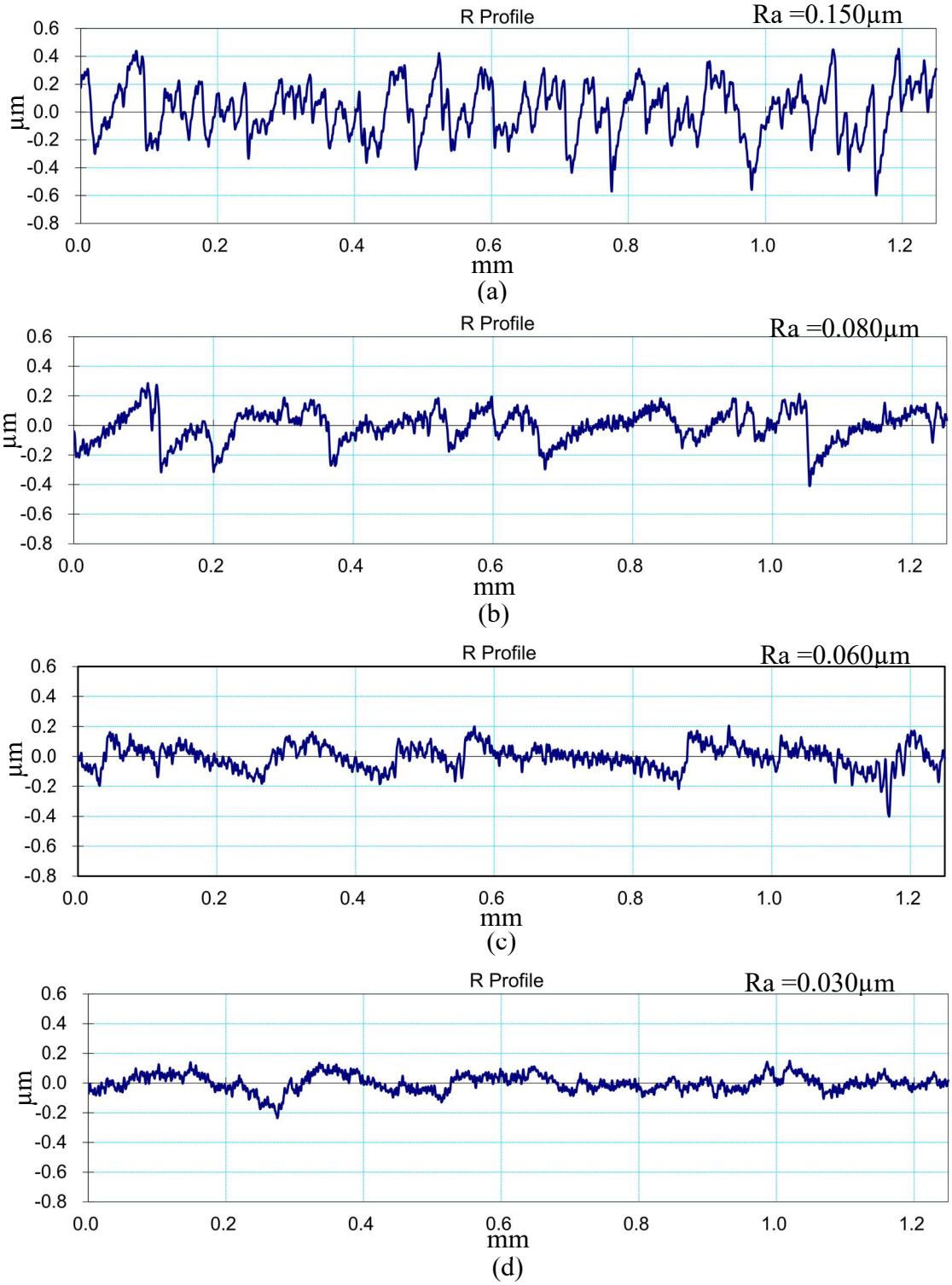

Figure 4.12 Experimentally measured surface roughness profiles on gear teeth surface initial surface and experimental in (µm) (a) initial grinded surface, (b) feed (50mm/min), rotation (500rpm), (c) feed (75), rotation (300) and (d) feed (100mm/min), rotation (400rpm)

$$\%\Delta R_a \text{ error} = \frac{E_{Ra} - T_{Ra}}{E_{Ra}} \times 100 \quad (4.34)$$

Where E_{Ra} is experimental surface roughness and T_{Ra} is theoretical surface roughness. The theoretical calculated surface roughness on the one left-side of the gear teeth profile is given in Table 4.9. It compares with experimental data, shown in Table 4.9. Initial average surface roughness 0.150 µm after gear grinding shown in Figure 4.12 (a), the surface roughness profile at different speeds and feeds are shown in Figure 4.12. After experimentation it was reduced to 0.03µm (Fig 4.12(d)), 0.06µm (Fig 4.12(c)) and 0.0.08µm (Fig 4.12(b)) in 100, 75 and 50 cycles respectively as reported in Table 4.9. The maximum error obtained was 15.00%.

Table 4.9 Represents the percentage error between theoretical and experimental data

S. No	Number of cycles	T_{Ra} in (µm)	E_{Ra} in (µm)	$\%\Delta R_a$ error
0	0	-	0.150	-
1	50	0.085	0.080	-6.25
2	75	0.063	0.060	-5.00
3	100	0.028	0.030	6.66

Mechanism of material removal was studied to predict the surface roughness reduction for finishing of gear tooth profile EN24 material using gear profile magnetorheological polishing wheel tool. In industries, process parameters are selected on basis of hit and trial. Selecting parameters by hit and trial is time consuming. This mechanism study will help to predict the results obtained after finishing as well as effect of selected parameters on the finishing performance for EN24 spur gear involute profile with 3-module. The predicted value will be having error in range of -5% to 6.66%. The change of percentage surface roughness error was higher means some causes not consider in the theoretical analysis study. These are in this way, after gear grinding tooth surface was not uniform, centrifugal force and gravity force on the active abrasive particle is not taken in study and the EN24 material characterization was not taken in the study. All these points are improving the percentage change of surface roughness error of the theoretical analysis model.

4.7 CONCLUSIONS

Theoretical analysis of gear teeth profile EN24 ferromagnetic material with the present magnetorheological gear profile finishing tool has been done. Magnetic flux density, indentation force, active abrasive area and theoretical surface roughness reduction were calculated. The main conclusion of the theoretical analysis of magnetorheological gear finishing modelling are drawn.

- Magnetic flux density on the left-side gear tooth profile, tool surface was found as 0.53T and it decreased towards the workpiece surface linearly to a value of 0.51T.
- Magnetic flux density on the right-side gear tooth profile, tool surface was found as 0.526T and it decreased towards workpiece surface linearly to value of 0.50T.
- The right-side gear tooth profile indentation force was 8.58×10^{-11} N and left-side gear tooth profile indentation was 7.40×10^{-11} N.
- The result obtained from the magnetic flux density and indentation forces on left and right sides of the gear tooth profile showed the present MR gear profile finishing tool is capable to perform uniform finishing.
- Surface roughness for the gear tooth profile workpiece was reduced from 0.15μm to 0.030μm, 0.060μm and 0.080μm respectively in 100, 75 and 50 number of finishing cycles.
- Percentage error in the theoretical as well as experimental data was found in range of -5% to 6.66%.
- Theoretically calculated surface roughness values are varying with number of cycles and their comparison with experimental data shows that the theoretical calculation accuracy can be increased with the consideration of centrifugal force. Initial surface roughness peaks are sharp edges. Therefore, material removal rate is higher in starting of running cycles.

CHAPTER 5

PARAMETRIC STUDY FOR FINISHING OF FERROMAGNETIC GEAR TEETH PROFILE WORKPIECE

The finishing of ferromagnetic gear teeth profile workpiece was done by using the newly developed magnetorheological gear profile finishing tool. The magnetorheological (MR) polishing fluid is functioned in the working gap between tool and workpiece perform the finishing operation. In this process various process parameters such as tool feed, tool rotation, working gap variation, current intensity through electromagnet and MR polishing fluid composition affects the performance of finishing process. In this chapter, parametric study was done on the process using response surface methodology (RSM). To perform the finishing operation more effectively, the optimum process parameters were calculated using analysis of variance (ANOVA). The percentage contribution of each parameter on the finishing performance of process was also calculated. The optimum parameters obtained from the parametric study was used to perform the finishing of spur gear tooth profile made with 3-module.

5.1 SELECTION OF MATERIAL

Material for gear manufacturing abide mechanical properties, it consists of fatigue strength, tensile strength, young modulus, high yield strength, hardness and easy to machine [65]. During meshing of gears, stresses are developed, on the face and flank of the gear teeth profiles due to the forces [45]. For absorbent power transmission by the gears, few metals and alloys are suitable for fabrication. Automotive industries choices for gears fabrication are steel, cast iron and malleable and modular irons. Selection of material matter on fatigue strength, bending fatigue strength and characterization of material composition play important role. For preparation of gear, from the American gear manufactures association (AGMA) standards the percentage of carbon (0.35 to 0.60 %) in steel and other important data given in Table 5.1 [45]. For the finishing of gear, the material should be carburized and case hardened after cutting of gear teeth [24]. To obtain the sufficient strength and wear resistance. The failure of gear modes depends on bending surface contact stresses it involves fatigue loading material and fatigue strength data needed. On the basis of the material characterization, EN24 steel material was selected for the development of gear, chemical composition EN24 is given in Table 5.2 [66]. After fabrication of EN24 gear, carburized and case hardening was done approximately 62HRC on Rockwell scale hardness.

Hardened material EN24 surface roughness much better than the other grade of steel (En series). From the industrial survey in GNA Gear Limited (Punjab), SHB (Punjab) and Kay-Kay Gear India Private Limited (Punjab) it has been found that En 24 steel material used in most of the industrial applications of gears.

Table 5.1 AGMA standards for gear material parameters [45]

Fatigue strength	Rockwell hardness (HRC)	Pressure	
		Psi*10^3	Mpa
Bending fatigue strength	55 – 64	50 – 75	380 – 520
Surface fatigue strength	55 – 64	50 – 75	1250 – 1300

Table 5.2 EN24 material chemical composition [66]

	Chemical composition wt. (%)									
Workpiece Material	C	S	P	Si	Mn	Cr	Ni	Mo	V	Al
EN24 steel (817 M 40)	0.40	0.048	0.039	0.26	0.68	0.86	1.47	0.20	0.09	0.034

5.2 PERPETRATION OF WORKPIECE

For the experimentation performance the spur gear profile is fabricated. In the present study, fabrication of spur gear with involute profile. EN24 steel blank was machined with pre-grinding (P.G) hob cutter tool. The pre-grinder tool machining specially used before the gear teeth profile grinder, it is left some margins for grinding operation at the tool face and flank profile. The general specification of straight teeth spur gear given in Table 5.3 [65]. On the basics of industrial requirements, the workpiece is fabricated based on process chart of fabrication shown in Figure 5.1. Heat treatment provided the fatigue strength to the material and increased the surface hardness. After that performance of surface quality increases and decrease the surface roughness value. Also, it is found from the literature review, gear material case hardening improves surface quality [49]. In the case hardening workpiece was heated up to a temperature 1100℃, treated in

muffle furnace for 15 min. and quenched in oil. To relieve the stresses and induce toughness in the material, tempered the workpiece with 300°C has been done for an hour.

Table 5.3 Spur gear dimensional characteristics

Module	3 mm
Pressure angle	20 deg.
Outer diameter	42.30 mm
Pitch circle diameter	36 mm
Face width	20 mm
Number of teeth	12 nos.

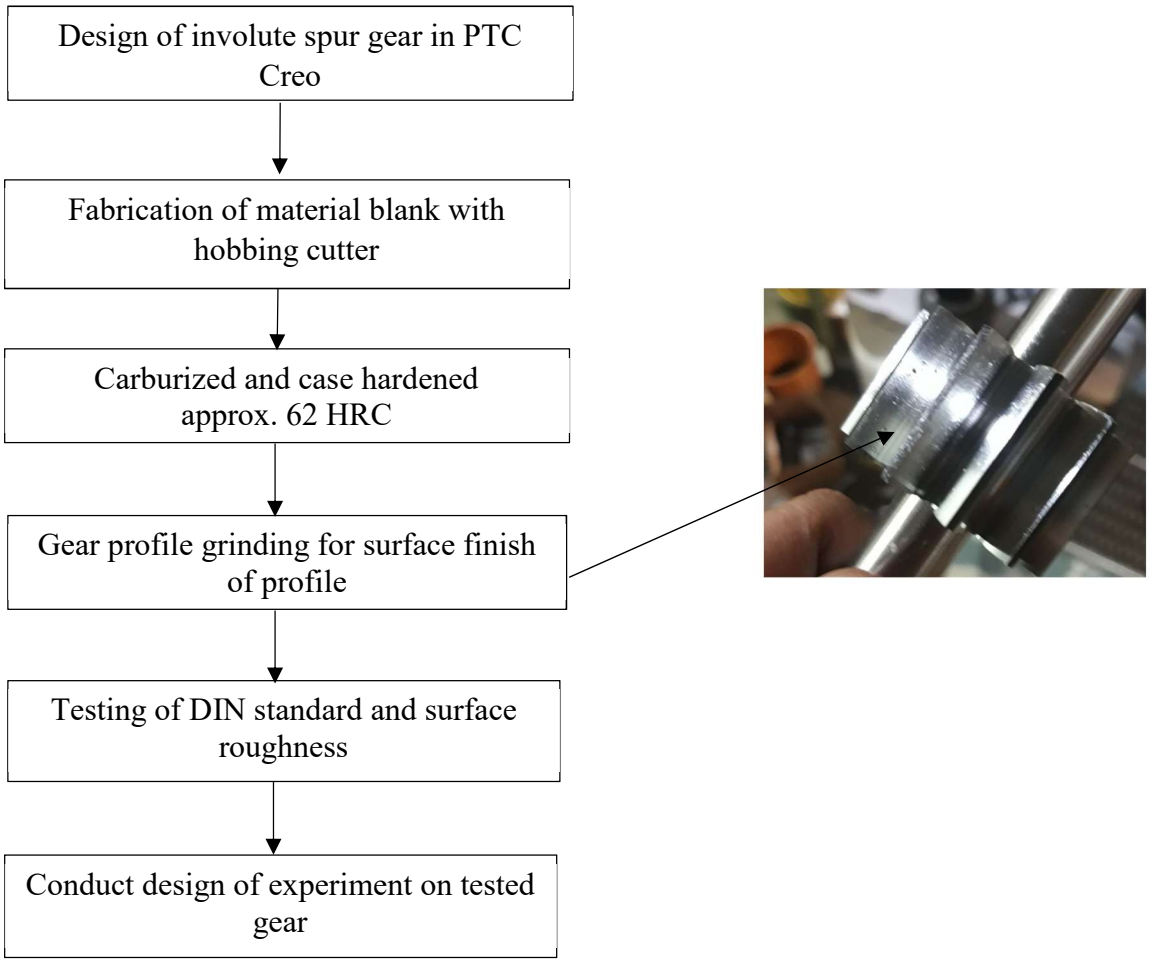

Figure 5.1 Fabrication process chart of ferromagnetic EN24 spur gear

The gear workpiece hardness was checked on Rockwell hardness and its value was found approximately 60±2 HRC. The gear teeth profile grinding operation was performed after the hardened of gear to get the required dimension. This process is material removal process, a margin left by hobbing cutter was removed to get the exact gear required dimension. The gear teeth profile grinder used in this study was 800 mesh size of silicon carbide (SiC) bonded. After gear teeth profile grinder, the DIN 3962 standard of the spur gear was checked for gear teeth lead and profile [21]. After grinding operation performance of gear was noticed in range of DIN 6 and surface roughness observed 0.12~0.16 μm.

5.3 EXPERIMENTAL SETUP

For the further finishing of the gear teeth profile after grinding to get the best dimensional accuracy and improved DIN standard. a new MR gear profile finishing (MRGPF) tool was used, with configuration has been already discussed in chapter 3. The existing developed set-up is shown in Figure 5.2 [67]. The new designed MRGPF tool was mounted on the Z axis horizontal slide and its motion controlled by the programmable logical controller (PLC) though. The gear workpiece was mounted on the indexing fixture set-up, after finished one tooth gear profile it was manually indexing to the next tooth precisely using indexing gear. The machine was operated using human machine interface (HMI). The electromagnet MRGPF tool movement (rotation and reciprocation) control by the PLC programming in HMI machine. The DC power supply was supplied to the electromagnet MRGPF tool. To cool the electromagnet, a coolant was supplied to the inlet of electromagnet. After extracting heat from the coiling in electromagnet, coolant returns to the coolant sump which is maintained at the temperature of -6℃.

5.4 PREPARATION OF MAGNETORHEOLOGICAL POLISHING FLUID

The MR polishing fluid is a Newtonian and viscous fluid when it is not present in magnetic field. When the magnetic field is applied the fluid become Non-newtonian fluid. It has been prepared in different composition as per the requirement of the finish process. The fluid applied on the tool profile surface it functioning in the working gap between tool surface and workpiece gear teeth profile surface. The MR polishing fluid is consisting of iron particle, silicon carbide (SiC) abrasive and base fluid. The base fluid was prepared with the paraffin oil and AP3 grease used.

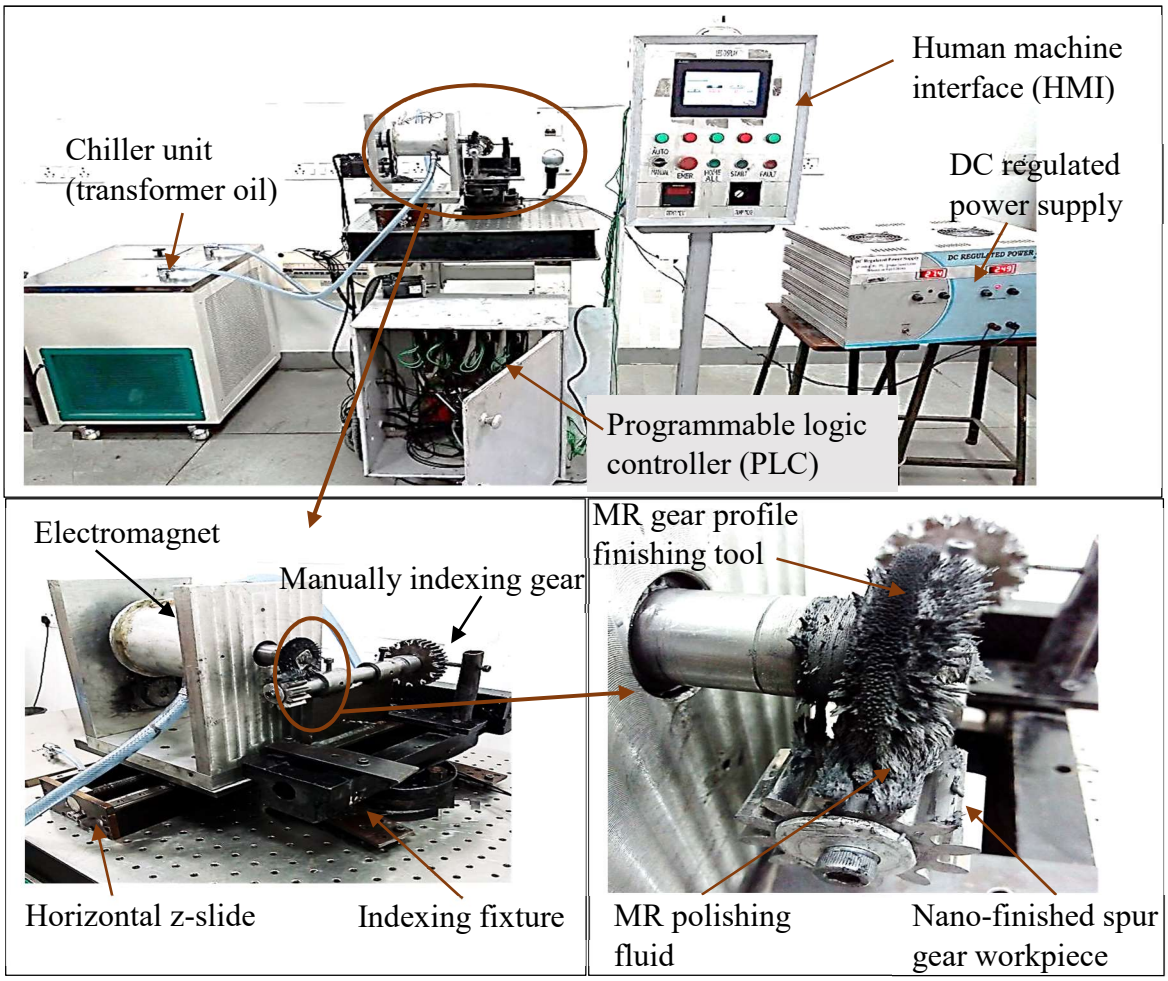

Figure 5.2 Photograph of a magnetorheological gear profile finishing (MRGPF) tool with the stiffened MR polishing fluid

From the literature reviewed found that the MR polishing fluid composition for maximum change in percentage of surface roughness while finishing of EN24 material [48], [49]. The MR polishing fluid composition are taken as concentration of iron particles is 20%, SiC abrasives is 20% and 60% base fluid [50], results as already discussed in section 4.1. The MR polishing fluid mixture (iron particle, SiC and base fluid) was applied on the tool profile before that stirring in stirring machine one hour.

5.5 PLAN OF EXPERIMENT

5.5.1 Experimentation Process Analysis

For the finishing of ferromagnetic gear workpiece using magnetorheological polishing fluid various parameter affecting the percentage change is surface roughness. From the literature found

that the parameters effecting the surface roughness are tool reciprocation speed, tool rotation, workpiece rotation, workpiece reciprocation, working gap, current density and MR polishing fluid composition. For the present study MR polishing fluid concentration already discussed in section 5.4. To finish the ferromagnetic workpiece with 2-D and 3-D geometry, literature review parameter study tells that the current varies (2~3 A) gives the best surface finish [54], [67]. Rest of the process parameters affecting the performance are discussed in preliminary experimentation.

5.5.2 Preliminary Experimentation

In order to determine the range of variable process parameter, a preliminary experiment was conducted. The experiment was conducted by using MR fluid concentration discussed in section 5.4, and optimum level of current 2~3 ampere taken, another parameter is studied. The working gap between the tool surface to workpiece surface is taken as 0.6 mm to finish ferromagnetic gear workpiece [60], [67]. In the preliminary experiments, tool rotation and tool reciprocation vary from 300 rpm to 700 rpm and 100 rpm to 200 rpm respectively. The observation of final change in surface roughness after 60 minutes of finish using Mitutoyo SJ-400 surftest, at different spur gear teeth, given in Table 5.4. From this studied it was found that, tool rotation and tool reciprocation are play an important role. Therefore, further study of gear tooth profile of EN24 material with 2A current. On the basics of the preliminary experiments, design of experiment study further.

5.6 EXPERIMENT

The MR gear profile finishing tool used to finish gear teeth profile for that conduct the design of experiment. To study the systematically investigate, the effect of process variables parameter to the change in surface roughness. From the plan of experiment, decided variable of process parameter are working gap (g), tool rotation (r) and tool reciprocation (f). To decide the five level of parameters on the basics of the preliminary experiments to make the accuracy, the response surface methodology. For the development and formation of new tool design as well as the improvement of the existing product design the response surface methodology (RSM) is utilized [68], [69], [70]. The present study has three parameter and five level for full factorial design of maximum change in surface roughness, the overall 5^3 =125 experiments made [41]. Ranges of the selected parameter and level shown in Table 5.5. Response surface methodology is a functional relationship between input and output. RSM used statically design of experiment

and least square fitting method for model generation [71]. The design of experiment performs on the Design- expert software.

Table 5.4 Preliminary experiment of spur gear finishing with the MR gear profile finishing tool

Parameters	Tool reciprocation feed (mm/min)	Tool rotation (rpm)	Final surface roughness (μm)
Concertation of MR fluid 20% SiC, 20% iron particles, 60% base fluid working gap = 0.6mm current = 2 A initial average surface roughness = 0.16 μm	300	100	0.05
	400	150	0.06
	600	50	0.07
	700	100	0.09
	400	200	0.08
Concertation of MR fluid 20% SiC, 20% iron particle, 60% base fluid working gap = 0.6mm current = 3 A initial average surface roughness = 0.16 μm	300	100	0.06
	400	150	0.05
	600	50	0.08
	700	100	0.09
	400	200	0.08

5.6.1 Central Composite Design

Generally, composite design planning adds some precise samples on the basis of regression design. thus, it reduces the number of experiments. On the reference bases of the first design of experiment, at the same time it can adjusting and satisfying the orthogonality of design experiment. Basically, three factors consist in composite design center point, factor point and the axial point. From this it is clear that three types of composite design make that are central composite face-centered (CCF), circumscribed central composite design (CCC), inscribe central composite design (CCI). CCF and CCC need 5 level and CCI need 3 level for every variable. On the basics of that CCI is selected for the further study and CCI design shown in Figure 5.3 [72].

Table 5.5 Coded level and corresponding actual values of process parameters

Factors		Levels				
Representations	Parameter description	-2	-1	0	1	2
f	Tool reciprocation feed (mm/min)	50	75	100	125	150
r	Tool rotation (rpm)	200	300	400	500	600
g	Working gap (mm)	0.5	0.55	0.6	0.65	0.7

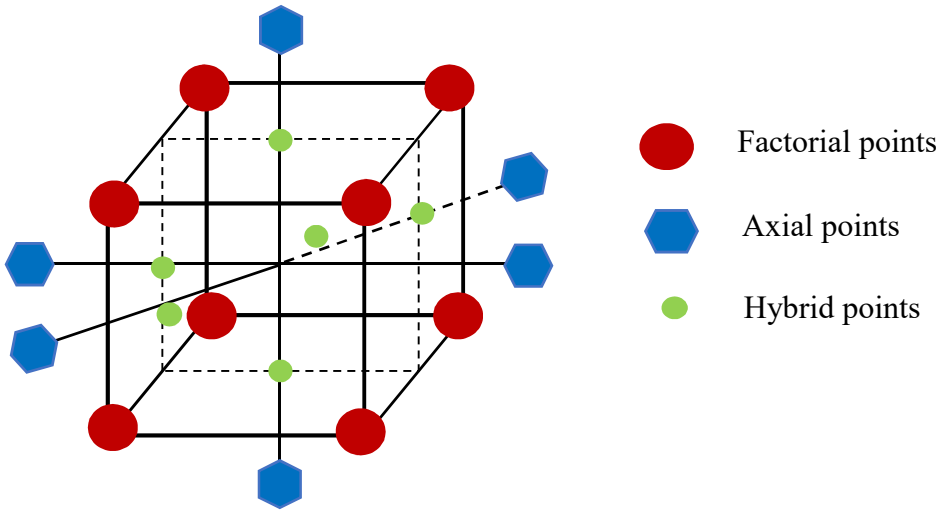

Figure 5.3 Central composite design [72]

5.6.2 Regression Model

The main objective of regression model to the percentage change of surface roughness, and the reduction of variability in process and improvement product and process quality. It can have accomplished in RSM model. In this model the relationship between the desired response that is

percentage change in surface roughness (%ΔRa) and independent input parameter relation given in Equation 5.1 [72].

$$\%\Delta Ra = F(f, r, g) \tag{5.1}$$

where (F) is the function of response, f is tool reciprocation feed, r tool rotation speed and g working gap.

In this study the effect of process parameter and percentage change in surface roughness for that second order mathematical regression method utilizes. Through this influencing the various process parameter, to the percentage change in surface roughness are accurately investigated given in Equation 5.2 [72]

$$\%\Delta Ra = b + \sum_{i}^{k} b_i x_i + \sum_{i}^{k-1} \sum_{i=j+1}^{k} b_{ij} x_i x_j + \sum_{i=1}^{k} b_{ii} x_i^2 + \delta \tag{5.2}$$

Where (x) represents the process parameter, (k) denotes the dimension of the design variable space, (b) represent predict coefficients, (δ) represents the residual measure. In reality to get optimum result 125 nos. of experiment conducted for the present selected parameter and their level. Hence, to analyze the effect of factor on response values for that adaptation shown in the response surface methodology method. Then the combination of the optimal processing parameter is able to achieve an optimal predicated change in surface roughness.

5.6.3 The Experimental Procedure

The Design-Expert 6.08 was used to establish the design of experiment and to fit the second order mathematical regression. From the user input in the software found the suitable 20 number of experiments using the CCI. In this work initial surface roughness of the workpiece measure at the face and flank of the gear tooth profile and found in the range of (120~160 nm). The table generated in software using regression second order. On the basis of the combination of all the process parameter, experiment perform and after 40 minutes final change in surface roughness measured using Mitutoyo SJ-400 surftest. Using initial surface roughness and the final result to get the percentage change of surface roughness of all the performed experiment are analyzed, as given in Table 5.6, using Equation 5.3.

$$\%\Delta \text{Ra} = \frac{\text{Intial surface roughness (Ra)} - \text{Final surface roughness (Ra)}}{\text{Intial surface roughess (Ra)}} \times 100 \quad (5.3)$$

Table 5.6 Summary of experiments and their response

Exp. No.	Tool feed (mm/min)	Tool rotation (rpm)	Working gap (mm)	Initial Ra (µm)	Final Ra (µm)	$\%\Delta Ra$
1	125	300	0.55	0.13	0.04	69.0
2	75	500	0.55	0.14	0.05	64.2
3	100	400	0.6	0.16	0.05	68.7
4	100	600	0.6	0.14	0.08	42.8
5	100	400	0.6	0.15	0.04	73.3
6	100	400	0.6	0.16	0.05	68.7
7	100	400	0.5	0.13	0.04	69.0
8	125	500	0.65	0.12	0.07	41.6
9	100	400	0.6	0.12	0.03	75.0
10	75	300	0.65	0.16	0.09	41.0
11	75	500	0.65	0.15	0.08	46.0
12	150	400	0.6	0.15	0.09	40.2
13	100	400	0.6	0.14	0.04	71.4
14	50	400	0.6	0.16	0.06	62.5
15	125	500	0.55	0.13	0.04	69.2
16	125	300	0.65	0.16	0.09	44.0
17	75	300	0.55	0.13	0.04	69.2
18	100	400	0.6	0.15	0.05	66.7
19	100	400	0.7	0.16	0.10	37.5
20	100	200	0.6	0.14	0.05	64.2

5.7 ANALYSIS OF EXPERIMENT

The change in term of percentage surface roughness and experimental factors converted into second order regression equation using analysis of variance (ANOVA) as reported in Table 5.7. The design expert suggests the quadratic equation for fitting in the model which is quite well for selecting the second order equation.

Table 5.7 ANOVA for percentage change in surface roughness

Source	Sum of squares	Degree freedom	Mean square	F-Value	Prob>F	
Model	*3062.41*	9	340.27	31	<0.0001	Significant
f	*285.63*	1	285.63	26.02	0.0005	
r	*385.48*	1	385.48	35.12	0.0001	
g	*916.13*	1	916.13	83.46	<0.0001	
f^2	*567.03*	1	567.03	51.66	<0.0001	
r^2	*765.67*	1	765.67	69.76	<0.0001	
g^2	377.32	1	377.32	34.38	0.0002	
fr	55.54	1	55.54	5.06	0.0484	
fg	124.85	1	142.85	11.37	0.0071	
rg	92.05	1	92.05	8.39	0.0159	
Residual	109.67	10	92.05	1.81	0.2656	Not significant
Lack of Fit	70.68	5	10.98			
Pure error	39.08	5	14.14			
Total	3172.17	19	7.82			

For the development of model for finishing of gear teeth and change of surface roughness was significantly shown by the model F (at 95%confidence) value. The model F value 30.74 indicating that the model is sufficient for the finish of gear. The values of “Prob > F” is less than the 0.0001 shows that the model terms are significant. Those model terms are less than 0.0001 are most

affecting the change of surface roughness and those are slight more than this affecting the model response less.

In the Table 5.7, observed that for the model significant, the p-value less than 0.05. For any value is higher than the p-value which is exclude from the model and perform the data again. The F value of lack of fit is 1.84 implies that the lack of fit not significant. The R^2 (0.96) value is close to 1 which is desirable. The difference between the adj. R-Squared (0.9337) and the pred. R-Squared (0.8043) is less than 0.20 for the model accuracy. The "Adeq Precision" is measure the signal to noise ratio (S/N) ratio of model. The S/N ratio is greater than 4 for the desirability of model. In the present model S/N ratio is 14.945 indicate an adequate signal.

From the ANOVA result it is concluded that the factor *f, r, g* and their interaction *fr, fg* and *rg* have significantly affect the surface roughness. Then the multivariant regression formula between percentage change of surface roughness and the process affecting parameter was established shown in Equation 5.4.

$$\%\Delta Ra = -809.933 + 2.958f + 0.579r + 227.370g - 0.007526f^2 - 0.0004234r^2 - 15.266g^2 + 1.008fr - 0.338fg - 0.065rg \quad (5.4)$$

5.8 RESULTS AND DISCUSSION

The accuracy of the regression model is fit for the experiment to check by the plot showing between the actual and predict values for percentage change in surface roughness, shown in Figure 5.4. The action of the model was tested through residual analysis. the residual fall on a straight inclined line which shows that the error is distributed normally through the predicted value. This graph shows that there is no unusual structure and no pattern, all the values are closer to the inclined line. Hence, the model provides reliable prediction.

5.8.1 Optimum Parameters

For the maximum percentage change in surface roughness design expert give three best optimum level solutions with desirability as 1. The three variable parameter tool reciprocation feed, tool rotation and working gap with their ranges reported in Table 5.8. From the response surface methodology, the obtained optimum parameters are given shown in Table 5.9.

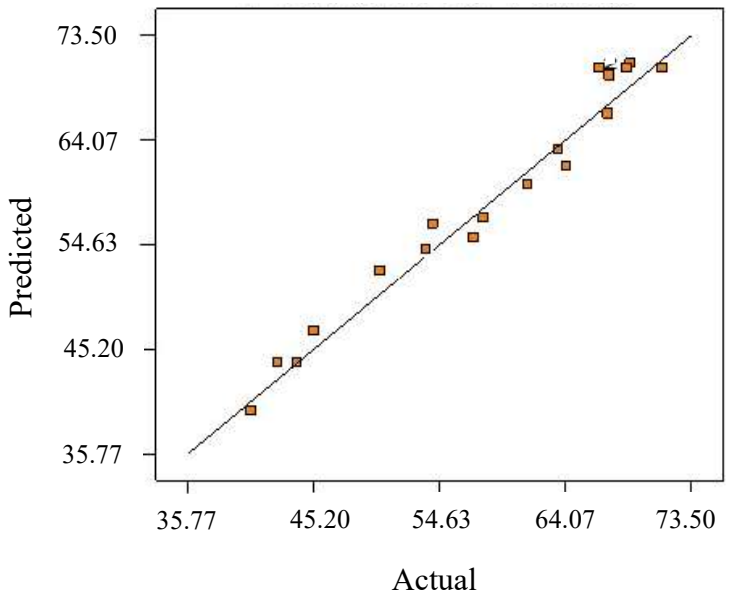

Figure 5.4 Variation between actual vs predicted value obtained from the experimental results

On the basics of this result take the average of the parameters, tool reciprocation feed 100mm/min, tool rotation 390rpm and working gap 0.55mm. After obtaining the optimum parameters as shown in Table 5.9, graphs were plotted for individual and interaction effect by keeping three variable constants for individual graphs and two parameters for interaction graphs. The parameters that was kept constant was at optimum value.

Table 5.8 Condition under which optimization of parameters performed

Name	Goal	Lower limit	Upper limit	Lower weight	Upper weight	Importance
Tool feed	Is in range	50	150	1	1	3
Tool rotation	Is in range	200	600	1	1	3
Working gap	Is in range	0.5	0.7	1	1	3
Response	Maximize	39.2	73.5	1	1	3

Table 5.9 Result obtained after optimization

Solution				
Tool feed (mm/min)	Tool rotation (rpm)	Working gap (mm)	Response (%ΔRa)	Desirability
102.59	390.82	0.55	73.99	1

5.8.2 Percentage Contribution of Each Factor on Percentage Change in Surface Roughness

Percentage contribution tells about the percentage weightage of each factor in regression model of the percentage change in surface roughness value. The analysis of the ANOVA table in term of percentage of contribution of all individual parameter, square of parameter and their interaction. This contribution shows that the change of percentage of surface roughness and their individual effect shown in Table 5.10. Pie chart is used to display the percentage share of each factors and their interaction on the response of experimentation as shown in Figure 5.5. Calculation of percentage of contribution of individual parameter has been calculated using Equation 5.4.

$$\text{Contribution individual parameter}(\%C) = \frac{\text{Indivisual sum of squares}}{\text{total sum of squares}} \times 100 \quad (5.4)$$

Table 5.10 ANOVA percentage contribution of the individual parameter

Parameters	Sum of squares	Total sum of squares	Percentage contribution (%)
f	*285.63*	3172.17	9.00
r	385.43		12.15
g	916.13		28.88
f^2	567.03		17.88
r^2	765.67		24.14
g	377.32		11.89
fr	*55.54*		1.75
fg	124.85		3.94
rg	92.05		2.90

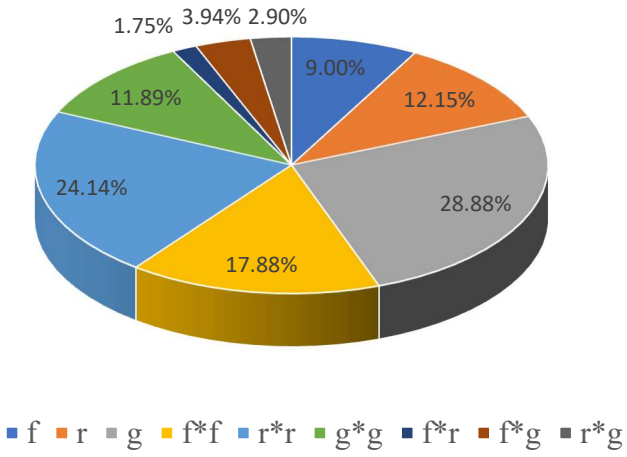

Figure 5.5 Contribution of individual parameter in percentage change of surface roughness

5.8.3 Effects of Feed Rate of Tool (*f*) on Percentage Change in Surface Roughness

The effect of feed rate of tool at tool rotation 400rpm and working gap 0.55mm is shown in Figure 5.6. As the feed rate increases, the percentage change in surface roughness increases up to some extent and start decreasing as the feed rate increases. At the feed rate of tool below 100mm/min, number of finishing cycles are increasing which results in increase of percentage change in surface roughness. Due to increase in number of finishing cycle, the collision between the active abrasives with roughness peaks increases. The stresses are being developed in MR polishing fluid column during rate of feed increasing. Beyond tool feed of 100mm/min, interaction between active abrasive particles with surface roughness peaks increases up to such an extent. The stresses induced in the MR polishing fluid column crosses the yield stress point for fluid column. Result for that deformation of MR polishing fluid column take place [51]. Due to deformation of iron particle chain, active abrasives are not able to remove the peaks more effectively as that at optimum level feed rate or below the optimum level feed rate.

5.8.4 Effects of Tool Rotation (*r*) on Percentage Change in Surface Roughness

The effect of tool rotation at tool feed 100mm/min and working gap 0.55mm is shown in Figure 5.7. As the tool rotation increases, the percentage change in surface roughness increases up to optimum level and start decreasing afterwards. The reason for that abrasive hold by the iron particle chains at the GPMRPW tool surface, when the speed is increasing the centrifugal force at the surface is increasing [73]. Result of that the iron particle trying to change their position or moving in outward direction, due to abrasive hold not tightly and after reaching optimum level

percentage change in surface roughness decreasing. The centrifugal force acting on the iron particle chain increases beyond 400rpm, which reduces the effect of magnetizing force acting on iron particles in the working gap. Due to the reduction of magnetizing force at iron particle chains in the working gap, the indentation force acting on the abrasive particles is reduced. This results in decrease the percentage change in surface roughness at higher tool rotation.

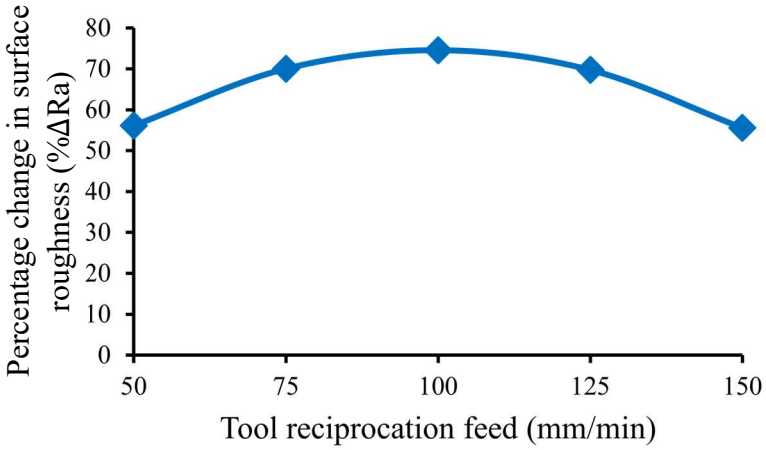

Figure 5.6 Percentage change in surface roughness value with respect to tool reciprocation feed

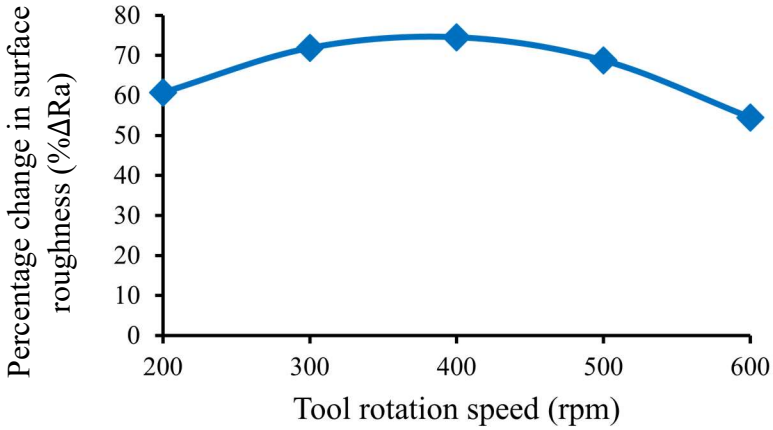

Figure 5.7 Percentage change in surface roughness value with respect to tool rotation speed

5.8.5 Effects of Working Gap (*g*) on Percentage Change in Surface Roughness

The effect of working gap between the tool surface and workpiece surface at tool feed 100mm/min and tool rotation 400rpm is shown in Figure 5.8. As the working gap increases, the percentage change in surface roughness increases up to optimum level and start fast decreasing afterwards. From the contribution of the working gap found that 0.5mm to 0.6mm percentage change of surface roughness is very small after the 0.6mm the percentage change of surface roughness is rapidly decrease. The reason for that when the gap is more the shear strength of the iron particle chains is not able to remove the material from the workpiece surface [51], [73]. If the working gap is optimum the shear strength of the iron particle chains enough to ploughing of material from workpiece surface.

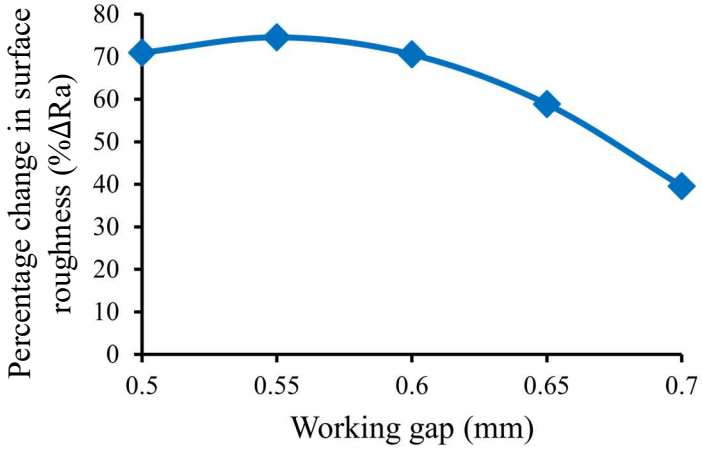

Figure 5.8 Percentage change in surface roughness value with respect to working gap

5.8.6 Effect of Interaction between Tool Reciprocation Feed and Tool Rotation

The effect of interaction between tool reciprocation feed and tool rotation at working gap of 0.5mm, is shown in Figure 5.9. The percentage change in surface roughness for individual effect of too rotation increase up to 400rpm and start decreasing afterwards. Figure 5.9, the optimum value of tool rotation for percentage change in surface roughness shifts after the interaction. For tool reciprocating feed at 150mm/min and 125mm/min, the optimum value of tool rotation shifts to 500rpm. The reason for this behavior is that as the tool feed increases, interaction between the active abrasive particles with surface roughness peaks increases. Effect of centrifugal force was less at high reciprocation feed because the active abrasive interaction fast with surface roughness peaks. Domination of this effect results in shifting of optimum value for tool rotation. For tool

reciprocating feed value at 50mm/min and 75mm/min, the optimum value of tool rotation shifts to 300 rpm. The shifting is due to reduction in number of cycles and effect of centrifugal force on active abrasive is less. Which results in decreasing of collision of abrasive particle with roughness peaks. Domination of this factor results in decreasing of optimum tool rotation to 300rpm. At the tool feed 100mm/min the tool rotation speed shift to 400rpm for maximum change in surface roughness. Reason for that the combined effect of number of cycle and centrifugal force at that range is optimum level.

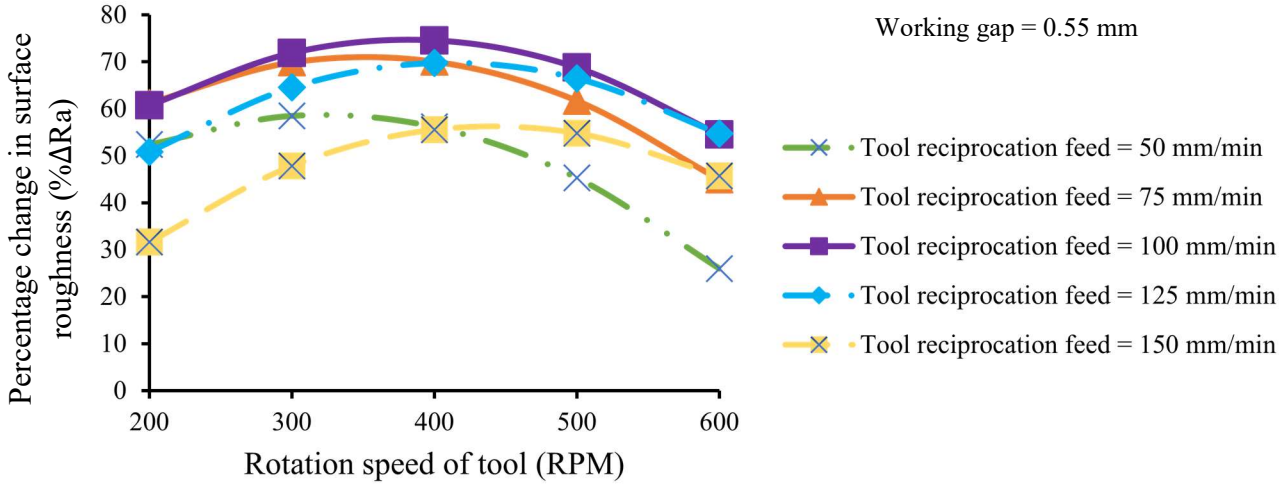

Figure 5.9 Percentage change in surface roughness value with respect to combine effect of tool reciprocation feed and tool rotation

5.8.7 Effects of Interaction between Tool Rotation Speed and Working Gap

The effect of interaction between tool rotation speed and working gap at tool reciprocation feed of 100mm/min, is shown in Figure 5.10. The percentage change in surface roughness for individual effect of working gap increase up to 0.55mm also small change from 0.5 to 0.6mm and start rapidly decreasing after 0.6mm. Figure 5.10, the optimum value of working gap for percentage change in surface roughness shifts after their interaction. For rotation at 600rpm, the optimum value of working gap shifts to 0.5mm. The reason for this behavior is that as the tool rotation increases, the centrifugal force increases due to the active abrasive indentation force decreases. Domination of this effect results in shifting of optimum value of working gap at minimum gap. For tool rotation value at 200rpm, the optimum value of working gap shifts to 0.6mm. The shifting is due to

centrifugal force are minimum due to that the less effect on indentation force and yielding strength of active abrasive are higher than the material resisting strength. Domination of this factor results in increasing of optimum working gap shift to 0.6mm. At the tool rotation 400rpm the working gap shift to 0.5 to 0.6mm for maximum change in surface roughness. Reason for that the combined effect of centrifugal force and higher yielding strength of iron particle chain in that range of optimum level.

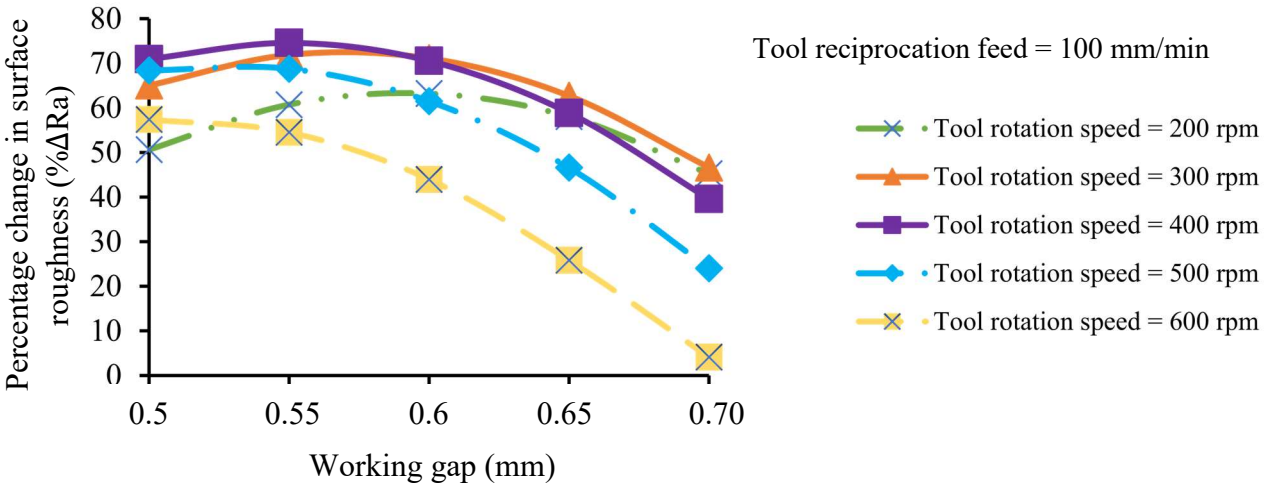

Figure 5.10 Percentage change in surface roughness value with respect to combine effect of working gap and tool rotation speed

5.8.8 Effects of Interaction between Tool Reciprocation Feed and Working Gap

The effect of interaction between tool reciprocation feed and working gap at tool rotation of 400rpm, is shown in Figure 5.11. The percentage change in surface roughness for individual effect of tool reciprocation feed increase up to 100mm/min and start decreasing afterwards. Figure 5.11, the optimum value of tool reciprocation feed for percentage change in surface roughness shifts after their interaction. For working gap at 0.7mm, the optimum value of tool reciprocation shifts to 75mm/min or less than this very small change. The reason for this behavior is that as the working gap increases, the shear strength of iron particle chain decreasing due to the active abrasive not indentation properly or says less indentation forces. Domination of this effect results in shifting of optimum value of tool reciprocation feed at minimum level 50 to 75mm/min. For working gap at 0.5mm, the optimum value of tool reciprocation feed shifts to 125mm/min. The shifting is due to shear strength of iron particle chains are sufficient to hold active abrasive and indentation force

are higher. Domination of this factor results in increasing of optimum tool feed reciprocation speed. At the working gap 0.55 to 0.6mm the change of tool reciprocation feed at 75 to 100mm/min effect are less. Reason for that the combined effect of shear strength of iron particle chains and number of cycle are at optimum level.

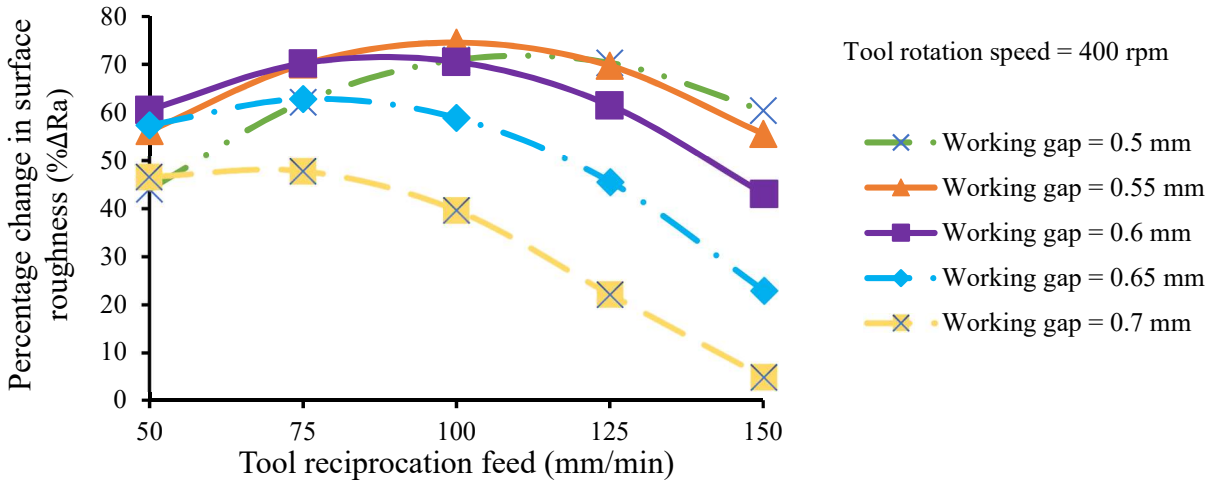

Figure 5.11 Percentage change in surface roughness value with respect to combine effect of tool reciprocation feed and working gap

5.8.9 Confirmatory Test for Regression Model Validation

In this section, the confirmatory test was carried out for checking the regression model accuracy. Three experiments were performed on optimum parameters. The percentage change in surface roughness was measured after experimentation using Mitutoyo SJ-400 surftest. Theoretically percentage change in surface roughness was calculated from the regression Equation 5.4, as given in Table 4.14. It can be seen that the maximum percentage change in roughness is -2.50% which shows the good agreement between regression model and experimental model. In the regression model the response was percentage change in surface roughness which has to be maximized. After regression analysis, the optimization of response was predicted on design-expert 6.0.8. It was found that optimized parameters were tool reciprocation speed 100mm/min, tool rotation 390rpm and working gap 0.55mm.

Table 5.11 Confirmatory tests and their comparison with the results during MR finishing of gear teeth profile

Solution number	Time (min)	Tool reciprocation (mm/min)	Tool rotation (rpm)	Working gap (mm)	Experimental %ΔRa	Predicted %ΔRa	Error (%)
1	40	100	390	0.55	71.42	73.99	-2.50
2	40	100	390	0.55	72.4	73.99	-1.59
3	40	100	390	0.55	74.55	73.99	0.56

5.8.10 Process Performance with the Optimum Parameters

After getting the model validation, the experiments were performed using optimum parameters. The present MR finishing with the optimum parameters performed on spur gear teeth profile after the gear grinding process. An EN24 material spur gear has involute profile with 3-module and 12 number of teeth. Implementing the optimum parameter tool reciprocation feed 100mm/min, tool rotation 390rpm and working gap 0.55mm to finish the gear teeth profile one by one. Checking surface roughness of gear teeth profile on Mitutoyo SJ-400 surface tester, after completing every cycle time, the results are reported in Table 5.12. The MR polishing fluid start working with average surface roughness 0.15µm and after 20 min 0.02µm achieved after that in next 20 minute there is no change in surface roughness, shown in Figure 5.12. There is no change in surface roughness after 20 min means the EN24 material saturation of finishing. Other parameter is same for this trial which used earlier such as current and MR fluid concentration use in response surface methodology.

Table 5.12 Effects of optimum parameters on process performance

Optimum parameters	Time (min)	Surface roughness Ra (µm)
Current = 2 A Tool reciprocation feed =100 mm/min Tool rotation speed = 390 rpm Working gap = 0.55 mm	0 (after grinding)	0.15
	10	0.04
	20	0.02
	40	0.02

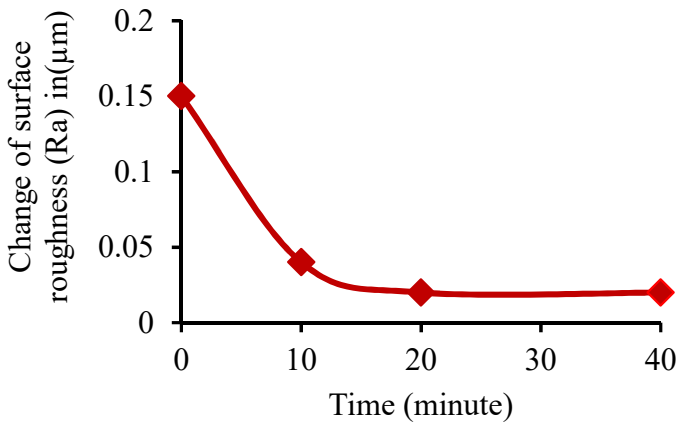

Figure 5.12 Change in surface roughness with time at optimum parameters during MR finishing of gear teeth profile

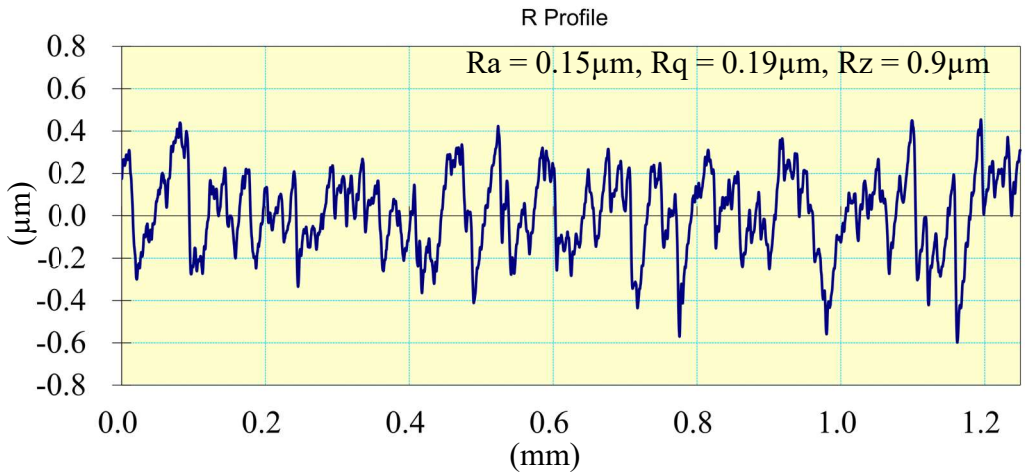

(a)

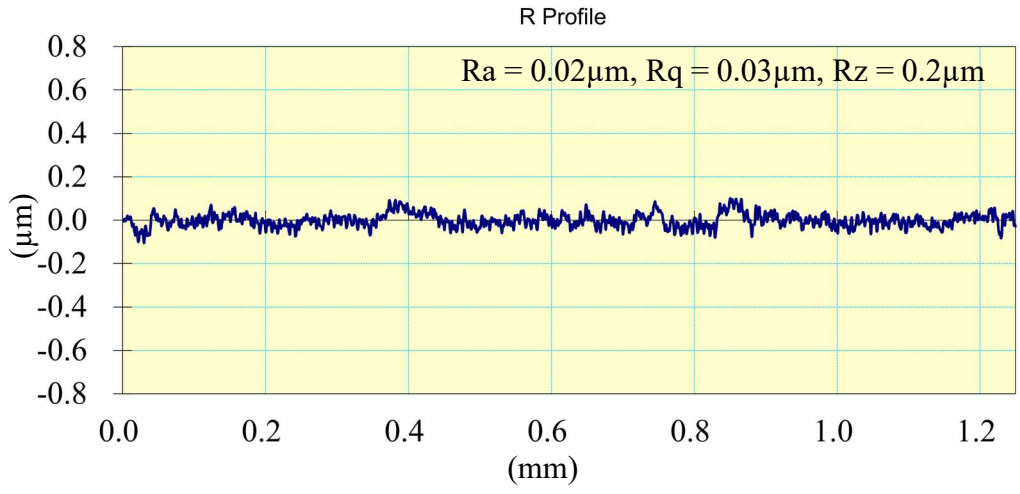

(b)

Figure 5.13 Surface roughness profiles of (a) gear ground surface and (b) after present MR finished process

Initial average surface roughness was 0.15µm to reduce up to 0.02µm on a single tooth with in 20 minute of process cycle, shown in Figure 5.13. Initial surface finish with gear teeth grinder (800-mesh size) of abrasive, which is mostly used in industry. Compare this gear grinder process with MRGPF a new designed tool, much better than the gear tooth profile grinder.

5.9 RESULT AND DISCUSSION

After completing the RSM model validation, the experimentation was done gear tooth profile using optimum parameter. Comparison of the new MR finishing with the gear profile grinder was done. Basically, the gear performance depends on their shape accuracy if it maintained as per standard it means gear life and performance best. In present study the gear life and best performance was compare with the same size industrial gear, which is used in motorcycle gear box.

Further, the comparison of spur gear tooth profile surface characterization with before gear profile grinder. Surface character measured in many ways, to see the mirror image, and after the MR finishing have been performed and scan electron microscopic (SEM) image. The surface gear performance and increase the life of gear finished surface with better texture improves.

The SEM images after gear grinding process are shown in Figure 5.14. The left-side and the right-side gear tooth profile cutting direction are same. Gear teeth profile grinder is material removal in straight line or horizontal line on the surface of gear tooth. The gear grinder abrasives for removing material are contact with gear workpiece in horizontal line. Reason for that the diametrical size of gear grinder is bigger than the workpiece gear outside diameter.

The new developed MR gear profile finishing process, removes roughness peaks on the surface of gear teeth with the present MR finishing process in 20 minutes. Which clearly seen in SEM image after MR gear profile finishing process as shown in Figure 5.15. The material removal in this MR finishing process are different from the gear grinding operation. In the SEM images the direction of material removal same on both left-side and right-side of the gear teeth. The new developed process removed almost the peaks and valley from the gear surface. Visual images of the gear teeth profile before and after MR gear profile finishing process is shown in Figure 5.16. After the MRGPF process, the gear tooth surface shine like a mirror, one tooth profile reflects to their adjacent tooth.

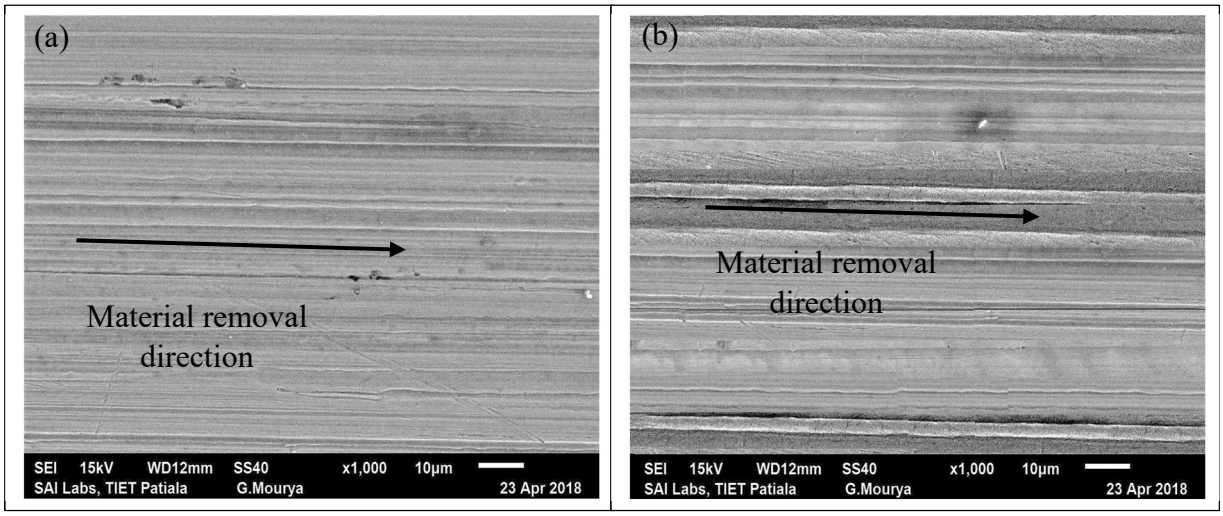

Figure 5.14 SEM images after gear grinding process (a) left-side gear tooth profile and (b) right-side gear tooth profile

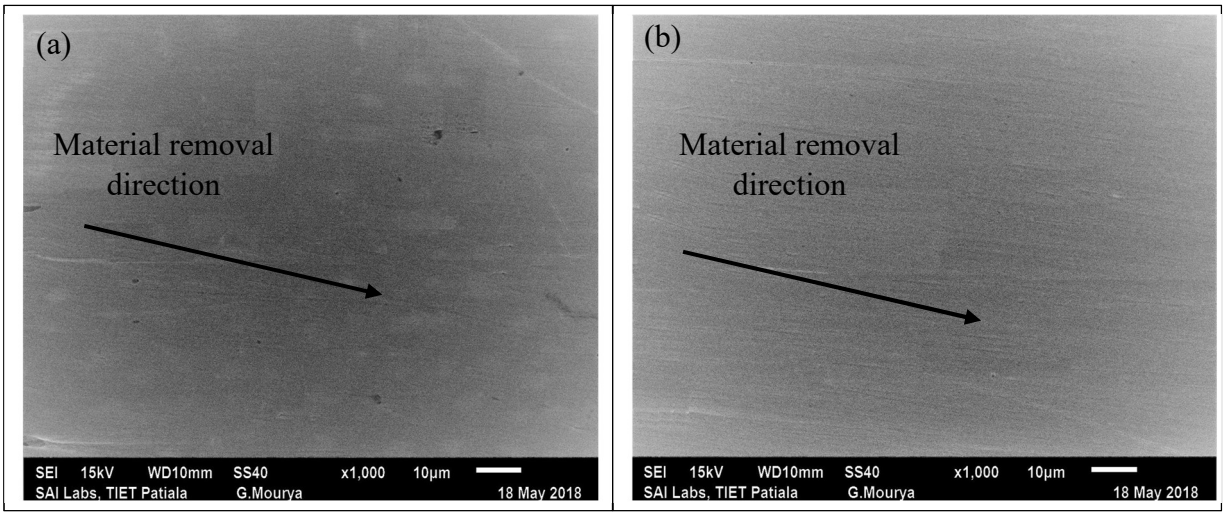

Figure 5.15 SEM images after the MR gear profile finishing process (a) left-side gear tooth profile and (b) right-side gear tooth profile after 20 min of finishing

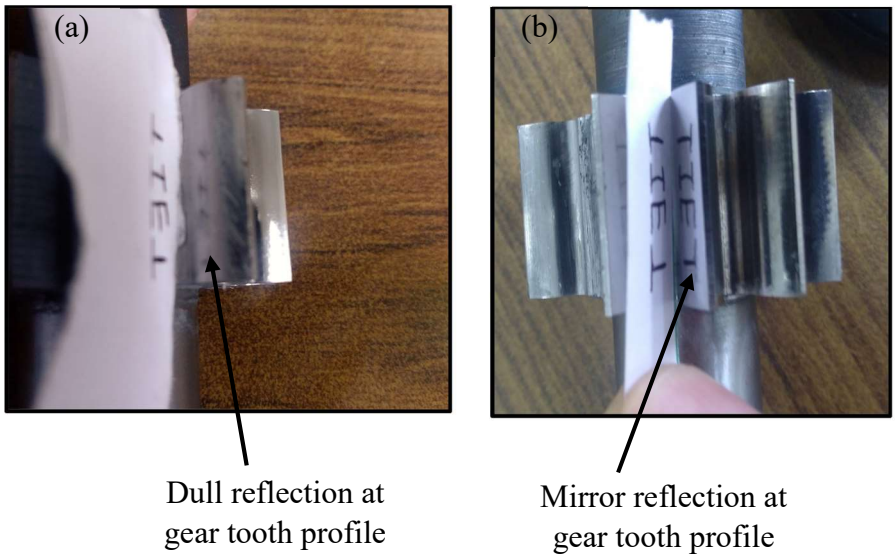

Figure 5.16 Mirror image of gear teeth profile (a) after gear grinding and (b) after MR finishing in 20 minutes

5.9.1 Improvement in Spur Gear Performance

Gear performance is depending upon the shape accuracy of gear teeth profile. Gear teeth profile can be measure with in the DIN standards. In the present study spur gear teeth profile measured with in DIN 3962 spur gear standard. This represent the gear teeth runout and gear teeth pitch deviation with any adjacent teeth in same spur gear. After gear tooth profile grinder finishing operation, gear profile and lead measured on both left and right-side of gear tooth and compare with any adjacent teeth.

From Figure 5.17, lead and profile parameter was checked in DIN 6 standard, on two teeth 1 and 5 numbers. Where left-side tooth profile compares with right-side tooth profile and left-side lead compares with the right-side tooth profile. For the left flank gear profile as the profile angle deviation (fHa), total profile deviation (Fa) and profile form deviation (ffa) are lies in DIN 7, 5 and 4 standards respectively. For the right flank gear profile as the profile angle deviation (fHa), total profile deviation (Fa) and profile form deviation (ffa) are lies in DIN 6, 6 and 3 standards respectively. Same as, the lead of the left and right-side gear such as the profile angle deviation (fHB), total profile deviation (FB) and profile form deviation (ffB) are lies in DIN 6, 5 and 2 standards respectively. For the right flank gear profile as the profile angle deviation (fHB), total profile deviation (FB) and profile form deviation (ffB) are lies in DIN 6, 6 and 5 standards

respectively. These data show that the gear tooth grinder was not precisely finish the gear tooth profile and can be their indexing was the measure issues, that why DIN standard variation are more.

On these two teeth checking the gear runout pitch deviation have been checked shown in Figure 5.18. After gear tooth profile grinder results came in DIN 6 standard. The pitch line runout (Fr) came in DIN 5 standard, total indexing variation for left side gear tooth profile are in DIN 5 and right-side total indexing variation are in DIN 6 standard. After achieved DIN 6 standard with gear grinder, again this ground surface was finished with the MR gear profile finishing process. After the MR finishing the DIN 4 standard has been achieved as gear profile and lead on same 1 and 5 number gear tooth.

From Figure 5.19, lead and profile parameter was checked in DIN 4 standard, on two teeth 1 and 5 numbers. Where left-side tooth profile compares with right-side tooth profile and left-side lead compares with the right-side tooth profile. For the left flank gear profile as the profile angle deviation (fHa), total profile deviation (Fa) and profile form deviation are lies in DIN 4, 4 and 3 standards respectively. For the right flank gear profile as the profile angle deviation (fHa), total profile deviation (Fa) and profile form deviation are lies in DIN 3, 4 and 3 standards respectively. Same as, the lead of the left and right-side gear such as the profile angle deviation (fHB), total profile deviation (FB) and profile form deviation (ffB) are lies in DIN 3, 3 and 4 standards respectively. For the right flank gear profile as the profile angle deviation (fHB), total profile deviation (FB) and profile form deviation (ffB) are lies in DIN 4, 4 and 3 standards respectively.

On these two teeth checking the gear runout pitch deviation have been checked shown in Figure 5.20. After gear tooth profile grinder results came in DIN 4 standard. The pitch line runout (Fr) came in DIN 2 standard, total indexing variation for left side gear tooth profile are in DIN 1 and right-side total indexing variation are in DIN 1 standard. This result shows that the newly designed MR gear profile finishing was better than the gear profile grinder.

This result shows that the MR polishing fluid finishing removes the material and gives the best shape accuracy. The pitch line runout is reduced from the 7.6µm to 4.0µm after MR finishing. Gear runout causes a problem of noise in gears and produce vibration when vehicle move at high rpm. Single pitch deviation (fp) reduces from 2.5µm to 1.3µm and total cumulative pitch deviation (Fp) reduced from 11.8µm to 4.2µm. Total profile deviation represents in distance, its total deviation reduces from 5.8µm to 2.5µm.

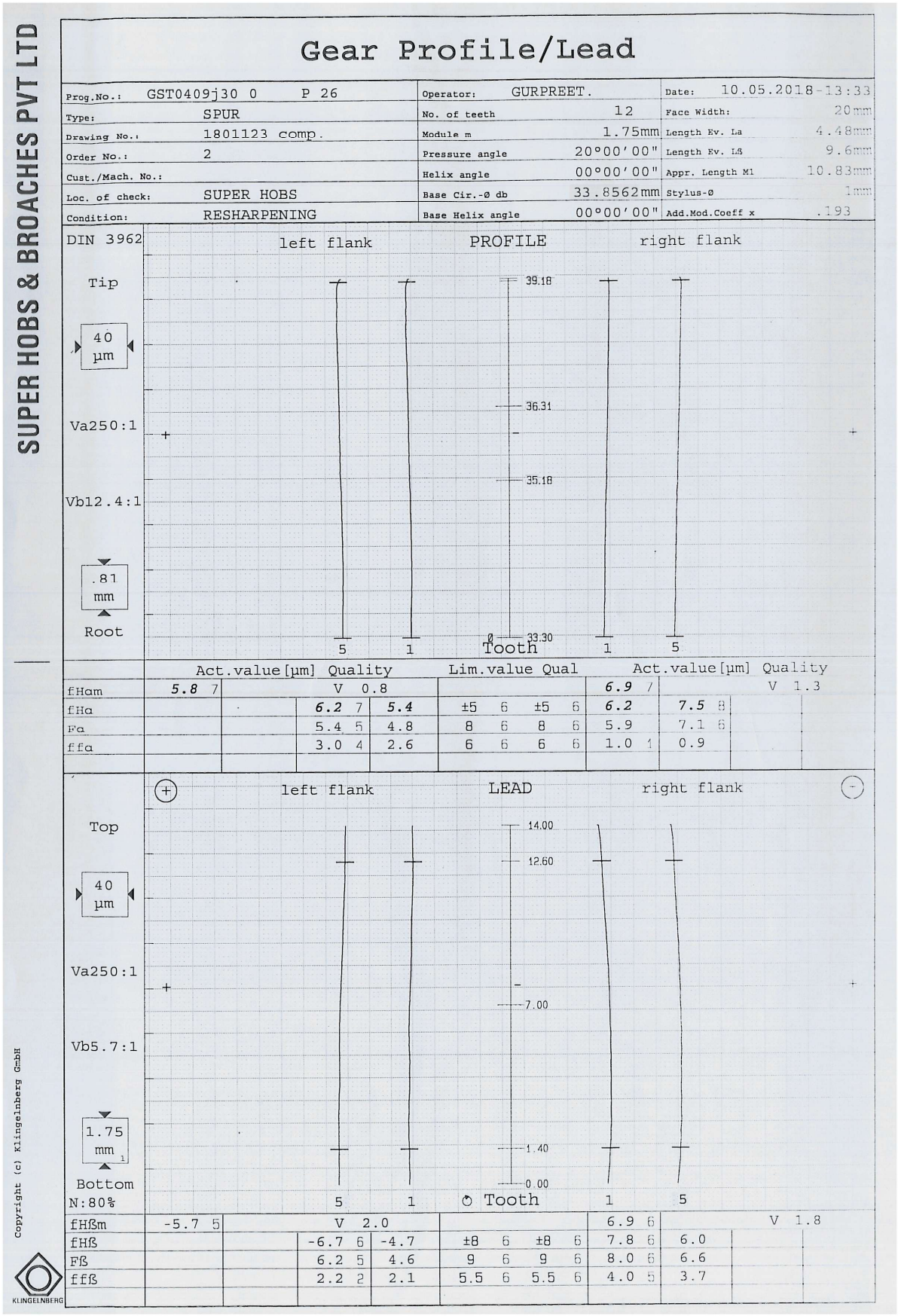

Figure 5.17 Spur gear teeth profile and lead in DIN 6 after gear profile grinder finishing process

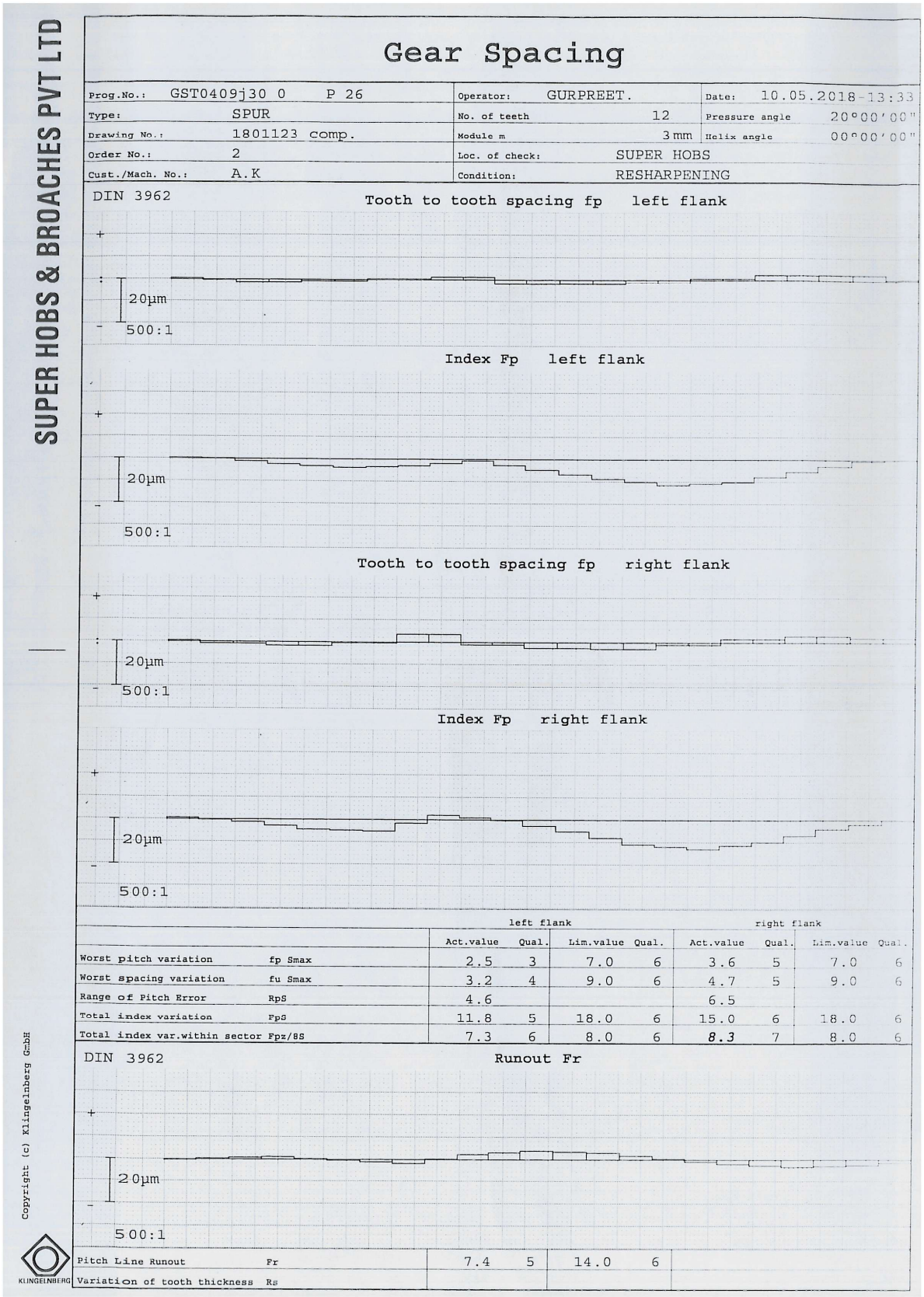

Figure 5.18 Spur gear runout in DIN 6 after gear profile grinder finishing process

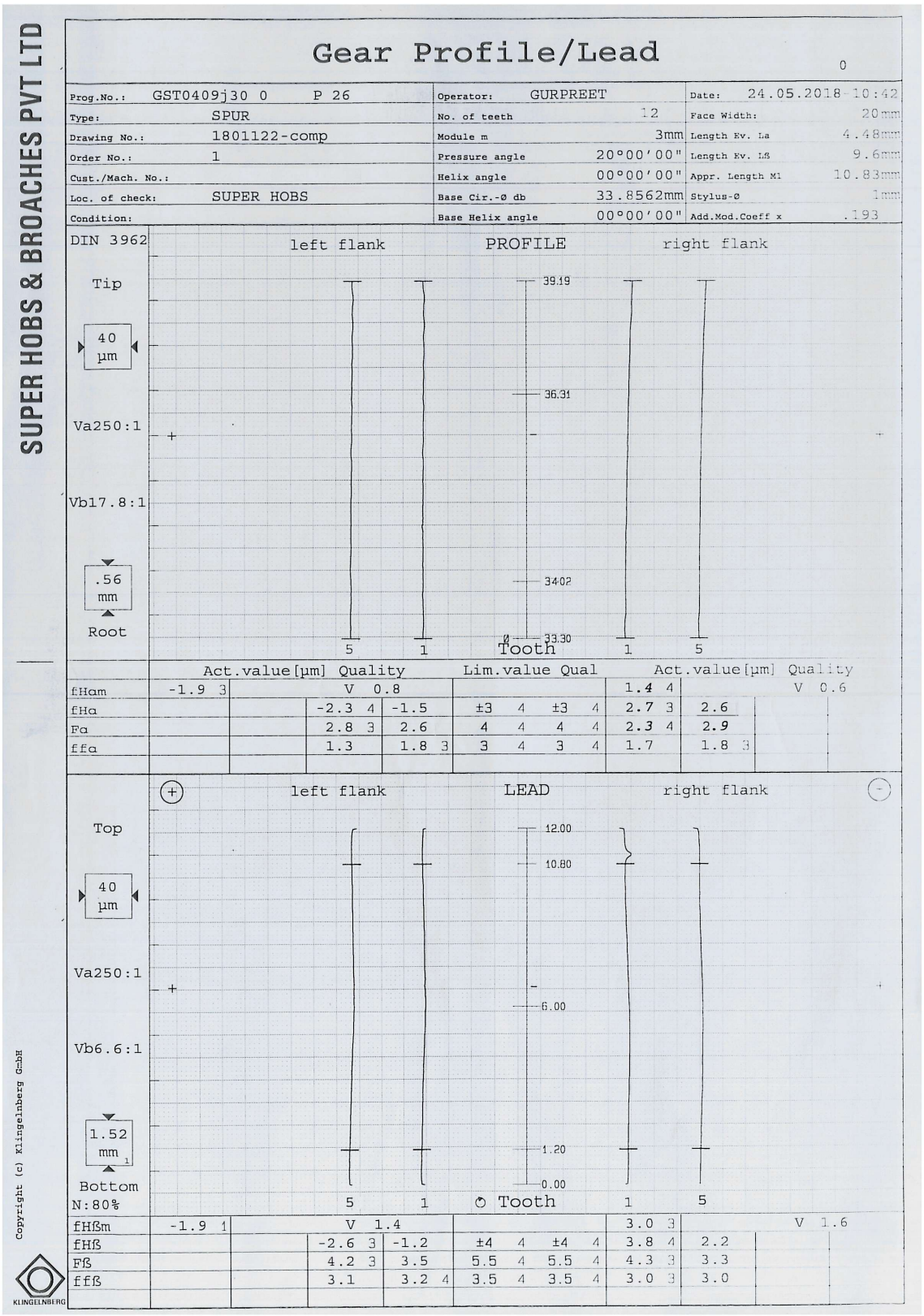

Figure 5.19 Spur gear teeth profile and lead in DIN 4 after the MR gear profile finishing process

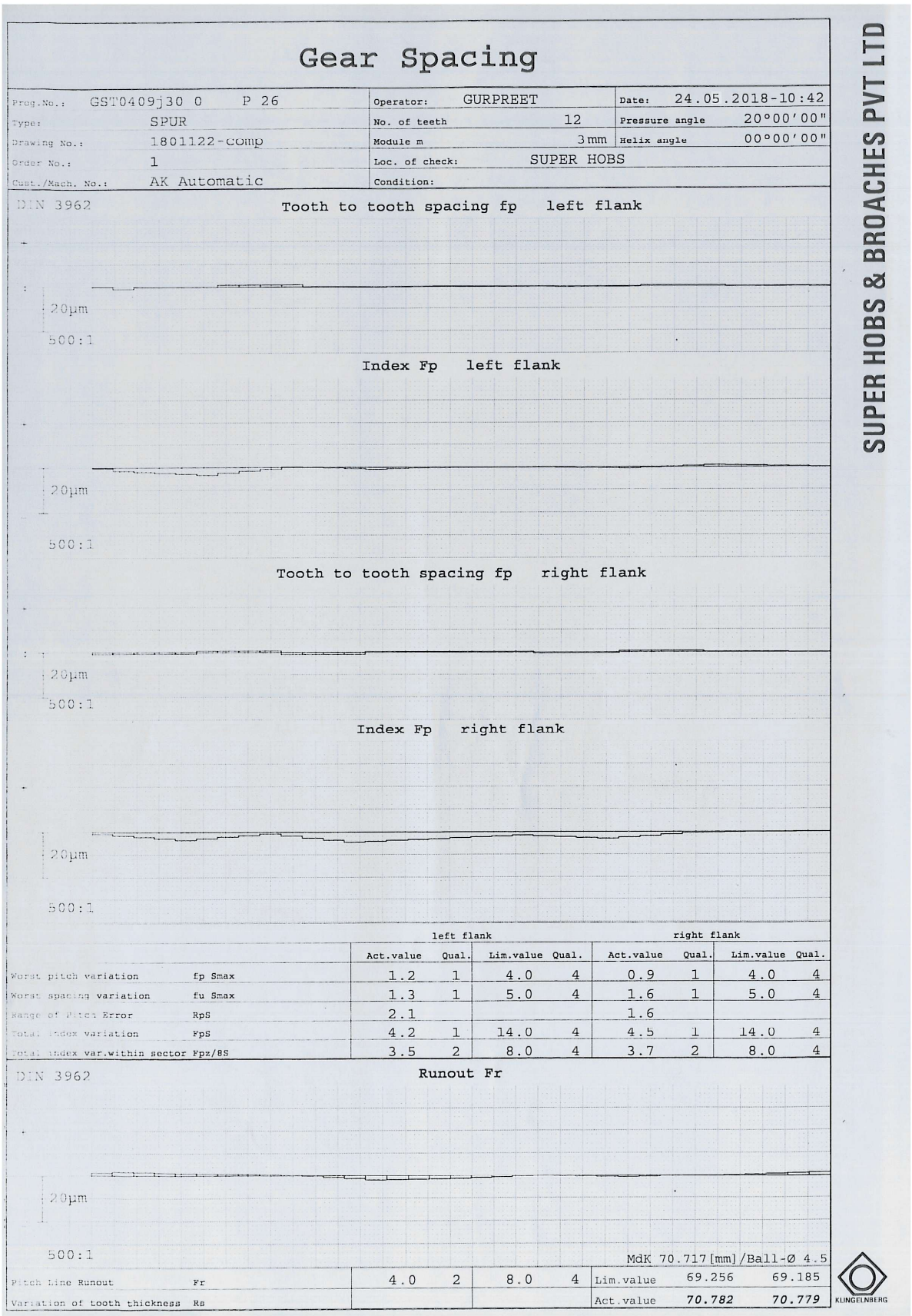

Figure 5.20 Spur gear runout in DIN 4 after the MR gear profile finishing process

5.10 CONCLUSIONS

The parametric study for the EN24 spur gear was carried out. The response surface methodology with central composite design has been used to statistically design the experiment. To analysis the response on percentage change in surface roughness with the effect of various parameters. Optimized parameters were obtained through the response surface methodology. There optimum parameters were used to finish the gear teeth profile with MR gear profile finishing tool. After MR finishing, gear teeth profile characteristics were compared to gear profile grinder. The following specific conclusion are drawn from this chapters

- Among all the parameters, the working gap between the tool surface to workpiece surface contributed the major role in finishing the EN24 steel spur gear. The contribution of parameters to percentage change in surface roughness was found with working gap as 28.88%, tool rotation 12.15% and followed by tool reciprocation feed 9.00%.
- The optimum parameters were obtained using response surface methodology are tool rotation 400rpm, tool reciprocation feed 100mm/min and working gap 0.55mm. Surface roughness of the specimen was reduced from 0.150µm to 0.020µm in 20 minutes.
- After performing the confirmatory test for regression model, the percentage error between the theoretical regression model observations and experimental observations was found in the range of 2.50% to 0.56 %. The range of percentage error showed good agreement between theoretical as well as experimental data.
- With the newly magnetorheological gear profile finishing process, the DIN standard of the finished surface reduced to DIN4 from DIN6.
- Improvement of gear single pitch deviation and total cumulative pitch deviation with any adjacent gear teeth revealed the shape accuracy of the gear improvement.
- The gear runout is reduced to almost 50% of the MR gear profile finishing process from the gear grinding surface. Gear runout is most important factor in gear manufacturing companies and assembly of gears in gear box to reduce the gear noise.

CHAPTER 6
CONCLUSIONS AND FUTURE SCOPE

In this chapter, the results obtained after design of magnetorheological gear profile finishing (MRGPF) tool, mathematical modelling, parametric study of process parameters and testing of gear teeth profile has been discussed.

6.1 CONCLUSIONS

- Uniform magnetic flux density was 0.64T at gear tooth surface was and decreases linearly to 0.54T towards gear tooth profile face. Similarly, magnetic flux density was 0.63T at gear tooth surface was and decreases linearly to 0.54T towards gear tooth profile flank.
- At the gear tooth profile magnetic flux density was 0.54T to 0.47T at left-side gear tooth profile, measured at gear tooth lead line. Similarly, magnetic flux was 0.53T to 0.46T at right-side gear tooth profile, measured at gear tooth lead line. This magnetic flux density increases the active area of abrasives.
- The distribution of magnetic flux density on both sides of gear tooth profile shows that the higher magnetic flux density region on gear tooth profile both sides is same.
- The theoretically result obtained from the magnetic flux density and indentation forces on left and right sides of the gear tooth profile showed the present MR gear profile finishing tool is capable to perform uniform finishing.
- Surface roughness for the gear tooth profile workpiece was reduced from 0.15µm to 0.030µm, 0.060µm and 0.080µm respectively in 100, 75 and 50 number of finishing cycles. Percentage error in the theoretical as well as experimental data was found in range of -5% to 6.66%.
- Theoretically calculated surface roughness values are varying with number of cycles and their comparison with experimental data shows that the theoretical calculation accuracy can be increased with the consideration of centrifugal force. Initial surface roughness peaks are sharp edges. Therefore, material removal rate is higher in starting of running cycles.
- Among all the parameter working gap plays the major role to finish the gear teeth profile EN24 steel material. The contribution of parameters to percentage change in surface roughness was found with working gap was 28.88% followed by tool reciprocation and tool feed was 12.15% and 9% respectively.

- The optimum parameters were obtained using response surface methodology are tool rotation 400rpm, tool reciprocation feed 100mm/min and working gap 0.55mm. Surface roughness of the specimen was reduced from 0.150μm to 0.020μm in 20 minutes.
- After performing the confirmatory test for regression model, the percentage error between the theoretical regression model observations and experimental observations was found in the range of 2.50% to 0.56 %. The range of percentage error showed good agreement between theoretical as well as experimental data.
- With the newly magnetorheological gear profile finishing process, the DIN standard of the finished surface reduced to DIN4 from DIN6.
- The newly designed MRGPF tool significantly improves the surface finish of gear teeth profile. The result is also ratified by the microscopic study of gear teeth surface with SEM images. After MR polishing fluid finish, all the peaks and valley equally remove the both gears left and right-side profile.
- The gear runout is reduced to almost 50% of the MR gear profile finishing process from the gear grinding surface.

6.2 FUTURE SCOPE

- A newly designed magnetorheological gear profile finishing (MRGPF) tool is used for a particular three module profile.
- While developing the mathematical model for surface roughness, rotation of tool has few effects on the surface roughness reduction. The main reason for this behavior is neglecting of centrifugal force on abrasive as well as iron particles. Percentage error can be reduced by eliminating the assumptions of the mathematical model.
- While performing the parametric experiment for EN24 steel spur gear, the colour of the surface changes to brown on reducing the gap. This change in characteristics needs to be further analyzed. The surface roughness was not reduced even after 20 minutes of operation.
- A manually designed gear indexing was done with finishing of gear teeth profile. Gear indexing play a major role for the reduction of gear DIN standard. If done with hydraulic system so reduce the DIN standard more rapidly and accurately with less skilled labor.

REFERENCES

[1] Jolivet S, Mezghani S, Mansori M E, Vargiolu R, and Zahouani H (2017). Experimental study of the contribution of gear tooth finishing processes to friction noise. *Tribology International*, 115, 70–77.

[2] Bot A Le (2017). Noise of sliding rough contact. *Journal of Physics: Conference Series,* 797, 012006.

[3] Mayer JE, Price AH, Purushothaman GK, and Dhayalan AK (2002). Specific grinding energy causing thermal damage in helicopter gear steel. *Journal of Manufacturing Processes*, 4(2), 142–147.

[4] Lewicki DG, Handschuh RF and Henry ZS (1994). Low-noise, high-strength, spiral-bevel gears for helicopter transmissions. *Journal of Propulsion and Power,* 10(3), 356–361.

[5] Jung B, Jang K, Min B, Jo S, and Seok J. (2009). Magnetorheological finishing process for hard materials using sintered iron CNT compound abrasives. *International Journal of Machine Tools & Manufacture,* 49, 407–418.

[6] Moriwaki I, Okamoto T, Fujita M and Yanagimooto T (1990). Numerical analysis of tooth forms of shaved gear. *JSME International Journal Series-3*, 33(4), 608–613.

[7] Tonshoff KH, Friemuth T and Marzenell C (2000). Properties of honed gears during lifetime. *CIRP Annals,* 49(1), 431–434.

[8] Jain NK and Petare AC (2017). Review of gear finishing processes, *Comprehensive Material finishing,* 1, 93–120.

[9] Chen CP, Jain L, Guo-chan W, Jian W and Lewi R (1981). Electrochemical honing of gear: a new method of gear finishing. *CIRP Annals,* 30(1), 103–106.

[10] Wei G, Wang H and Chen CP (1987). Field controlled electrochemical honing of gears. *Procedia Engineering,* 9(4), 218–221.

[11] Mishra JP, Jain PK and Dwivedi DK (2011) Precision finishing of gears by electrochemical honing process: a state of art review. *Journal of Advanced Manufacturing Systems,* 10(2), 309–327.

[12] Venkatesh G and Sharma AK. (2014). Finishing of bevel gears using abrasive flow machining. *Procedia Engineering*, 97, 320–328.

[13] Masseth J and Kolivand M (2008). Lapping and superfinishing effects on hypoid gears surface finish and transmission errors. *Gear Technology magazine,* 72–78.

[14] Mutschler E and Nicholson M (2004). The basics of brush deburring. *Gear Solutions Magazine,* 11, 40–47.

[15] Bertsche R (2009). High pressure deburring. *Gear Solutions Magazine,* 20–25.

[16] Sroka G and Winkelmann L (2003). Superfinishing gears: the state of the art. *Gear Solutions Magazine,* 28–33.

[17] Vibro PDJ. Gear maker invests in vibratory finishing. Available at https://www.vibratoryfinishing.co.uk/deburring-machines/gear-maker-invests-in-vibratory-finishing.html (Accessed on 4th March 2018).

[18] Pa PS (2010). A super surface finish module by simultaneous influences from electromagnetic force and ultrasonic vibrations. *Materials and Manufacturing Processes,* 25(5), 288–292.

[19] Wei BY, Denga XZ and Fang ZD (2007). Study on ultrasonic-assisted lapping of gears. *International Journal of Machine Tools & Manufacture*, 47, 2051–2056.

[20] Yang JJ, Zhang H, Deng XZ, and Wei BY (2013). Ultrasonic lapping of hypoid gear: System design and experiments. *Mechanism and Machine Theory,* 65, 71–78.

[21] Shaikh JH and Jain NK (2015). Effect of finishing time and electrolyte composition on geometric accuracy and surface finish of straight bevel gears in ECH process. *CIRP Journal of Manufacturing Science and Technology*, 8, 53–62.

[22] Singh H and Jain PK (2015). Role of the Power Supply and Inter-Electrode Gap in Electrochemical Honing Process. *Procedia Engineering*, 100, 907–911.

[23] Jain VK. *Advanced Machining processes.* Allied Publishers; New Delhi, 2002.

[24] Britton RD, Elovate CD, Alanou MP, Evans HP and Snidle RW (2009). Effect of surface finish on gear tooth friction. *American Society of Mechanical Engineers,* 99, 354–360.

[25] Klocke F, Lopenhaus C and Sari D (2016). Process concepts for gear finish hobbing. CIRP Conference on Manufacturing Systems, 41, 875–880.

[26] Jolivet S and Mansori ME (2015). Numerical simulation of tooth surface finish effects on gear noise. *Conference on Engineering Systems Design and Analysis 2014* [12th Biennial 2014] ESDA2014–20575.

[27] Sekar RP and Kumar RS (2017). Enhancement of wear resistance on normal contact ratio spur gear pairs through non-standard gears. *Wear*, 380, 228–239.

[28] Karpuschewski B, Knoche HJ and Hipke M (2008). Gear finishing by abrasive processes. *CIRP Annals - Manufacturing Technology,* 57, 621–640.

[29] Kumar SS and Hiremath SS (2016). A review on abrasive flow machining. *Procedia Technology,* 25, 1297–1304.

[30] Antoniadis A, Vidakis N and Bilalis N (2004). A simulation model of gear skiving. *Journal of Materials Processing Technology*, 146, 213–220.

[31] Fuentes A, Nagamoto H, Litvin FL, Gonzalez-perez I, and Hayasaka K (2010). Computerized design of modified helical gears finished by plunge shaving. *Computer Methods in Applied Mechanics and Engineering*, 199, 1677–1690.

[32] Heinzel C and Wagner A (2013). Fine finishing of gears with high shape accuracy. *CIRP Annals - Manufacturing Technology*, 62, 359–362.

[33] Oobayashi K, Irie K and Honda F (2005). Producing gear teeth with high form accuracy and fine surface finish using water-lubricated chemical reactions. *Tribology International*, 38, 243–248.

[34] Lopatin BA and Plotnikova SV (2016). Finishing of the helical-bevel gear teeth flanks. *Procedia Engineering*, 150, 889–893.

[35] Niranjan MS, Jha S and Kotnala RK (2014). Ball end magnetorheological finishing using bidisperse magnetorheological polishing fluid. *Materials and Manufacturing Processes*, 29, 487–492.

[36] Degroote JE, Marino AE, Wilson JP, Bishop AL, Lambropoulos JC, and Jacobs SD (2007). Removal rate model for magnetorheological finishing of glass. *Applied Optics,* 46(32), 7927–7941.

[37] Barman A, Das M and Singh A (2014). Modelling and simulation of magnetic field assisted finishing process [12th-14th Design and Research Conference (AIMTDR) December 2014, IIT Guwahati, Assam, India], pp. 481–486.

[38] Jha S and Jain VK (2006). Modelling and simulation of surface roughness in magnetorheological abrasive flow finishing process. *Wear*, 261, 856–866.

[39] Li Y, Shen X and Wang A (2009). Nano-precision finishing technology based on magnetorheological finishing. *Key Engineering Materials*, 416, 118–122.

[40] Sagbas A (2011). Analysis and optimization of surface roughness in the ball burnishing process using response surface methodology and desirability function. *Advanced in Engineering Software,* 42, 992–998.

[41] Oktem H, Erzurumlu T and Kurtaran H (2005). Application of response surface methodology in the optimization of cutting condition for surface roughness. *Journal of Material Processing Technology*, 170, 11–16.

[42] Bedi TS and Singh AK (2017). Magnetorheological fluid of ferromagnetic blind hole type surfaces. *Materials and Manufacturing Processes,* 1–8.

[43] Singh AK, Jha S and Pandey PM (2013). Mechanisms of material removal in ball end magnetorheological finishing process. *Wear,* 302, 1180–1191.

[44] Ramesh R and Gnanamoorthy R (2006). Fretting wear behavior of liquid nitride structural steel EN24 and En31. *Journal of Material Processing Technology,* 171, 61–67.

[45] Norton LR. Machine Design an Integrated Approach. North America: Pearson Education, 2013.

[46] Singh AK, Jha S and Pandey PM (2011). Design and development of nano-finishing process for 3D surface using ball end magnetorheological finishing process. *International journal of machine tool and manufacturing*, 51(2), 142–151.

[47] Sawhney A.K. *Electrical Machine Design*. Dhanpat Raj and Co, 2016.

[48] Das M, Jain VK and Ghoshdastidar PS (2008). Analysis of magnetorheological abrasive flow finishing process. *Machining Science and Technology,* 98(1), 613–621.

[49] Bedi TS and Singh AK (2016). Magnetorheological methods for finishing- a review. *Particulate Science and Technology.* 34(4), 412–422.

[50] Singh AK, Jha S and Pandey PM (2009). Nano finishing of a typical 3D ferromagnetic workpiece using ball end magnetorheological finishing process. *International journal of machine tool and manufacturing*, 63, 21–31.

[51] Sidpara A, Das M and Jain VK (2009). Rheological characterization of magnetorheological finishing fluid. *Materials and Manufacturing Processes,* 24(12), 1467–1478.

[52] Pattanaik LN and Agarwal H (2014). Development of magnetorheological finishing process for freeform surfaces. *International Journal of Advanced Mechanical Engineering*, 4(6), 611–618.

[53] Kirk, D. A quick and easy formula for mesh-micron particle size conversions. Available at https://www.powderbulk.com/wp-content/uploads/2014/05/pbe_20081201_0018.pdf (Accessed on 10th February 2018).

[54] Singh AK, Jha S and Pandey PM (2012). Magnetorheological ball end finishing process. *Materials and Manufacturing Processes,* 27, 389–394.

[55] Kumar S, Jain VK and Sidpara A (2015). Nano finishing of freeform surfaces (knee joint implant) by rotational-magnetorheological abrasive flow finishing (R-MRAFF) process. *Precision Engineering*, 42, 165–178.

[56] Jha S and Jain VK (2006). Nano finishing of silicon nitride workpieces using magnetorheological abrasive flow finishing. *International Journal of Nanomanufacturing,* 1(1), 17–25.

[57] Seok J, Lee SO, Jang KI, Min BK and Lee SJ (2007). A study on the fabrication of curved surfaces using magnetorheological fluid finishing. *International Journal of Machine Tool and Manufacturing*, 47, 2077–2090.

[58] Sidpara A and Jain VK (2012). Theoretical analysis of forces in magnetorheological fluid-based finishing process. *International Journal of Mechanical Sciences,* 56, 50–59.

[59] Xudong G, Cheng W and Rongguo Y. An electromagnetic localization method for medical micro-devices based on adaptive particle swarm optimization with neighborhood search. *Measurement*, 44, 852–858.

[60] Paswan SK, Bedi TS and Kumar A (2017). Modeling and simulation of surface roughness in magnetorheological fluid based honing process. *Wear*, 376–377, 1207–1221.

[61] Jolly MR, Carlson JD and B. C. Munoz CB (1996). A model of the behavior of magnetorheological materials. *Smart Material Structure*, 5, 607–614.

[62] Sidpara A and Jain VK (2012). Nano-level finishing of single crystal silicon blank using magnetorheological finishing process. *Tribology International,* 47, 159–166.

[63] Alam Z and Jha S (2017). Modeling of surface roughness in ball end magnetorheological finishing process. *Wear*, 374-375, 54–62.

[64] Jain R.K, Jain V.K and Dixit P.M (1999). Modeling of material removal and surface roughness in abrasive flow machining process, *Machine Tools and Manufacture,* 39, 1903–1923.

[65] Gupta K and Chatterjee S (2018). Analysis of design and material selection of a spur gear pair for solar tracking application. *Material Today: Proceedings*, 5, 789–795.

[66] Sarmah BP and Khare MK (1988). Some investigation of the wear mechanisms of widalon carbide insert in machining En 24 steel. *Wear*, 127, 229–240.

[67] Bedi TS and Singh AK (2016). A new magnetorheological finishing process for ferromagnetic cylindrical honed surfaces. *Materials and Manufacturing Processes,* DOI.10.1080/10426914.2016.1269925.

[68] Baligidad SM, Chandrasekhar U, Elangovan K and Shankar S (2018). RSM optimization of parameter influencing mechanical properties in selective inhibition sintering. *Material Today: Proceedings*, 5, 4903–4913.

[69] Kant S and Jawalkar CS (2018). Modeling in drilling of die steels using taguchi method-based response surface analysis. *Material Today: Proceedings,* 5, 4531–4540.

[70] Vardhan MV, (2017). Optimization of parameters in CNC milling of P20 steel using response surface methodology and taguchi method. *Material Today: Proceedings,* 4, 9163–9169.

[71] Sun G, Sankaraiah G, Yohan M and Rao HJ (2018). Reinforcement of thermoplastic chitosan hydrogel using chitin whiskers optimized with response surface methodology. *Carbohydrate polymers,* 189, 280–288.

[72] Yang A, Han Y, Pan Y, Xing H, and Li J (2017). Optimum surface roughness prediction for titanium alloy by adopting response surface methodology. *Results in Physics*, 7, 1046–1050.

[73] Maan S and Singh A.K (2017). Nano surface finishing of hardened AISI 52100 using magnetorheological solid core rotating tool. *International Journal of Advanced Manufacturing Technology,* 95, 513–526.